Molecular Mechanism Underlying Dissociation of the Coat of COPI Vesicles

DISSERTATION

submitted to the
Combined Faculties for the Natural Sciences and for Mathematics
of the Ruperto-Carola University of Heidelberg, Germany

for the degree of
Doctor of Natural Sciences

presented by
Iva Ganeva
2016

DISSERTATION

submitted to the
Combined Faculties for the Natural Sciences and for Mathematics
of the Ruperto-Carola University of Heidelberg, Germany
for the degree of

Doctor of Natural Sciences

presented by

Iva Ganeva, Diplom-Ingenieurin Biotechnology (FH)

born in Sofia

Oral examination:

…….

Molecular Mechanism Underlying Dissociation of the Coat of COPI Vesicles

Referees: Prof. Dr. Felix T. Wieland

Prof. Dr. Britta Brügger

На татко

Abstract

In Eukaryotes vesicular transport mechanisms collectively ensure the transport and distribution of proteins and lipids between cellular compartments to maintain their unique composition and their specialized functions. COPI vesicles mediate retrograde transport from the ERGIC/Golgi to the ER as well as intra-Golgi transport. Formation as well as consumption of COPI-coated transport vesicles is directly controlled by small GTPases of the Arf family, which in turn are regulated via specific Guanine nucleotide exchange factors (GEFs) and GTPase Activating Proteins (GAPs). COPI vesicle formation is initiated by recruitment of Arf1 to membranes, which subsequently recruits the heptameric coat complex coatomer. GTP hydrolysis within Arf1 is a prerequisite for COPI vesicle uncoating. Three ArfGAPs are associated with COPI vesicle formation in mammalian cells: ArfGAP1, ArfGAP2 and ArfGAP3. During the course of this work mechanistic aspects of COPI vesicle biogenesis were investigated: i) the interaction of ArfGAPs with coatomer isoforms, ii) the regulation of ArfGAP activity by p24 family proteins, and iii) the molecular mechanism of COPI vesicle uncoating. We have determined the dissociation constants of the ArfGAPs for each of the four individual coatomer isoforms and found that all three ArfGAPs displayed a higher affinity for the $\gamma_1\zeta_1$ isoform than for the other isoforms. This result is in accordance with the localization of both ArfGAP2/3 and $\gamma_1\zeta_1$ to the cis-Golgi, whereas ArfGAP1 is equally distributed throughout the Golgi apparatus. Furthermore, we have investigated an effect on the GAP activity of ArfGAP1 and ArfGAP2 of the cytoplasmic tail of the transmembrane protein p23, a COPI vesicle machinery protein. p23 was reported to induce a conformational change in coatomer, resulting in a structure that resembles coatomer conformation within the polymerized COPI coat. Interestingly, p23 influenced the activity of ArfGAP1 and ArfGAP2 in an opposite fashion: whereas ArfGAP2 displayed a higher rate of Arf1 GTP hydrolysis in the presence of p23, ArfGAP1 displayed a lower rate. Thus, ArfGAP2/3 might preferentially interact with polymerized coatomer as found on a completed COPI vesicle. Although GTP hydrolysis in Arf1 is commonly considered necessary for coat disassembly, it remains obscure whether it is sufficient to complete this process. To investigate this pivotal mechanistic question, we have established a real-time assay to follow the fate of the COPI coat components of purified vesicles upon addition of ArfGAPs, and discovered an unanticipated essential role of the non-catalytic domains of ArfGAPs. While GTP-hydrolysis within Arf1, induced by the isolated catalytic domain of the ArfGAP, released the small GTPase from the coat, the network of coatomer remained associated with vesicle membranes. Only in the presence of full-length ArfGAP1, including the non-catalytic part, the coat network was completely disassembled. We propose that the energy released upon GTP-hydrolysis in Arf1 is coupled by GAP-coatomer interactions to mediate conformational changes in coatomer that are required for COPI coat disassembly.

Zusammenfassung

In Eukaryoten stellt das Zusammenwirken vesikulärer Transportmechanismen den Transport und die Verteilung von Proteinen und Lipiden zwischen zellulären Kompartimenten sicher, um ihre spezifische Zusammensetzung aufrecht zu erhalten und ihre spezialisierte Funktion zu gewährleisten. COPI-Vesikel vermitteln den retrograden Transport vom ERGIC/Golgi zum ER sowie den intra-Golgi-Transport. Die Bildung sowie der Verbrauch von COPI-umhüllten Transportvesikeln wird direkt durch kleine GTPasen der Arf-Familie kontrolliert, die wiederum von spezifischen GTP Austauschfaktoren (GEFs) und GTPase aktivierende Proteine (GAPs) reguliert werden. Der erste Schritt bei der Bildung von COPI Vesikeln wird durch Aktivierung von Arf1 durch Beladung mit GTP und Bindung an die Donormembran eingeleitet. Arf1-GTP rekrutiert anschließend den heptameren Hüllkomplex Coatomer. Die Hydrolyse von GTP in Arf1 ist Voraussetzung für die Freisetzung der Vesikelhülle von COPI Vesikeln. In Säugerzellen sind drei ArfGAPs mit der Bildung von COPI-Vesikeln assoziiert: ArfGAP1, ArfGAP2 und ArfGAP3.

Im Verlauf dieser Arbeit wurden verschiedene Aspekte der COPI-Vesikel-Biogenese untersucht: i) die Interaktion von ArfGAPs mit Coatomer-Isoformen, ii) die Regulation von ArfGAPs durch p24 Proteine und iii) der molekulare Mechanismus der Freisetzung der COPI-Hüllproteine.

Wir haben die Dissoziationskonstanten für ArfGAPs mit allen Coatomer-Isoformen bestimmt, wobei alle ArfGAPs eine höhere Affinität zur $\gamma_1\zeta_1$ Isoform im Vergleich zu den anderen Isoformen aufwiesen. Dieses Ergebnis steht in Einklang mit der Lokalisation von sowohl ArfGAP2/3 als auch $\gamma_1\zeta_1$ am cis-Golgi, wohingegen ArfGAP1 eine gleichmäßige Lokalisation überall im Golgi-Apparat aufweist. Des Weiteren haben wir den Effekt des zytoplasmatischen Teils des Transmembranproteins p23, eines Proteins der COPI Vesikel Maschinerie, auf die GAP-Aktivität von ArfGAP1 und ArfGAP2 untersucht. Es ist beschrieben, dass p23 eine Konformationsänderung in Coatomer induziert. Die resultierende Konformation ähnelt der Struktur des Komplexes in der polymerisierten COPI-Hülle. Interessanterweise beeinflusst p23 die Aktivität von ArfGAP1 und ArfGAP2 in gegenläufiger Weise. Während ArfGAP2 eine höhere Arf1-GTP-Hydrolyserate in Gegenwart von p23 aufwies, zeigte ArfGAP1 eine geringere Rate. Demnach interagiert ArfGAP2/3 möglicherweise bevorzugt mit Coatomer in polymerisierter Form, wie er auf COPI-umhüllten Vesikeln vorliegt.

Obgleich die GTP-Hydrolyse in Arf1 für die Freisetzung der Proteinhülle im Allgemeinen als notwendig betrachtet wird, ist bisher unklar, ob sie auch ausreichend ist, um diesen Prozess zu komplettieren. Um diese zentrale mechanistische Frage zu untersuchen, haben wir einen Echtzeit-Assay etabliert, um das Schicksal einzelner COPI-Hüllkomponenten aus gereinigten Vesikeln nach Gabe von ArfGAPs zu verfolgen. Unsere Ergebnisse haben zur Aufdeckung einer unvorhergesehenen, essentiellen Rolle der nicht-katalytischen Domäne von ArfGAP

geführt. Während die durch die katalytische Domäne der ArfGAPs alleine vermittelte GTP-Hydrolyse zur Freisetzung der kleinen GTPase von der Vesikelhülle führt, bleibt das Coatomer-Netzwerk mit der Vesikelmembran assoziiert. Nur in Gegenwart des vollständigen ArfGAP1 inklusive des nicht-katalytischen Teils erfolgte die vollständige Auflösung des Hüll-Netzwerks. Wir schlagen vor, dass die durch die GTP-Hydrolyse in Arf1 freigesetzte Energie an eine Interaktion des GAP Proteins mit Coatomer gekoppelt ist. Diese Interaktion ist notwendig, um die für das Zerlegen der COPI-Hülle benötigte Konformationsänderungen im Coatomer zu bewirken.

1 Introduction

Eukaryotic cells feature an elaborated internal membrane system. The individual compartments of a cell are able to communicate with one another, a process which is to a large extend achieved by coated vesicles. These coated vesicles are thought to mediate sorting and transport of proteins and lipids between adjacent membranes in the secretory and endocytic pathways.

In eukaryotic cells, each organelle has a distinct lipid and protein composition. In order to make possible the constant communication between compartments while keeping their identity intact, numerous transport vesicles bud off from one membrane and fuse with another. This traffic is strictly organised, the secretory pathway leads outwards from the ER through the Golgi apparatus and to the cell surface while the endocytic pathway leads inwards from the cell surface via endosomes and to lysosomes. The tight regulation of these processes ensures that a transport vesicle budding from an individual compartment incorporates only specific cargo and fuses with no other but the target membrane.

1.1 The Secretory Pathway

Transport of cargo along the secretory pathway has been first described based on an electron microscopy study performed on exocrine pancreatic cells (Caro and Palade, 1964; Jamieson and Palade, 1967). These early findings and a series of follow-up studies led to the postulation of the vesicular transport hypothesis (Palade, 1975) according to which transport between individual compartments of a cell is mediated by directed and strictly regulated vesicular transport.

The secretory pathway involves various vesicular transport systems, of which COPI-, COPII- and Clathirin-coated vesicles (working with a variety of adaptor proteins) are the best characterized ones. COPII-mediated vesicular transport is involved in the export of secretory cargo from the ER (Barlowe et al., 1994; Kuehn et al., 1998) (Figure 1.1). COPI coated vesicles are responsible for the retrieval of ER resident and cycling machinery proteins from the ER Golgi intermediate compartment (ERGIC) and the Golgi apparatus to the ER (Cosson and Letourneur, 1994; Letourneur et al., 1994), for retrograde (Lanoix et al., 1999; Lanoix et al., 2001; Love et al., 1998) and aterograde (Orci et al., 1997) intra Golgi transport. The late endocytic pathway is governed by clathrin-coated vesicles, and various less well characterized vesicular coats and comprises transport between the plasma membrane, the trans Golgi network (TGN), lysosomes and endosomes (reviewed in Robinson and Pimpl, 2014).

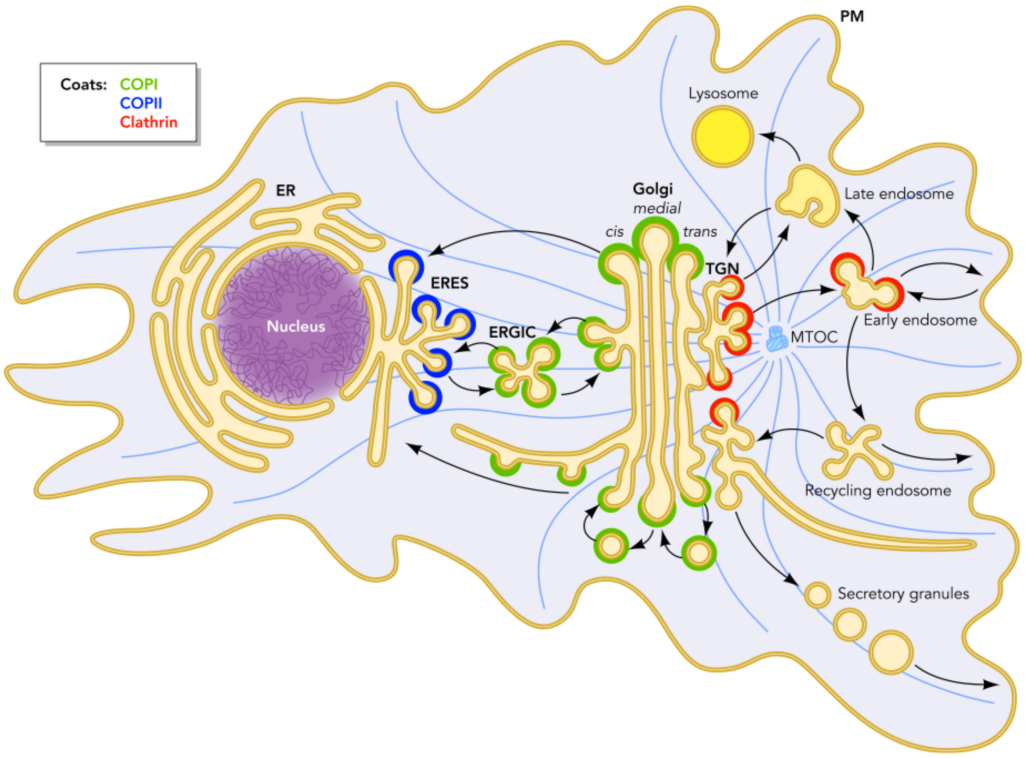

Figure 1.1: Intracellular Transport Pathways. The three main coating systems: COPI, COPII and Clathrin share structural and mechanistic features. Proteins transported along the early secretory pathway are secreted proteins, soluble proteins and lysosomal/vacuolar proteins with a common signal sequence. Secretory protein transport can be subdivided into four steps: ER import/quality control, transport from the ER to the Golgi, intra-Golgi transport/ER retrival and post Golgi transport, reviewed in (Barlowe and Miller, 2013). COPI vesicular transport is involved in retrograde transport from the Golgi/ERGIC to the ER as well as in intra Golgi transport. COPII vesicles are responsible for anterograde transport from ERES to the ERGIC and to the Golgi. Post-Golgi transport is governed by the Clathrin system involving various adaptor proteins. Figure adapted from (Szul and Sztul, 2011).

1.1.1 ER to Golgi Transport

ER to Golgi transport is bidirectional: the anterograde direction goes to the Golgi while the retrograde one from the Golgi back to the ER. Forward transport comprises uptake of cargo by both bulk flow (reviewed in Thor et al., 2009), and by specific cargo recognition (Kuehn et al., 1998). Most secreted proteins undergo the conventional ER to Golgi pathway. After completion of folding and initiation of glycosylation, those soluble and membrane proteins that have passed the ER quality control systems (ERQC) are packed into COPII vesicles and transported to the ERGIC/Golgi apparatus. The budding sites of the COPII carriers are restricted to long-lived subdomains, termed ER exit sites (ERES) (Bannykh et al., 1996; Hammond and Glick, 2000). According to some of the current views, the ERES scaffold is organized by the large multidomain protein Sec16, and in turn recruits the COPII machinery via multiple interactions with the coat (reviewed in Miller and Barlowe, 2010). Dependent on

the cell type, the COPII carriers need to cover varying distances in order to reach the target membrane.

In mammalian cells, COPII vesicles form the ERGIC by homotypic fusion (Xu and Hay, 2004). Anterograde carriers are than guided from the ERGIC via microtubules towards the Golgi complex (Mogelsvang et al., 2003; Presley et al., 1997) (reviewed also in Appenzeller-Herzog and Hauri, 2006).

1.1.2 Structure and Function of the Golgi apparatus

The mammalian Golgi apparatus, described for a first time by Camillo Golgi in 1898, consists of four to six cisternae and is localized in an area near the nucleus and the centrosome (Rambourg and Clermont, 1990). Anterograde cargo enters the Golgi at the cis-Golgi network (CGN) and exits at the trans-Golgi network (TGN). Once at the TGN, the cargo molecules are sorted and subsequently transported to the endo-lysosomal compartments, the plasma membrane or the extracellular space (reviewed in Gu et al., 2001; Rodriguez-Boulan and Musch, 2005). Vesicle machinery is recycled to earlier compartments by COPI vesicular transport (Cosson and Letourneur, 1994; Letourneur et al., 1994; Majoul et al., 2001). On their way through the Golgi apparatus secretory proteins can undergo a large variety of post-translational modifications: glycosylation, sulfatation and phosphorylation. To facilitate this process, each cisterna is equipped with a unique set of enzymes: in this way the individual steps are spatially and temporally separated (de Graffenried and Bertozzi, 2004; Munro, 2001; Nilsson et al., 2009; Opat et al., 2001; Schoberer and Strasser, 2011; Tu and Banfield, 2010).

1.1.3 Structure of the Golgi apparatus

The Golgi apparatus takes a central position in the secretory pathway as here takes place the sorting of proteins into anterograde and retrograde cargo. While highly conserved, the structure of the Golgi apparatus still differs in certain aspects between organisms. The budding yeast *Saccharomyces cerevisiae* features unstacked Golgi compartments distributed along the cytoplasm. In contrast, *Schizosaccharomyces pombe*, *Pichia pastoris* and mammalian cells display a stacked Golgi with 4 to 11 independent cisternae, the number being depended on the organism and the cell type. Golgi architecture is maintained by tethering proteins of the GRASP and golgin family. These very long rod-like proteins create a structural scaffold (Goud and Gleeson, 2010; Munro, 2011; Ramirez and Lowe, 2009). The mammalian Golgi apparatus can be subdivided into five distinct regions: ,1) cis-Golgi network (CGN), 2) cis-Golgi, 3) medial-Golgi, 4) trans-Golgi and 5) trans-Golgi network (TGN), which display different functions and posses a distinct set of enzymes, respectively (Dunphy et al.,

1981; Dunphy and Rothman, 1983; Griffiths et al., 1983; Quinn et al., 1983). Mannosidases are located in the cis-Golgi, glycosyl transferases in the medial-Golgi and acid phosphatases as well as the galactosyl transferases in the trans-Golgi. ER resident proteins that have escaped from the ER in COPII vesicle, are returned back to the ER via COPI vesicles budding from the ERGIC and cis-Golgi membranes.

The TGN is the next sorting hub. Proteins destined for constitutive and regulated secretion are sorted into secretory vesicles. Proteins marked with a Mannose-6-phospate and destined to the lysosomes are packed in AP-1/GGA-dependent Clathrin-coated vesicles, whereas proteins destined to other organelles of the endo-lysosomal system (e.g. early and late endosomes or lysosome-related organelles (LRO)), as well as proteins of the plasma membrane are sorted into distinct transport vesicles. For a more comprehensive reviews see (Bonifacino and Glick, 2004; Hinners and Tooze, 2003; Nakatsu and Ohno, 2003; Robinson, 2004).

1.1.4 Intra-Golgi Transport: lateral Diffusion versus Vesicular Transport

The exact mechanism of intra-Golgi transport is still under debate and two main current hypotheses exist: cisternal progression/maturation versus vesicular transport (reviewed in (Glick and Luini, 2011; Glick and Malhotra, 1998; Glickman et al., 1989; Pfeffer, 2010; Rothman and Wieland, 1996; Suda and Nakano, 2012). According to the vesicular transport model, cargo is transported along the Golgi apparatus by COPI vesicles that bud from one stationary cisterna and fuse with the next. This model requires the existence of two distinct populations of COPI vesicles, one responsible for anterograde and the other one for retrograde transport. On the contrary, in the cisternal progression/maturation model anterograde cargo is transported through the Golgi without leaving the cisterna (Glick and Malhotra, 1998). Anterograde carriers coming from the ER fuse with each other at the CGN and form a new cisterna at the cis-Golgi. Then machinery from the previous cis-most cisterna is recycled in COPI vesicles to the new cisterna. The cisterna move stepwise through the stack and mature by recycling machinery in the cis direction and receiving machinery from the trans direction, and are eventually consumed at the trans Golgi. Nevertheless, both models fail to account for the complete mechanism. While the cisternal progression/maturation model cannot explain the varying rates of anterograde transport (Bonfanti et al., 1998; Karrenbauer et al., 1990), the vesicular model fails to explain the mechanism by which cargo bigger than COPI vesicles is transported (Bonfanti et al., 1998). Recently a new model, the cisternal progenitor model, has been proposed, which combines the cisternal progression/maturation model with the vesicular transport (Pfeffer, 2010). According to this model, the Golgi is a stable structure, which is able to generate subsequent

compartments. A different Rab protein governs each of the tightly packed stacks. RabA recruits a guanine nucleotide exchange factor, which subsequently activates RabB. An interaction with an effector protein stabilizes the activated Rabs on the membrane. RabB in turn recruits a GTPase activating protein, which inactivates RabA creating a separate RabB domain. The RabB domain, including its cargo, can now undergo fission and fuse with a stable RabB cisterna. In this way sequential domains are built from stable progenitor domains. Likewise, vesicles budding from the RabA domain and fusing with the RabB domain can transport cargo.

1.2 Classes of Coated Vesicles within the Secretory Pathway

1.2.1 Clathrin-Coated Vesicle

Clathrin-coated vesicles are involved both in the late secretory pathway and the endocytic pathway (Mellman, 1996; Pearse and Robinson, 1990). The late secretory pathway includes transport between the trans Golgi network (TGN), lysosomes, endosomes and the plasma membrane. Clathrin consists of three large (Clathrin heavy chain) and three small (clathrin light chain) polypeptide chains that together form a three-legged structure called a triskelion (Kirchhausen and Harrison, 1981; Ungewickell and Branton, 1981). Clathrin triskelions assemble into a basket-like convex framework of hexagons and pentagons to form coated pits on the cytoplasmic surface of membranes and subsequently organise recruitment of proteins to these coated pits and facilitates vesiculation of the lipid bilayer (Kirchhausen, 2000). The clathrin terminal domain is a seven-blade beta propeller, a structure well adapted to interact with multiple partners, such as the AP-1 and AP-2 sorting adaptor complexes but also monomeric clathrin adaptor proteins, e.g. Golgi-localised γ-ear-containing Arf-binding proteins (GGAs), Epsin1-3; EpsinR, AP180, and beta-arrestins (reviewed in Robinson and Pimpl, 2014).

The numerous Clathrin mediated transport processes are promoted by the use of different adaptor complexes (AP), which build the inner coat of the vesicle (Bonifacino and Glick, 2004; Owen et al., 2004; Robinson, 2004). AP1, AP2, AP3, AP4, AP5 belong to a family of homologous tetrameric adaptor protein complexes, which show distant sequence and structural homology to the tetrameric subcomplex of coatomer (β-, δ-, γ-, ζ-COP) (reviewed in Kirchhausen et al., 2014; Paczkowski et al., 2015). AP1 localizes to the TGN and endosomes (Ahle et al., 1988) and functions with Arf1 (Stamnes and Rothman, 1993; Traub et al., 1993). AP2 is recruited by a direct interaction with $PI(4,5)P_2$ (Collins et al., 2002; Gaidarov et al., 1996; Gaidarov and Keen, 1999; Rohde et al., 2002) and mediates vesical formation of endocytic Clathrin-coated vesicles from the plasma membrane (Ahle et al., 1988). The endosomal AP3 (Dell'Angelica et al., 1997; Simpson et al., 1997) has also been

shown to be recruited via the small GTPase Arf1 (Ooi et al., 1998), however, its potential role as a cargo adaptor and its acossiation with clathrin remains to be clarified (Dell'Angelica et al., 1998; Peden et al., 2002; Rehling et al., 1999). AP4 localizes to the TGN (Dell'Angelica et al., 1999; Hirst et al., 1999) and like AP1 and AP3 functions with Arf1 (Boehm et al., 2001), however, it seems not to be accociated with clathrin (Borner et al., 2012). The last adaptor protein to be discovered is AP5 (Hirst et al., 2011) and while it is known to localize to endosomes, its membrane recruitment mechanism has not been elucidated yet. Another independent class of adaptor proteins are the Golgi-localised γ-ear-containing Arf-binding proteins (GGAs) (Boman et al., 2000; Dell'Angelica et al., 2000; Hirst et al., 2000; Puertollano et al., 2001). There are three mammalian GGAs, which are involved in transport between the trans-Golgi and the endosome/lysosome system (reviewed in Bonifacino and Glick, 2004; Robinson and Pimpl, 2014).

1.2.2 COPI Vesicles

The COPI minimal machinery consists of the small GTPase Arf1, dimeric proteins of the p24 family and the heptameric coat protein coatomer (Bremser et al., 1999), which occurs in four different isoforms. Escaped ER resident proteins are retrieved to their proper location by a direct interaction between their conserved C-terminal KKXX or KXKXX motif (Jackson et al., 1990), or KDEL motif (Arakel et al., 2016) and the coat complex of COPI vesicles (Duden et al., 1991; Serafini et al., 1991b; Waters et al., 1991). For more details see 1.3.1

1.2.3 COPII Vesicle

COPII-mediated vesicular transport is involved in the export of secretory cargo and proteins destined for almost all organelles from the ER (Adolf and Wieland, 2013; Miller and Schekman, 2013). Most of the components of the COPII vesicular system were first discovered in a screen in *S. cerevisiae*, where temperature-sensitive mutants displaying a defect in protein secretion and cell surface growth (Novick et al., 1980). These vesicles, which are destined for the ERGIC and/or the Golgi apparatus, bud from a specialised region of the ER called ER exit sites (ERES) or transitional elements, whose membrane lacks bound ribosomes. ERES acumulate at regions juxtaoposed to the Golgi apparatus, but can be found also spread throughout the cell.

The protein coat of COPII vesicles is made of one inner layer: the Sec23/24 complex and one outer layer: the Sec13/31 complex (Barlowe et al., 1994). The formation of COPII vesicles at the ER is induced by the activation of the Ras-like small GTPase Sar1, which undergoes a GDP to GTP exchange facilitated by the COPII specific GEF: a type 2 integral membrane glycoprotein termed Sec12 (Barlowe and Schekman, 1993; d'Enfert et al., 1991;

Nakano and Muramatsu, 1989). Sar1 is soluble and located in the cytosol in its inactive GDP-bound state but becomes membrane associated when transferred to its active GTP form. The interaction of Sar1 with the membrane is mediated by an intramolecular conformation change within Sar1 involving a reorientation of the two switch regions and a subsequent exposure of the N-terminal, non-acylated helix, which then anchors the protein to the ER membrane (Bi et al., 2002; Huang et al., 2001). Activated Sar1 recruits the COPII inner complex subunits, Sec23/24, from the cytosol to the membrane via an interaction between Sec23 and Sar1-GTP. Once associated, the Sec23/24/Sar1 complex recruits the Sec13/31 heterotetramer from the cytosol, leading to polymerization of the COPII coat (Matsuoka et al., 1998). The binding site for Sec23/Sec24 in Sec13/31 includes a 50-residue long stretch of an unstructured prolin-rich region within Sec31. This stretch is sufficient to trigger GTP hydrolysis in the Sar1/Sec23 complex. COPII vesicle targeting is governed by Rab1 GTP, which recruits p115 and thus tethers the vesicles to the final destination. Fusion is then mediated by the Q-SNARE complex comprising Syntaxin5, GS27 (also known as membrin), Bet1, and the R-SNARE Sec22b (Parlati et al., 2000; Weber et al., 1998).

As the pathway from the ER via the Golgi apparatus to the cell surface is considered to be the default pathway, vesicles budding from the ER transitional elements were initially thought to be non-selective (Karrenbauer et al., 1990; Wieland et al., 1987). In later studies, a variety of biochemical and genetic studies have identified individual cargo binding sites in the COPII coat subunit Sec24 pointing that sorting of some cargo proteins into COPII vesicles is mediated by specific export signals (Buchanan et al., 2010; Miller et al., 2002; Miller et al., 2003; Mossessova et al., 2003).

1.3 Components and Molecular Mechanism in COPI Vesicles Biogenesis

1.3.1 The small GTPases of the Arf family

Small GTPases of the Ras superfamily are key regulators of a number of important cellular functions (Vetter and Wittinghofer, 2001). The Arf subfamily is highly conserved and is itself subdivided into Arfs and Arf-like (Arls) proteins. In mammals, there are six Arf isoform, which function as molecular switches and cycle between an inactive GDP-bound state and an active GTP-bound state. Arf's soluble GDP state is transformed to a membrane bound GTP state by an ArfGEF. Arf1 is reversed to its soluble from by ArfGAPs mediated GTP hydrolysis. The six Arfs can be allocated to three different classes (Kahn et al., 2006). Arf1, Arf2 and Arf3 belong to class I, Arf4 and Arf5 to class II and Arf 6 to class III. While Arf6 is localized at the plasma membrane (Cavenagh et al., 1996; D'Souza-Schorey et al., 1998; Peters et al., 1995), Arf1-5 are primarily found at the Golgi (Chun et al., 2008) and to some extent at the endosomes (Lenhard et al., 1992; Volpicelli-Daley et al., 2005).

Arf1 recruits the COPI coat protein, the clathrin adaptor proteins (APs) AP1 and AP3, the Golgi-localized γ-ear-containing Arf-binding proteins (GGAs) (D'Souza-Schorey et al., 1998), and the Mints (Hill et al., 2003) to Golgi membranes. In addition, Arf1 associates with AP4 in the late secretory pathway (Boehm et al., 2001). It has been found in a recent study that not only Arf1 but also Arf4 and Arf5 associate with *in vitro* generated COPI vesicles (Popoff et al., 2011b). Furthermore, Arf1, Arf4 and Arf5 proved to be sufficient to individually mediate COPI vesicle formation *in vitro* (Popoff et al., 2011b). Interestingly, Arf3, which was not found in the vesicle fraction by mass spectrometry analysis, was also able to initiate COPI vesicle biogenesis *in vitro* when incubated with purified coatomer, nucleotide and isolated Golgi membranes (Popoff et al., 2011b).

The small GTPase Arf1 is a structural coat component of COPI vesicles (Bremser et al., 1999; Serafini et al., 1991a; Spang et al., 1998). It regulates both coating (Donaldson et al., 1992; Orci et al., 1993; Ostermann et al., 1993; Serafini et al., 1991a; Palmer et al., 1993) and uncoating of the vesicles (Tanigawa et al., 1993). Likewise, Arf1 plays a key role in the recruitment of the tetrameric adaptor protein complexes AP1 (Austin et al., 2000), AP3 (Ooi et al., 1998) and AP4 (Boehm et al., 2001). Although the subunits of coatomer and tetrameric adaptor protein complexes share only weak sequence homology (Schledzewski et al., 1999), they are comprised of conserved structural elements (McMahon and Mills, 2004), indicating mechanistic similarities between vesicle biogenesis mediated by COPI and these adaptor protein complexes.

1.3.2 Coatomer - the COPI Coat Complex

Coatomer is the coat protein complex of COPI vesicles, which consists of seven subunits: α-, β-, β`-, γ-, δ-, ε- and ζ-COP. Higher eukaryotic organisms possess two isoforms of γ- and ζ-COP, which are termed γ1-, γ2-, and ζ1-, ζ2-COP, respectively (Wegmann et al., 2004) (Figure 1.2). According to a immunoelectron microscopy study, coatomer isoforms display heterogeneity in their localisation within the Golgi apparatus: while γ1- and ζ2-COP is mainly located at the pre-Golgi and early Golgi compartment, the γ2-COP isotype is found preferentially at the trans side of the organelle (Moelleken et al., 2007).

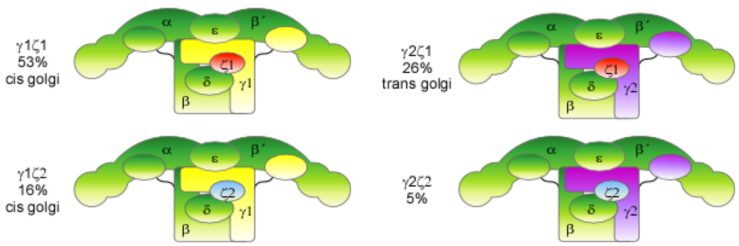

Figure 1.2: Coatomer Isoforms. Coatomer consists of seven subunits α-, β-, β`-, γ-, δ-, ε- and ζ-COP. Higher eukaryotes feature two isoforms of γ- and ζ-COP, which allows assembly of four possible complexes (γ1ζ1, γ1ζ2, γ2ζ1, and γ2ζ2). Approximated abundance and preferential localization of the four coatomer isoforms within NRK cells are indicated.

1.3.3 p24 Family Proteins in the Early Secretory Pathway

The p24 proteins comprise a family of type I transmembrane proteins of 23 to 27 kDa that can be subdivided into four subfamilies (p24α, -β, -γ and -δ) (Dominguez et al., 1998). The six best understood family members in mammalian systems are p23, p24, p25, p26, p27 and tp24. All p24 proteins cycle between the Golgi and the ER in different oligomeric forms (Dominguez et al., 1998; Emery et al., 2000; Gommel et al., 1999; Sohn et al., 1996; Blum et al., 1999; Fullekrug et al., 1999; Nickel et al., 1997) and share similar domain architecture: an N-terminal Golgi-dynamics domain (Anantharaman and Aravind, 2002), a predicted coiled-coil region, a membrane spanning domain and a short cytoplasmic tail (13 to 20 amino acids). Within the sequence, several highly conserved motifs required for the binding of COPI and COPII coat complexes are distinguishable. Interactions between the p24 proteins occur via their cytoplasmic tails (Reinhard et al., 1999; Weidler et al., 2000) and presumably also via their predicted coiled-coil regions (Ciufo and Boyd, 2000). The cytoplasmic tails have two conserved motifs: a diphenylalanine motif and a dibasic motif. While in mammalian p25 and its yeast orthologs the dibasic motif is identical to the KKXX motif, this is not the case for the other family members.

p24 proteins are strictly dependent on each other in terms of localisation, stability and transport. The overexpression of a single member leads to the mislocalisation of the entire p24 family in ER-derived structures (Emery et al., 2000; Fullekrug et al., 1999; Gommel et al., 1999). Knock out of all the p24 family proteins in yeast leads only to a minor defect in cargo transport and thus the strain remains viable (Springer et al., 2000). In contrast, in mice even a single homozygous knock out is lethal at an early embryonic stage (Denzel et al., 2000). This discrepancy might be based on the different levels of complexity of the early secretory pathway in the two systems. The early secretory pathway is relatively simple in yeast as it contains an unstacked Golgi and involves only limited N-glycan processing. The disruption of the system activates the unfolded protein responce (UPR), which enables the

p24-deficient cells to counteract the transport defects (Aguilera-Romero et al., 2008; Belden and Barlowe, 2001a). On the other hand, mammals possess a more complex early secretory pathway, which might be more sensitive to the absence of the p24 family and is more likely to be affected to a degree that cannot be compensated by the UPR.

The exact function of the p24 family is under debate and still remains to be elucidated. In one of the models, p24 proteins are suggested to be cargo receptors for the specific incorporation of secretory molecules into transport vesicles (Stamnes et al., 1995). Evidence for that is provided by the finding that a deletion of one of the p24 family members disrupts the anterograde transport of certain cargo proteins in yeast (Gas1p and invertase), but not of others (α-factor, acid phosphatase, carboxypeptidase Y, alkaline phosphatase and Gap1p) (Belden and Barlowe, 2001b; Marzioch et al., 1999; Muniz et al., 2000; Schimmoller et al., 1995; Stamnes et al., 1995). In another model, p24 proteins are proposed to play a role in COPI vesicle biogenesis and function as machinery (Bremser et al., 1999). Here, dimeric p24 recruits Arf1 to sites of COPI vesicle formation and thus functions as an Arf1 receptor at the cis-Golgi (Gommel et al., 2001; Majoul et al., 2001).

1.3.4 ArfGEFs in COPI-mediated Transport

The 15 eukaryotic ArfGEFs can be divided into five families based on overall structure and domain organisation: Golgi BFA resistance factor 1/BFAinhibited GEF (GBF/BIG), Arf nucleotide binding site opener (ARNO)/cytohesin, exchange factor for Arf6 (EFA6), Brefeldin resistant Arf GEF (BRAG) and F-box only protein 8 (FBX8). Every mammalian cell expresses at least six different GEFs and some isoforms display a tissue-specific pattern. It has been proposed that each GEF functions in a specific subcellular compartment and thus is dependent on different kinds of upstream regulation (reviewed in Casanova, 2007).

Arf GEFs are characterised by a central catalytic Sec7 domain of approximately 200 amino acids. It is named based on its homology to the yeast protein Sec7p. The Arf1 specific GEFs are GBF1, BIG1 and BIG2. While GBF1 activates Arf1 at the cis-Golgi, BIG1 and BIG2 govern the Arf1 activation at the trans-Golgi and the trans-Golgi network. Once in its GTP bound state, Arf1 is able to interact with various effectors and to recruit coat components to specific sites of vesicle formation.

The COPI-specific GEF is the Golgi-specific BFA resistance factor 1 (GBF1), which binds to the cis-Golgi elements as well as to the ERGIC, where it undergoes an interaction with the tethering protein p115 (Garcia-Mata et al., 2003; Zhao et al., 2006) (Figure 1.3). A treatment of cells with the fungal toxin Brefaldin A (BFA) leads to the dissociation of coatomer from the membrane. This effect can be abolished by the overexpression of GBF1 (Claude et al., 1999) and mimicked by the overexpression of the catalytically inactive GBF1 mutant E794K (Garcia-Mata et al., 2003).

Figure 1.3: Domain structure of the ArfGEF GBF1. ArfGEFs are characterised by a central catalytic Sec7 domain of approximately 200 amino acids. The N-terminal DCB domain plays a role in dimerization. The highly conserved HUS1 domain and the HDS1, 2 and 3 domains are of unknown function. Figure adapted from (Casanova, 2007)

It has been shown via fluorescence recovery after photobleaching (FRAP) that GBF1 has a shorter residence time on the Golgi membrane in comparison to Arf1 (Niu et al., 2005; Szul et al., 2005; Zhao et al., 2006), suggesting that the GEF dissociates rapidly from Arf1-GTP once nucleotide exchange has taken place while the activated Arf1 remains tightly associated with membrane (Niu et al., 2005; Szul et al., 2005).

GBF1 and its two yeast homologues Gea1 and Gea2 bind directly to coatomer (Deng et al., 2009). In a yeast two-hybrid screen, Sec21p (the homologue of γ-COP) proved competent to bind the N-terminus of Gea1 (Deng et al., 2009). The interaction site was mapped to the C-terminal domain of Sec21p (Deng et al., 2009). Furthermore, the N-terminus of the human GBF1 binds bovine γ1-COP in a co-immunoprecipitation experiment when both proteins are co-expressed in COS7 cells (Deng et al., 2009). This interaction is even enhanced in the presence of BFA (Deng et al., 2009). In addition, Gea1 and Gea2 interact with TRAPPII, a tethering complex, which as well directly interacts with coatomer and thus assists COPI vesicle trafficking (Chen et al., 2011). Interestingly, neither of the interactions is necessary to recruit coatomer to liposomes *in vitro* (reviewed in (Jackson, 2014). It is solely the interaction with Arf1-GTP that is responsible for coat membrane association. Based on this data, it was speculated that the interaction between the coat protein and the corresponding GEF is rather needed in order to increase the local concentration of the coat at sites where Arf1 activation takes place (Jackson, 2014).

Based on the experimental data, two different models have been proposed for the role of GBF1 in the temporal and special organisation of COPI coat recruitment and vesicle biogenesis. According to the widely accepted model, the association of GBF1, Arf1 and coatomer with the Golgi membrane are sequential events. GBF1 is first recruited to the membrane by a direct interaction with a still unknown receptor. Then Arf1 is recruited to the membrane and undergoes the GBF1-mediated GDP to GTP exchange. Finally, Arf1-GTP recruits coatomer. In a newer model, the interaction between Arf1, coatomer and GBF1 takes place on the membrane prior to the GDP to GTP exchange (Deng et al., 2009). Here Arf1, GBF1 and coatomer are recruited individually and once present at the membrane, they undergo a direct transient interaction with each other. This interaction plays a critical role in

the specific recruitment of coatomer only at the site of Arf1 activation at the cis-Golgi (Deng et al., 2009).

1.3.5 ArfGAPs in COPI-mediated Transport

The ArfGAP family of proteins consists of more than 30 members in mammals. It is characterised by a conserved, catalytic ArfGAP-domain of approximately 130 amino acids containing a characteristic zinc finger motif (Cukierman et al., 1995; Goldberg, 1999). The non-catalytic domains of these proteins differ significantly, which underlines their individual mechanisms of recruitment.

There are four ArfGAPs that function within the Golgi apparatus and are responsible for the hydrolysis of Arf-GTP to Arf-GDP (Cukierman et al., 1995; Frigerio et al., 2007). Three of the ArfGAPs, namely ArfGAP1, ArfGAP2 and ArfGAP3 interact with coatomer, indicating a role in COPI transport (Frigerio et al., 2007; Goldberg, 1999; Lee et al., 2005) (Figure 1.4). Whereas the catalytic parts of the three proteins share 80 % identity, the non-catalytic domains of ArfGAP1 differs significantly from the non-catalytic domains of ArfGAP2 and ArfGAP3. The three proteins are believed to originate from a common ancestor, as there is a single gene in *G. lamblia*. Very early in evolution the family split into ArfGAP1 and ArfGAP2 subfamilies. In *S. cerevisiae*, there are only two homologous of the three mammalian ArfGAPs. Gcs1 is the ArfGAP1 homologue and Glo3 is the ArfGAP2/3 homologue (Poon et al., 1999). For more details see 1.4.

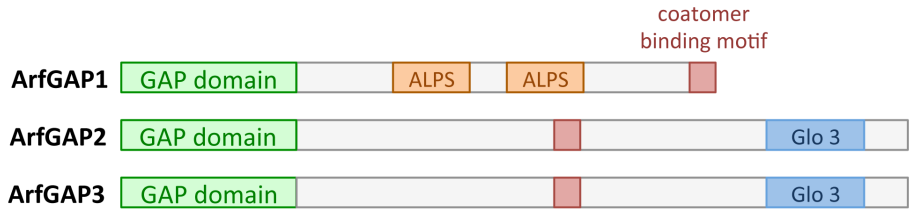

Figure 1.4: Structure of the ArfGAPs involved in COPI vesicle biogenesis: ArfGAP2, ArfGAP2 and ArfGAP3. All three ArfGAPs feature a conserved catalytic zinc finger GAP domain but differ in their non-catalytic domains. Whereas ArfGAP1 contains two ALPS domains, which can sense membrane curvature, ArfGAP2 and ArfGAP3 are display 58 % identity and contain a highly conserved Glo 3 motif of unknown function (Frigerio et al., 2007).

1.3.6 COPI Vesicle Biogenesis

COPI vesicle biogenesis is initiated by the recruitment of the small GTPase Arf1 (ADP-ribosylation factor 1) from the cytosol, where it is located in its inactive, soluble form, to Golgi membranes (Figure 1.5) by a direct interaction with p23/p24. A unique feature of Arfs and Arls is their N-terminal, amphipathic helix, which is myristoylated on its N-terminal glycine residue and is hidden within the protein core in the GDP-bound state. At the membrane Arf1

is activated by GBF1 (Claude et al., 1999). Once in its GTP bound state, Arf1 dissociates from p23/p24 dimers (Gommel et al., 2001), exposes its N-terminal α- helix and inserts the myristic acid residue in the lipid bilayer, which leads to its stable association with the membrane. Upon activation on the membrane, Arf1 was suggested to from a dimer (Beck et al., 2008). This dimerization seems to be essential for vesicle formation as a mutant not able to dimerize leads to a scission arrest of COPI vesicles (Beck et al., 2011b). In a more recent cryo-EM structure (Dodonova et al., 2015; Faini et al., 2012) only monomeric Arfs bound to coatomer were observed. This, however, does not exclude a potential role of dimeric Arfs at the vesicle bud neck required for vesicle scission. Subsequently, Arf1 GTP recruits coatomer *en bloc* (Hara-Kuge et al., 1994) via multiple interactions with its subunits (Bethune et al., 2006; Harter and Wieland, 1998; Sun et al., 2007; Zhao et al., 1997; Zhao et al., 1999). Activated Arf1 binds to the trunk domains of β- and γ-COP and to δ-COP (Sun et al., 2007; Yu et al., 2012; Zhao et al., 1997; Zhao et al., 1999) whereas p24 proteins bind to the trunk and appendage domains of γ-COP (Bethune et al., 2006). The interaction with the p24 family proteins induces a conformational change within coatomer (Bethune et al., 2006; Langer et al., 2008; Langer et al., 2007; Reinhard et al., 1999). The polymerizing coat deforms the membrane, which leads to the formation of COPI coated vesicles.

Prior to fusion with the target membrane, vesicles must be uncoated (Tanigawa et al., 1993). This process is at least partly mediated by the enzymatic activity of the ArfGAPs, which catalyse the hydrolysis of the GTP within the Arf1, returning it to its inactive cytosolic conformation (Cukierman et al., 1995; Reinhard et al., 2003; Tanigawa et al., 1993) and presumably leads to the release of coatomer to the cytosol.

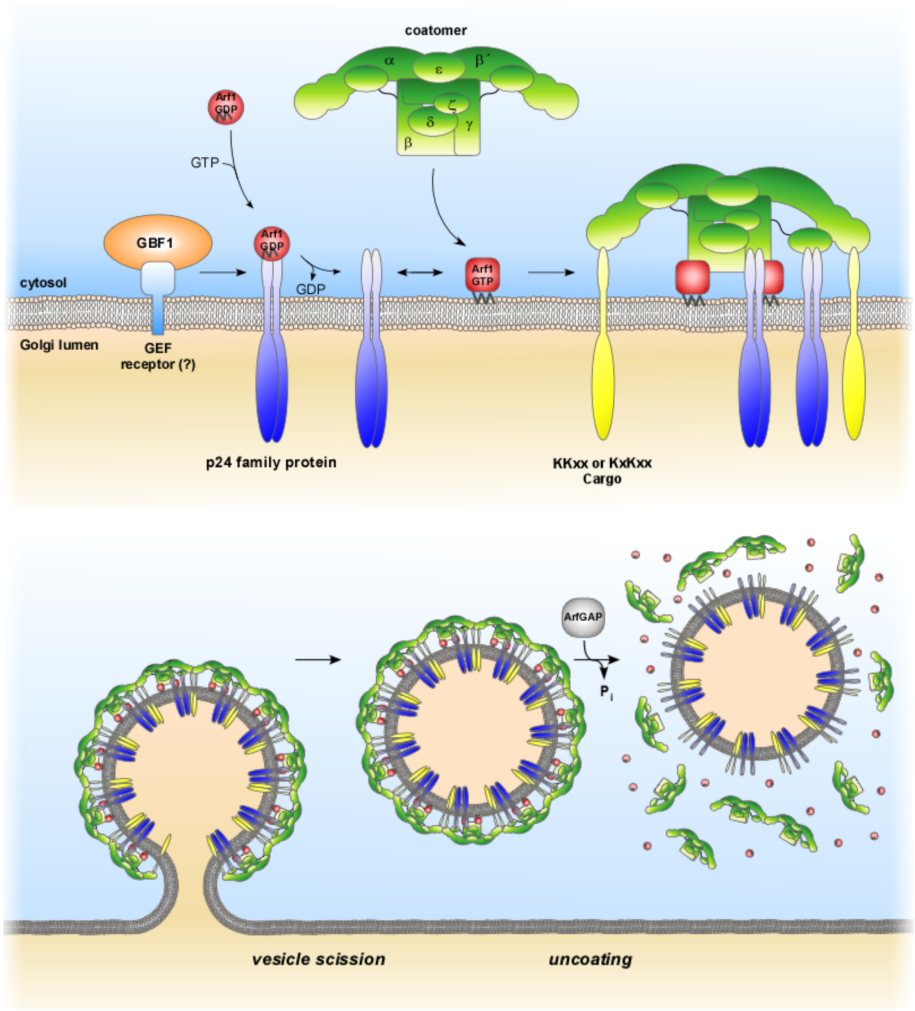

Figure 1.5: COPI vesicle biogenesis. The small GTPase Arf1 is recruited to Golgi membranes in its GDP bound state by an interaction with dimeric p23/p24 tails. It is then transferred to its active GTP state by the guanine nucleotide exchange factor GBF1. Upon activation, Arf1 disassembles from p23/p24 and the transmembrane proteins together with Arf1 recruit coatomer. Membrane budding occurs and the newly formed vesicles are released. Figure adapted from (Popoff et al., 2011).

1.4 Arf GTPase Activating Proteins

1.4.1 ArfGAP Superfamily of Proteins

The ArfGAP superfamily of proteins comprises of 10 subfamilies with more than 30 different members in humans, which are responsible for GTP hydrolysis within the Ras superfamily of GTPases including Ras, Rho, Rab, Arf and Ran. Each family of small GTPase has a distinct set of GAPs, which do not only serve as molecular switches but also play a key role as effectors in vesicle biogenesis (Gillingham and Munro, 2007; Inoue and Randazzo, 2007).

The highly conserved catalytic ArfGAP domain was first identified in rat ArfGAP1 and was shown to catalyze GTP hydrolysis on Arf1 (Cukierman et al., 1995). It consists of

approximately 130 amino acids and contains a characteristic C4-type zinc finger motif and a conserved arginin. Based on the crystal structure the zinc finger was proposed to have a structural role (Goldberg, 1999), while the arginin finger seems to play a catalytical role, a mechanism also proposed for other GAPs (Scheffzek et al., 1998).

The various members of the ArfGAP family display a different degree of specificity for certain Arf GTPases. Most of the ArfGAPs possess an activity on one or more Arfs (Arf1-6), while the Arf-like (Arls) and Sar GTPases work with distinct subset of GAPs. However, the yeast orthologue of ArfGAP1, Gcs1p can hydrolyse GTP both within Arf1p and Arl1p (Liu et al., 2005).

1.4.1.1 ArfGAP1

ArfGAP1 shuttles between the cytosol and the Golgi. It has been shown to interact with coatomer, clathrin and AP-1 (Watson et al., 2004). The activity of ArfGAP1 was initially reported to be dependent on coatomer in a membrane-free system (Goldberg, 1999). Later studies show, however, that in a liposomal system the activity of ArfGAP1 is dependent on membarne curvature rather than on coatomer (Bigay et al., 2003; Weimer et al., 2008). For more details see 1.4.2.

1.4.1.2 ArfGAP2 Subfamily

ArfGAP2 and ArfGAP3 belong to the ArfGAP2 subfamily of proteins. The two proteins display 58 % identity to each other. Both ArfGAP2 and ArfGAP3 have been found to strongly interact with coatomer (Frigerio et al., 2007; Watson et al., 2004), which in turn regulates the activity of the two ArfGAPs (Weimer et al., 2008). For more details see 1.4.2.

1.4.1.3 ADAP Subfamily

ArfGAPs with dual PH domains (ADAPs) are Arf6 GAPs and are thus involved in actin cytoskeleton remodelling, neuronal differentiation and membrane trafficking (Thacker et al., 2004; Venkateswarlu et al., 2004). The ADAP family consists of two members ADAP1 and ADAP2. ADAP1 displays a high affinity for Ins(1,3,4,5)P_4 and PI(3,4,5)P_3. In accordance with its role in neuronal differentiation, ADAP1 localizes at dendrites, spines and synapses of developing and adult neurons.

1.4.1.4 SMAP Subfamily

The human small ArfGAP proteins (SMAPs) are approximately 50 kDa and are involved in endocytosis and oncogenesis (Tanabe et al., 2006). Two SMAP proteins, which share 47 % identity, are expressed in humans. SMAP1 function with Arf6 and SMAP2 also Arf1 (Tanabe

et al., 2006; Tanabe et al., 2005). SMAPs bind via their LLGLD binding motif to clathrin heavy chain and to the clathrin assembly protein, CALM (Natsume et al., 2006). The primarily cytosolic SMAP1 is recruited to membranes where it plays a crucial role in the regulation of constitutive endocytosis. SMAP2 is membrane bound and localizes to endosomes. It has been implicated in the retrograde transport of TGN46 from early endomes back to the TGN (Natsume et al., 2006).

1.4.1.5 AGFG Subfamily

Two members of the nucleoporin-related Arf-GAP domain and FG repeats-containing proteins (AGFG) subfamily were identified up to date: AGFG1 and AGFG2. Their corresponding small GTPases still remain unknown. The AGFG1 protein contains 10 phenylalalnin-glycin (FG) repeats similar to the ones found in nucleoporins. It has been shown to be an important HIV Rev cofactor as it seems that the ArfGAP domain of AGFG1 is essential for the release of Rev-directed HIV-1 RNAs from the perinuclear region (Sanchez-Velar et al., 2004).

1.4.1.6 GIT Subfamily

Two G-protein-coupled receptor (GPCR)-kinase-interacting proteins 1 and 2 (GIT) genes are expressed in vertebrate, expressing GIT1 and GIT2. The two proteins presumably serve as GTPase activating proteins for Arf6 (Claing et al., 2000; Di Cesare et al., 2000; Vitale et al., 2000). GIT1 is predominately expressed in endothelial cells and completely lacking in muscle cells, hepatocytes, pneumocytes and adipocytes (Schmalzigaug et al., 2007). GIT2 is ubiquitous in most cells types. A hallmark of the proteins of the GIT subfamily is that they form oligomeric complexes together with the PIX/Cool proteins (Premont et al., 2004), which serve as GEFs for Cdc42 and Rac1 GTPases. These complexes play a role as scaffolds for different signalling enzymes and thus receive multiple inputs from different GTPases and function as signal integration sites. Among the signalling enzymes are p21 activated kinases, MEK/Erk, phospholipase Cγ and some G protein receptor kinases. The recruitment of GIT/PIX to specific cellular locations is achieved by a direct interaction with a distinct set of proteins.

1.4.1.7 ASAP Subfamily

The ArfGAP with SH3 Domain, Ankyrin Repeat and PH Domain (ASAP) subfamily of proteins are encoded in three genes in humans expressing ASAP1, ASAP2 and ASAP3 respectively. ASAPs are found at specializations of the plasma membrane like in filodopodia and focal

adhesions and have been reported to play a regulative role in actin remodelling and endocytic traffic (Inoue and Randazzo, 2007; Nie et al., 2006). Thus, ASAP1-3 are involved in Arf1 and presumably Arf5 activation (Andreev et al., 1999; Brown et al., 1998). The three human ASAPs share multiple domains but possess distinct C termini. ASAP1 features a SH3 domain and tandem repeats of D/ELPPKP and directly interacts with CrkL, Src, CD2AP and CIN85. ASAP2 has an SH3 domain as well but lacks D/ELPPKP repeats and associates with the focal adhesion kinase pyk2. ASAP3 has neither SH3 domain nor D/ELPPKP repeats but also localizes at focal adhesions and has been implicated in stress fibers regulation (Ha et al., 2008).

1.4.1.8 AGAP Subfamily

Simmilar to the ASAP subfamily, the ArfGAP with GTPase Domain, Ankyrin Repeat and PH Domain (AGAP) subfamily is exclusively found in mammals. Eleven genes in humans have been predicted to encode AGAP proteins. AGAPs are implicated in Arf1 (Jacques et al., 2002), and probably also Arf5 (reviewed in Randazzo and Hirsch, 2004), activation as well as in regulation AP-3 (Nie et al., 2003a). AGAPs contain a GTP-binding domain, which directly associates with Akt and Ras effectors, an interaction required for the activation of Akt and Ras (Ye and Snyder, 2004). The most studied members AGAP1 and AGAP2 play a role in the endocytic system. AGAP1 functions with AP3 and AGAP2 with AP1 (Nie et al., 2005; Nie et al., 2003b).

1.4.1.9 ACAP Subfamily

The ACAPs are found already in Dictyostelium and metazoans and consist of three genes in humans. ACAP stands for ArfGAP with coiled coil, ankyrin repeat and PH domains. The coiled coil has been later shown to be a BAR domain. The ACAPs play a regulative role in endocytosis, Arf6-dependent actin remodelling and receptor tyrosin kinase-dependent cell movement (Inoue and Randazzo, 2007). ACAP1 serves as a part of an Arf6-regulated clathrin coat (Li et al., 2007).

1.4.1.10 ARAP Subfamily

The ARAPs are a distinct feature of chordates and are represented by three genes in humans. They are involved in EGF receptor signalling, the dynamics of focal adhesions and lamellipodia formation (Inoue and Randazzo, 2007). The Arf specificity of the individual ARAPs remains unclear. ARAP1 and ARAP2 were proposed to function with Arf1 and Arf5 rather than Arf6 (Miura et al., 2002). With respect to ARAP3, contradictory results can be

found in the literature. Earlier studies implicated ARAP3 in Arf6 activation (Krugmann et al., 2002) whereas later ones showed that it functions with Arf1 and Arf5 rather than with Arf6 (I et al., 2004) The ARAPs possess ArfGAP, RhoGAP and Ras association domains as well as ankyrin repeats. This elaborated domain combination implies that they might be involved in the coordination of two or more GTPase signalling pathways. The three human ARAPs display similar domain architecture, however, they differ in function and cellular localization and thus show distinct preferences for Arf, Rho or Ras.

1.4.2 Functions of ArfGAPs in COPI Vesicular Transport

1.4.2.1 ArfGAP1

ArfGAP1 is a 45 kDa protein, which cycles between the cytosol and the Golgi, and was the first member of the family to be identified (Cukierman et al., 1995; Randazzo and Hirsch, 2004). ArfGAP1 binds via its N-terminal catalytic domain to switch 2 and the α3 helix within Arf1 and thus orients an Arf1 residue, and stimulates GTP hydrolysis (Goldberg, 1999). The crystal structure of the catalytic domain in a complex with Arf1 reveals that the catalytic domain does not supply an arginine to the active site of the GTPase (Goldberg, 1999). However, newer evidence based on a cryo EM structure of the COPI coat on a membrane challenges this hypothesis (Dodonova et al., 2015). The C-terminal region was predicted to be largely unstructured. It contains two ALPS motifs (amphipathic lipid packing sensor), which are unstructured in solution but are capable of forming an amphipathic helix on highly curved membranes by inserting bulky hydrophobic residues between loosely packed lipids (Bigay and Antonny, 2005; Bigay et al., 2003; Levi et al., 2008; Mesmin et al., 2007) (Figure 1.6). These helixes differ from classical amphipathic helices by the abundance of serine and threonine residues on their polar face. Lipid packing is a physical parameter, which depends on the shape of the lipid molecules as well as on the curvature of the membrane. ArfGAP1 was shown to have a higher activity in the presence of conical lipids (dioleolylglycerol) then in the presence of cylindrical lipids (phosphatidylcholine) at a constant liposomal radius (Antonny et al., 1997). Furthermore, at a constant lipid composition, the activity of ArfGAP1 increases with decreasing liposomal radius (Bigay et al., 2003). This sensitivity of ArfGAP1 to membrane curvature might play a key functional role in the temporal and spatial organisation of GTP hydrolysis within a coated membrane area. Once associated with the membrane, ArfGAP1 would gradually eliminate Arf1-GTP molecules from the coat area with positive curvature leaving intact the molecules at the edge where the membrane curvature is negative (Bigay et al., 2003).

ArfGAP1 interacts with coatomer via a tryptophane based stretch in the most C-terminal part of the protein (Rawet et al., 2010). The motif was identified to be 405AADEGWDNQNW415. The binding site within coatomer is localized in the C-terminus of δ-COP (Rawet et al., 2010). Recent studies have revealed that ArfGAP1 also interacts with components of the Clathrin system, namely clathrin, AP-1 and AP-2 (Bai et al., 2011; Watson et al., 2004) . However, the biological relevance of these interactions still remains to be elucidated.

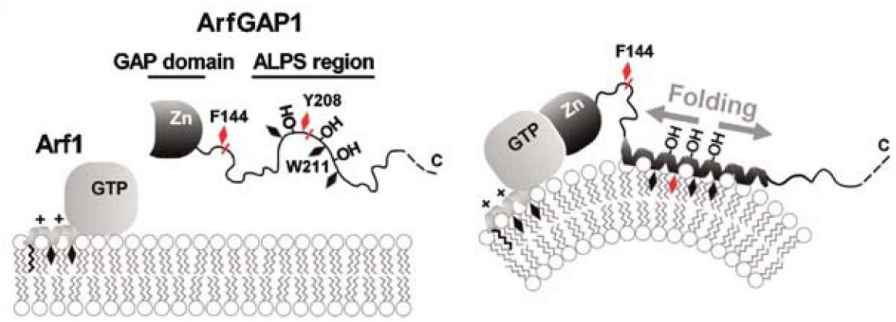

Figure 1.6: Model for curvature sensitivity of ArfGAP1. ArfGAP1 has two ALPS (amphipathic lipid packing sensor) motifs within its noncatalytic region. These ALPS motifs are unstructured in the presence of flat membranes. Upon curvature induction, they recognise the defects in the lipid packing, fold into an amphipathic helix and insert into the membrane. Figure adapted from (Bigay and Antonny, 2005).

1.4.2.2 ArfGAP2 and ArfGAP3

Less is known about the more recently discovered ArfGAP2 and ArfGAP3. These two proteins are closely related and show 58 % identity to each other (Frigerio et al., 2007). The non-catalytic domains of ArfGAP2 and ArfGAP3 lack classical ALPS motifs. A sequence comparison between different species has led to the identification of a highly conserved Glo3 motif at the C-terminus (Yahara et al., 2006), whose function is not yet known.

ArfGAP2 and ArfGAP3 are dependent on the COPI coat protein for their association with the Golgi membrane (Kliouchnikov et al., 2009; Weimer et al., 2008). The Golgi localization of ArfGAP2 and ArfGAP3 is based on two different motifs within the proteins: a central basic stretch and a C-terminal amphipathic motif (Kliouchnikov et al., 2009). The central basic stretch, 235QKL237 in ArfGAP3 (QKV in ArfGAP2), binds to the γ-COP subunit of coatomer (Eugster et al., 2000; Kliouchnikov et al., 2009; Watson et al., 2004). This stretch is also governing the catalytic activity of ArfGAP3 (Kliouchnikov et al., 2009). The carboxy terminal motif, residues 485-510 in ArfGAP3, is conserved in ArfGAP2, ArfGAP3 and the yeast Glo3. It contains predominantly hydrophobic residues on the one face and primarily hydrophilic ones on the other thus representing an amphipathic helix. Despite its pronounced differences in terms of length and types of hydrophobic residues to the ALPS motifs described within ArfGAP1, the carboxy stretch in ArfGAP3 also assumes helical fold in the presence of liposomes. This effect was, however, observed only with the peptide stretch on its own and

not with the full-length protein. Nevertheless, mutations in the carboxy stretch abrogated the Golgi localization of ArfGAP3 pointing to a direct interaction with the lipid bilayer (Kliouchnikov et al., 2009).

In a recent study, it was shown that coatomer components also modulate the activity of ArfGAP2 (Pevzner et al., 2012). Based on homology to the clathrin adaptor complexes, coatomer can be subdivided into two subcomplexes. The adaptor-like CM4 comprises β-, δ-, γ- and ζ-COP, and the cage-like CM3, which contains α-, β`- and ε-COP. ArfGAP2 binds a hydrophobic pocket within the γ1-appendage domain of CM4 (Pevzner et al., 2012). CM4 becomes membrane associated via a direct interaction with Arf1 and in turn recruits ArfGAP2 (Pevzner et al., 2012). Nevertheless, a stimulation of ArfGAP2 activity has been observed only when the fully assembled heptameric coat protein was present (Pevzner et al., 2012).

1.4.2.3 Functions of ArfGAP1, ArfGAP2 and ArfGAP3

ArfGAPs were shown to function both in cargo sorting (Malsam et al., 1999; Nickel et al., 1998; Pepperkok et al., 2000) and coat disassembly (Tanigawa et al., 1993). Although the precise mechanism of cargo sorting is unknown, a current hypothesis suggests that a cycle of Arf1 activation by GBF1 and Arf1 deactivation by an ArfGAP plays a key role in this process. The role of the ArfGAPs as a prerequisite for uncoating is well established, however, what is not completely understood is the molecular mechanism that underlies this process, and whether additional factors are required for completing coat disassembly. In an electron microscopy study Golgi-derived vesicles generated in the presence of the constitutively GTP loaded Arf variant ArfQ71L, vesicles remained coated and failed to fuse with the target membrane (Tanigawa et al., 1993).

A series of contradictory studies have proposed a role of the ArfGAPs as coat components rather than accessory proteins. Hsu and collegues performed *in vitro* COPI vesicle reconstitutions using purified Golgi as donor membranes and observed an increased effciency of COPI vesicle formation in the presence of ArfGAP1 (Yang et al., 2002). GTPγS controls showed lower effciency of vesicle formation and a defect in uncoating, which led the authors to conclude that both effects are due to inefficient GAP recruitment (Yang et al., 2002).

1.5 Coat Disasembly of Transport Vesicles

1.5.1 Uncoating of COPII Vesicle

According to the prevalent view, GTP hydrolysis in the small GTPase is a prerequisite for vesicle uncoating. Early studies have shown that vesicles are incompetent to fuse with the

target membrane when GTP hydrolysis in Sar1 is blocked (Aridor et al., 1995; Barlowe et al., 1994). Thus, both polymerisation and depolymerisation of the COPII coat is regulated by the small GTPase Sar1 (Barlowe et al., 1993; Nakano and Muramatsu, 1989). Sar1-bound GTP undergoes hydrolysis, promoting depolymerisation of the coat proteins, which are then recycled for further rounds of vesicle formation. The GTP hydrolysis in Sar1 is mediated by the coat component Sec23 (Yoshihisa et al., 1993). The catalytic mechanism involves an arginine residue provided by Sec23, which inserts in the catalytic site of Sar1 and stabilizes the phosphate groups of GTP (Bi et al., 2002). Sec23 GAP-activity is further enhanced by an interaction of Sec23 with the outer shell Sec13/31 complex, leading to re-orientation of the arginine finger (Antonny et al., 2001; Yoshihisa et al., 1993).

Initial data points out to an essential role of post-translational modifications within Sec23 for COPII vesicle formation and trafficking. The Ferro-Novick lab, in a series of studies, has shown that the phosphorylation state of Sec23 is crucial for its interaction pattern, which in turn affects vesicle delivery. A phosphorylation site in the vicinity of the Sar1 interaction site is responsible for both Sar1 and transport protein particle (TRAPP) release. Sar1 presumably first binds Sec23 in order to trigger vesicle formation, then in turn Sec23 catalyses GTP hydrolysis and Sar1 is released from the membrane. As the binding site is now free, TRAPP can associate at the same position and recruit Ypt1/Rab1. Hrr25, which is a Golgi-localized kinase, is then able to phosphorylate Sec23 leading to TRAPP dissociation and potentially facilitatiing uncoating. This temporal organisation might be important for maintaing the directionality of COPII trafficking (Lord et al., 2011).

As the Sec23 coat component both supports coat assembly and promotes uncoating, the COPII is stabilized by additional components. The cytosolic factor Sec16 is a large multidomain protein, which is crucial for ER export *in vivo* (Novick et al., 1980; Kaiser and Schekman, 1990). It is associated with the ER exit sites (ERES), which serve as platforms for COPII vesicle budding, and participates in their organisation and structural maintenance (Hughes et al., 2009; Watson et al., 2006). Sec16 interacts with all components of the COPII coat, can directly bind to membranes *in vitro* and remains longer membrane-associated in comparison to the COPII coat components (Espenshade et al., 1995; Gimeno et al., 1996; Hughes et al., 2009; Montegna et al., 2012; Supek et al., 2002; Whittle and Schwartz, 2010; Yorimitsu and Sato, 2012). Furthermore, Sec16 inhibits the Sec31-driven increase of GTPase activity in Sar1 and can thus control COPII vesicle biogenesis (Kung et al., 2012; Yorimitsu and Sato, 2012). However, Sec16 does not display an effect on the GAP activity of Sec23 (Supek et al., 2002). These findings imply that Sec16 can act as a scaffold for the COPII coat components, thus favouring ERES formation and stabilizing the COPII coat by modulating Sar1 GTPase activity (Hughes et al., 2009; Ivan et al., 2008; Kung et al., 2012; Supek et al., 2002; Yorimitsu and Sato, 2012).

Sec12, the COPII-specific GEF, seems also to play a role in the maintainance of coat stability. Sar1p, Sec23/24p, Sec13/31p and GTP do not suffice for vesicle budding *in vitro* as the GTP hydrolysis within Sar1p leads to a coat too unstable to allow vesicle formation. However, if GTP is substituted by its non-hydrolyzable analogue GMP-PNP, *in vitro* COPII budding reactions generate vesicles (Matsuoka et al., 1998). When the reaction was performed in the presence of GTP and the catalytic domain of Sec12p, Sar1p activity was 10-fold higher than the enhanced GAP activity stimulated by the full coat, which led to a stable coat assembly at the liposomal membrane (Futai et al., 2004).
Cargo proteins probably also play a role in the maintenance of coat stability as coat cargo interactions increase the dwelling time of the coat on membranes (Forster et al., 2006; Sato and Nakano, 2005).

1.5.2 Uncoating of Clathrin-Coated Vesicle

Uncoating of an endocytic vesicles requires the heat-schock cognate protein-70 (Hsc 70) (Braell et al., 1984; Schlossman et al., 1984; Ungewickell et al., 1995). The clathrin coat is build up of individual triskelions, comprising three clathrin molecules, which form a lattice upon polymerization (Fotin et al., 2004). Each clathrin molecule consists of a 30-kDa light chain and a 180-kDa heavy chain (Kirchhausen, 2000). After the fully formed vesicle pinches off, the coat needs to be disseassembled so that fusion with the target membrane can occur. The temporal regulation of the uncoating reaction is governed by the recruitment of auxillin, which in turn recruits Hsc70. Auxilin contains an C-terminal J-domain interacting with chaperons of the Hsp70-family and N-terminal PTEN-like region, which can distinguish between a vesicle still associated with the membrane and a vesicle that has already undergone fission (Massol et al., 2006). Hsc70 as a member of the Hsp70-family contains a substrate binding domain and an ATPase domain. Cryo-EM structures of the clathrin coat shed light on the uncoating mechanism (Fotin et al., 2004; Xing et al., 2010). Auxilin binds in such a way that three J-domains are positioned in the vicinity of each vertex of the clathrin coat. Auxilin binding brings about a conformational change, which allows Hsc70, recruited via a direct interaction with the J-domain of auxilin, to reach its target sequence QLMLT near the C-terminus of clathrin (Rapoport, 2008). As Hsc70 binds the peptide in a groove on its substrate binding domain, ATP hydrolysis occurs. This leads to two simultaneous events: the J-domain is released and the substrate becomes tightly clamped in the groove. In such a way, Hsc70 stabilizes the distorted conformation. Once a critical concentration of auxilin/Hsc70 is reached, the coat becomes irrevocablly destabilized and falls apart in a all-or-none fashion (Bocking et al., 2011).

1.5.3 Uncoating of COPI Vesicle

1.5.3.1 Role of the ArfGAPs in COPI Vesicle Coat Disassembly

Simmilar to COPII, the older and still prevailing modell states that GTP hydrolysis within Arf1 is the driving force for coat disassembly (Reinhard et al., 2003; Tanigawa et al., 1993). Initially this hypopthesis was based on two sets of experimental data. First it was discovered that GTPγS blocks transport and leads to the accumulation of coated vesicles (Melancon et al., 1987), and a few years later that Arf1 is a subunit of the COPI coat (Serafini et al., 1991a). The effect of GTPγS on transport can be mimicked by an Arf1 mutant. Arf1Q71L-GTP in its myristoylated form is competent to bind to membranes and recruit coatomer, however, in contrast to wild type fails to hydrolyse GTP (Tanigawa et al., 1993). Although the amount of vesicles formed in the presence of Arf1-Q71L is comparable to the one in the presence of wild type Arf1, cis to medial Golgi transport is inhibited by the mutant in a cell free system (Tanigawa et al., 1993). As observed by EM, vesicles displaying a distinct electron-dense coat accumulated as they probably failed to fuse with the target membrane (Tanigawa et al., 1993). Furthermore, the role of the ArfGAP induced GTP hydrolysis in uncoating was studied on artificial membranes. It was shown in a liposome based system that the GTP hydrolysis mediated by the catalytical domain of ArfGAP1 is sufficient to initiate uncoating (Reinhard et al., 2003). As the catalytical domains of the three ArfGAPs involved in COPI trafficking display 80 % identity, this rose the question if all three ArfGAPs: ArfGAP1, ArfGAP2 and ArfGAP3, are able to meadiate uncoating. Although the three Golgi associated ArfGAPs have been described to have overlapping functions (Cukierman et al., 1995; Frigerio et al., 2007), recent evidence suggests that the three enzymes might fulfill different purposes in COPI transport. Based on their distinct recruitment mechanisms: via the ALPS motifs for ArfGAP1 and via coatomer for ArfGAP2 and 3, two different hypotheses have been proposed. According to the Antonny lab, ArfGAP2/3 can be recruited to the flat Golgi membrane via a direct interaction with coatomer and remove single coatomers from the membrane thus antagonising the formation of COPI vesicles when not enough cargo is present. ArfGAP1, on the other hand, is recruited to the curved membrane of a fully formed COPI vesicle and is rather responsible for uncoating and so rendering a fusogenic vesicle. In accordance with the same data, the Wieland lab suggested that ArfGAP2/3 are the uncoating ArfGAPs and are recruited by a direct interaction with coatomer to the polymerized COPI coat. ArfGAP1 is rather involed in the early steps of vesicle biogenesis and is recruited to the highly curved regions of COPI vesicle formation thus playing a role in cargo uptake.

1.5.3.2 Role of Tethering factors in COPI Coat Disassembly

According to a newer model, vesicle tethering might occur prior to uncoating and facilitate this process as tethers seem to directly interact with coat components (reviewed by Szul and Sztul, 2011). Dsl1p binds directly to α-COP and δ-COP (Andag and Schmitt, 2003; Reilly et al., 2001). More recently it has been shown that the interaction sites between Dsl1p and α-COP are simmilar to the interaction sites between α-COP and ε-COP, suggesting that the Dsl1p-coatomer interaction might destabilize the polymerized coat (Zink et al., 2009). Downregulation of the Dsl1 gene leads to an accumulation of COPI and COPII coated vesicles in cells. Based on this data a model has been proposed, in which Dsl1p facilitates uncoating by a direct interaction with coatomer subunits and might even be the factor initiating the uncoating event once the vesicle has been tethered to the ER membrane. This specific interaction between Dsl1p and coatomer was further proposed to prevent repolymerisation of the COP-subunits and thus facilitate coat disassembly (Zink et al., 2009).

On the basis of these data in the literature, the goals of my thesis were a biochemical analysis of the role of ArfGAP1, ArfGAP2 and ArfGAP3 in COPI vesicle biogenesis. To this end, the following issues were addressed:

1. Determining the kD-values for the interaction between the four coatomer isoforms and the three ArfGAPs.
2. Influence of the conformational state of the COPI coat on its affinity for ArfGAPs.
3. Effect of type I transmembrane protein p23 on ArfGAP activity.
4. Establishing a real-time assay with single molecule sensitivity to monitor the dynamics of COPI coat disassembly.

2 Results

2.1 Cloning, Expression and Purification of S-tagged ArfGAPs

2.1.1 Cloning and expression of S-tagged ArfGAPs

One of the goals of this thesis was to study the interactions of ArfGAP1, ArfGAP2 and ArfGAP3 with the four different coatomer isoforms. In order to address a potential difference in affinity of the ArfGAPs for the coatomer isoforms, a detection method was required, which recognizes all three GAPs with the same efficiency. For this purpose, ArfGAP1, ArfGAP2 and ArfGAP3 were recloned in such a way that they contain a S-tag. This tag allows a direct detection of the protein of choice with a secondary antibody coupled to horseradish peroxidase. ArfGAP1, ArfGAP2 and ArfGAP3 were previously cloned in a pFastBacHTB vector (Weimer et al., 2008). The S-tag was ordered as a synthetic oligomer and cloned in the ArfGAP containing pFastBacHTB vector via SfoI and Bam HI. This resulted in a vector containing first a S-tag and then a His-tag prior to the N-terminus of the ArfGAPs. In order to express S-tagged ArfGAP1, ArfGAP2 and ArfGAP3 in a baculoviral expression system, Sf9 cells were infected with the corresponding amount of P2 virus (for preparation of the virus see Materials and Methods). The insect cells were then incubated for 72h at 27°C and the cell pellets, containing the expressed protein, were harvested (Figure 2.1).

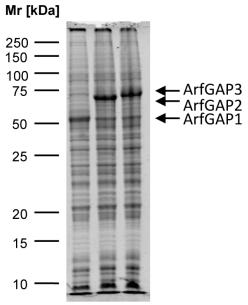

Figure 2.1: Expression of S-tagged ArfGAP1, 2 and 3 in a baculo virus expression system. After 72-hour infection of Sf9 cells with a virus stock containing S-tagged ArfGAP1, 2 and 3, the cells were harvested and a fraction was lysed and loaded on a SDS-PAGE to test the expression efficiency. Bands appear at the corresponding molecular weight of S-tagged ArfGAP1, 2 and 3.

2.1.2 Purification of S-tagged ArfGAPs

After lysis of the Sf9 cells, the protein containing supernatant was separated from the cell debris by a centrifugation step. The protein was then purified by Immobilized Metal Affinity Chromatography (IMAC) purification and a subsequent gel filtration step on a Superdex200 column (for more details see Materials and Methods). All three S-tagged ArfGAPs displayed no differences from the His-tagged ArfGAPs described in (Weimer et al., 2008) in terms of

their behavior during the purification. Figures 2.2 to 2.5 show representative purifications of S-tag ArfGAP1, ArfGAP2 and ArfGAP3.

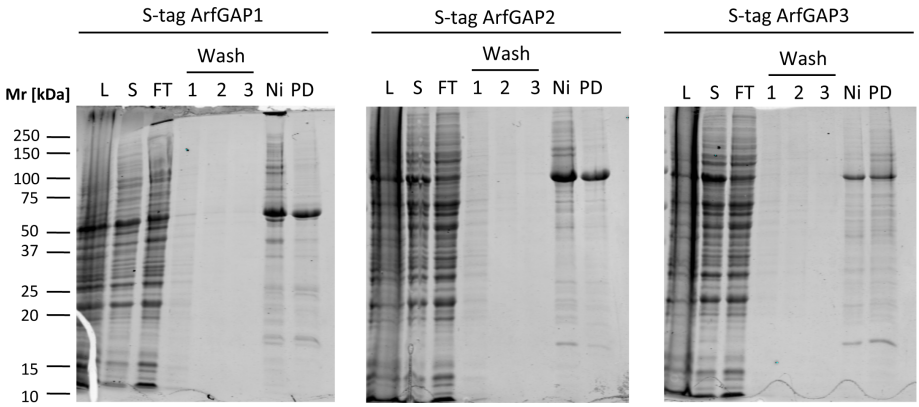

Figure 2.2: Purification of S-tag ArfGAP1, ArfGAP2 and ArfGAP3. S-tagged ArfGAPs were purified via Immobilized Metal Affinity Chromatography (IMAC). Equal volumes of the different purification steps were loaded on a 12 % SDS gel and separated by SDS gel electrophoresis. Staining was performed with coomassie brilliant blue. L= Lysate, S= supernatant after 100 000 x g ultracentrifugation, FT= flow through after incubation with Ni-Sepharose, 1, 2, 3= washing steps, Ni= pool after elution from Ni-Sepharose, PD= final pool after buffer exchange on a PD10 column.

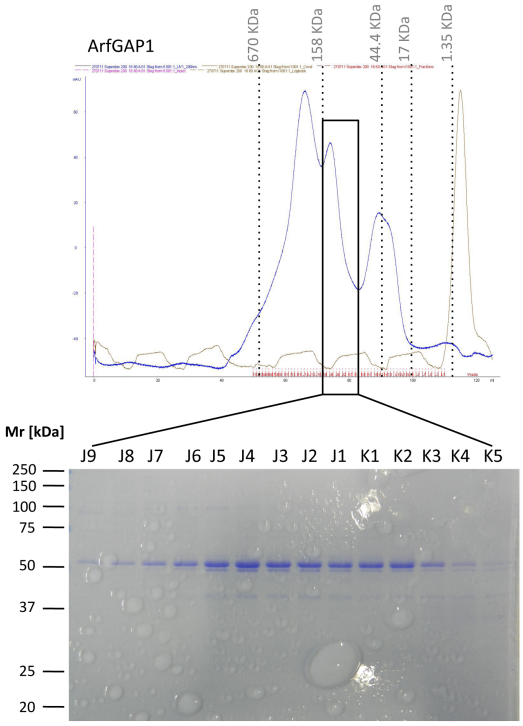

Figure 2.3: Gel filtration of S-tag ArfGAP1. The PD pool of IMAC-purified S-tag ArfGAP1 was further purified via size exclusion chromatography on a Superdex200 column. Fractions corresponding to S-tag ArfGAP1 were separated by SDS-PAGE on a 12 % gel and stained with coomassie brillian blue. Dashed lines correspond to the peaks of standard proteins. Black box indicates fractions loaded on the gel.

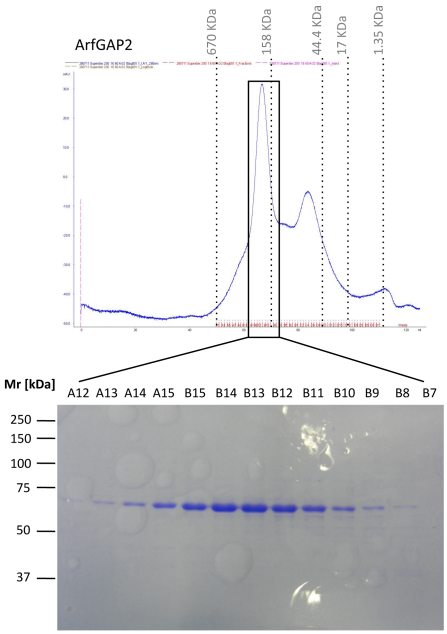

Figure 2.4: Gel filtration of S-tag ArfGAP2. The PD pool of IMAC-purified S-tag ArfGAP1 was further purified via size exclusion chromatography on a Superdex200 column. Fractions corresponding to S-tag ArfGAP2 were separated by SDS-PAGE on a 12 % gel and stained with coomassie brillian blue. Dashed lines correspond to the peaks of standard proteins. Black box indicates fractions loaded on the gel.

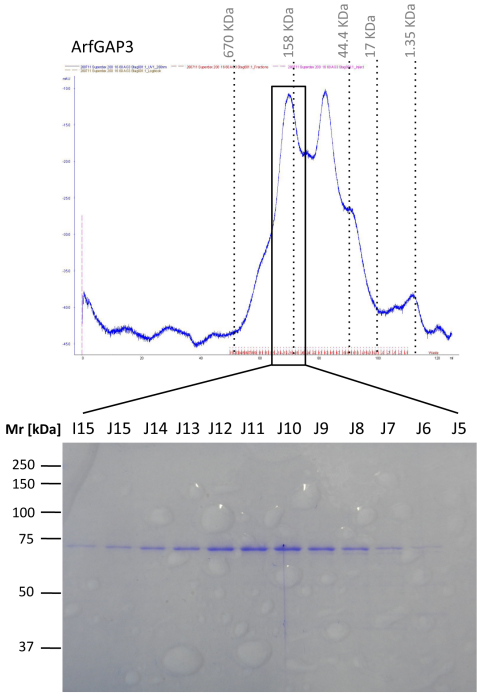

Figure 2.5: Gel filtration of S-tag ArfGAP3. The PD pool of IMAC-purified S-tag ArfGAP1 was further purified via size exclusion chromatography on a Superdex200 column. Fractions corresponding to S-tag ArfGAP3 were separated by SDS-PAGE on a 12 % gel and stained with coomassie brillian blue. Dashed lines correspond to the peaks of standard proteins. Black box indicates fractions loaded on the gel.

2.1.3 Functionality test of the S-tagged ArfGAPs

To make sure that the addition of the S-tag did not compromise the functionality of ArfGAP1, 2 and 3, we performed a tryptophane fluorescence based binding assay. To this end, we prepared liposomes with Golgi-like composition (for details see Materials and Methods) and incubated them with Arf1, coatomer and GTP. GDP to GTP exchange within Arf1 was triggered by the addition of EDTA and monitored as change in tryptophan fluorescence. Upon the conformational change of Arf1 associated with GTP binding, a conserved tryptophan in switch region one gets exposed and an increase in tryptophane fluorescence was observed. Once a plateau was reached, the GTP state was stabilized by the addition of $MgCl_2$ and uncoating was subsequently triggered by the addition of ArfGAP. The GTP to GDP exchange resulted then in a decrease in tryptophan fluorescence. As depicted in Figure 2.6, the addition of the S-tag did not alter the functionality of ArfGAP1, 2 and 3.

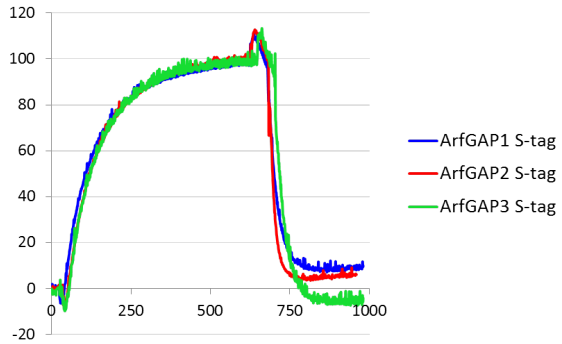

Figure 2.6: S-tagged ArfGAPs are able to hydrolyse GTP within Arf1. The functionality of the S-tagged ArfGAPs was probed in a tryptophane fluorescence based assay. Liposomes of Golgi-like composition were incubated with Arf1, coatomer, GTP and EDTA in a quartz cuvette. The GDP to GTP exchange within Arf1, triggered by EDTA, leads to a conformational change within the protein and to the exposure of a tryptophane within switch region 1. Thus, the measured tryptophane fluorescence increases. Upon the addition of 50nM ArfGAP, GTP is hydrolysed and tryptophane fluorescence signal decreases again.

2.2 Differential interactions of ArfGAP1/2/3 with coatomer isoforms

One of the initial goals of this thesis was to investigate potential differences in the functions of ArfGAP2 and ArfGAP3. While different roles of ArfGAP1 on one side and ArfGAP2/3 on the other side were reported in the literature, up to date no functional difference between ArfGAP2 and ArfGAP3 were described. One aspect, which has not been addressed so far, is a potentially differential interaction of the three ArfGAPs with the four coatomer isoforms.

2.2.1 Analysis of ArfGAP interactions with coatomer isoforms by ELISA

In order to investigate coatomer- ArfGAP interactions, we have established an enzyme-linked immonosorbent assay (ELISA)-like assay. In this assay, specific coatomer isoforms were immobilized on a surface and subsequently the individual ArfGAPs were added in solution. Binding of ArfGAPs was detected by an anti-ArfGAP specific primary antibody and visualized by a secondary antibody coupled to horseradish peroxidase (HRP). In these experiments we determined dissociation constants (K_D-values) in the low micromolar range for the ArfGAP-coatomer interaction. We observed a preference of all three ArfGAPs for the γ1-isoforms (Figure 2.7). ArfGAP1 displayed the highest affinity for all four coatomer isoforms (0.1-0.6μM) followed by ArfGAP2 (0.5-1.2μM). ArfGAP3 showed the weakest interaction (1.2-4.3μM).

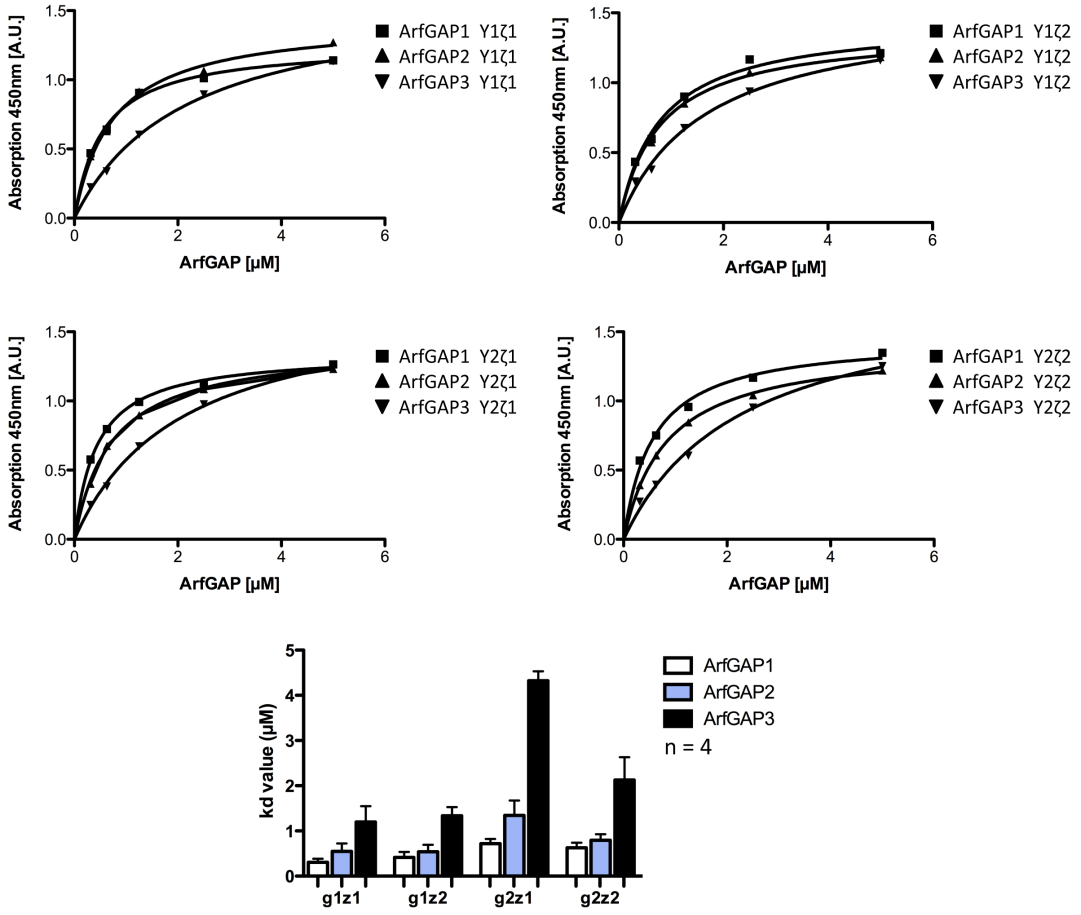

Figure 2.7: Differential interactions between the ArfGAPs and coatomer isoforms. 96-well plates were coated with recombinant coatomer isoforms. Subsequently, the wells were incubated with ArfGAPs and then anti-ArfGAP antibodies. Detection was performed via secondary antibodies coupled to HRP and addition of 3,3´,5,´5-Tetramethylbenzidine. After measurement of the fluorescence at 450nm, the absorbance values were plotted against the ArfGAP concentration. For the analysis, one site binding hyperbola model was fitted. The obtained k_D values were plotted as a bar diagram. (N=4)

2.3 Effect of coatomer conformation on ArfGAP affinity

Another aspect studied in this thesis is the mode of recruitment of ArfGAP2 and 3 from the cytosol to the Golgi membrane. While it was shown earlier that ArfGAP2 and 3 depend on coatomer for their association with the Golgi membrane (Weimer et al., 2008), the spatial and temporal regulation of this process remains unknown. In one model, ArfGAP2 and 3 bind to soluble coatomer already in the cytosol and are recruited *en block* with the heptameric complex to Golgi membranes. In another model, ArfGAP2 and 3 are recruited only once coatomer has polymerized on the donor membrane and the corresponding binding site was formed. In order to address this mechanistic question, we utilized an ELISA-like binding assays as well as a conventional pull down assay.

2.3.1 Effect of coatomer conformation on ArfGAP affinity studied by ELISA-like assay: direct immobilization of coatomer

To quantitatively analyse the interactions between the three ArfGAPs and coatomer, we used a modified version of the ELISA-like binding assay described above. As ArfGAP2 and ArfGAP3 show 49,6 % protein sequence identity and have a single homologue in yeast, Glo3 (Frigerio et al., 2007), we used ArfGAP2 in most of the assays as a representative of both ArfGAP2 and ArfGAP3. The most abundant coatomer isoform *in vivo* is γ1ζ1 and thus only the affinity of ArfGAPs to this particular isoform was assessed.

Coatomer was immobilized on a polystyrene surface directly. In order to change the conformation of coatomer to a conformation resembling the one on a COPI vesicle, the coatomer coated plate was incubated with peptides corresponding to the cytoplasmic tails of p23 dimer, which was shown previously to induce a conformational change in coatomer (Langer et al., 2008; Reinhard et al., 1999). As a negative control we used a C-terminal peptide of the ER resident protein Wbp1, a type I glycosyltransferase. In the next step, ArfGAP1, 2 (or 3) was added to the polymerized or non-polymerized coatomer samples. Bound ArfGAPs were detected using a primary antibody directed against ArfGAP1, 2 or 3 and a secondary antibody conjugated to HRP. The determined k_D values of ArfGAP1, 2 and 3 for both coatomer treated with p23 and coatomer treated with Wbp1 were in the low micromolar range (Figure 2.8). In this *in vitro* system, no significant differences in the dissociation constants were observed.

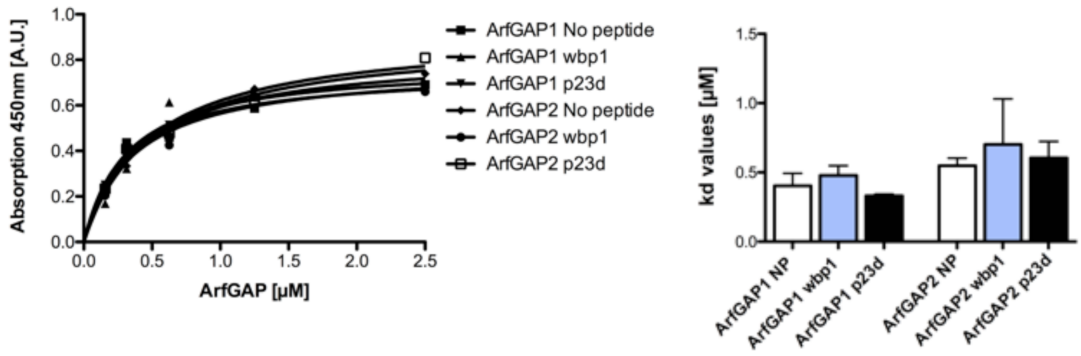

Figure 2.8: Effect of the conformational state of coatomer on ArfGAP activity: direct immobilization of coatomer. 96-well plates were coated with recombinant coatomer of the isoform γ1ζ1. Subsequently, the wells were incubated with dimeric p23 peptide in order to alter the coatomer conformation or dimeric Wbp1 peptide or no peptide as a control. In the next step the different ArfGAPs and anti-ArfGAP antibodies were added. Detection was performed as described in Figure 2.7. Absorbance values were plotted against the ArfGAP concentration. For the analysis, one-site binding hyperbola model was fitted. Dissociation constants (k_D) were determined by fitting one-site binding hyperbola model and plotted as a bar diagram. (N=3)

2.3.2 Effect of coatomer conformation on ArfGAP affinity studied by ELISA-like assay: immobilization of coatomer via CM1

One potential limitation of the direct immobilization of coatomer is that the conformational change within coatomer might not take place as efficiently on the surface as it does in solution. In addition, the interaction with the polystyrene plate could lead to a perturbation of the functionality of coatomer. In order to select one specific orientation of coatomer and immobilize the protein more gently, we first coated the 96-well plate with CM1, a structure-specific antibody against fully assembled coatomer, and then added coatomer in a second step.

For this purpose, we recloned the ArfGAPs and added an S-tag to allow their direct detection with a HRP substrate (for more details see 2.1). Here, we measured significantly higher k_D values in comparison to the ones measured in the set up based on direct coatomer immobilization (compare Figure 2.8 to Figure 2.9). In order to exclude a possibility that the addition of the S-tag has an effect on binding, we performed the experiment described in 2.2 with the S-tagged ArfGAPs. Here, the 96-well plates were coated only with the coatomer isoform γ1ζ1. In the set up relying on direct immobilization (Figure 2.10), the S-tagged ArfGAPs displayed k_D values similar to the ArfGAPs lacking the S-tag. However, upon coatomer immobilization via CM1, both ArfGAP1 and ArfGAP2 displayed higher k_D values and thus significantly lower affinity for coatomer (Figure 2.11). Thus, it is possible that either the CM1 antibody masked the ArfGAP binding sites in coatomer or that the concentration of immobilized coatomer in these set-ups was lower than in the set-up relying on direct

immobilization. Thereby, this experimental approach proved not to be suitable to address the question of interest.

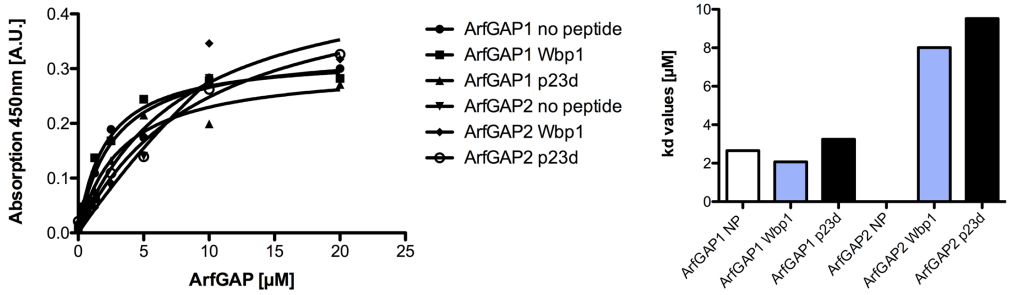

Figure 2.9: Effect of the conformational state of coatomer on ArfGAP activity: coatomer immobilization via CM1. 96-well plates were coated overnight with 100µL of CM1 antibody, generated from hybridoma supernatant. Subsequently, the wells were incubated with coatomer of the γ1ζ1 isoform and the three individual ArfGAPs. Detection was performed with HRP substrate and the plate was measured at 450nm. The absorbance values were plotted against the ArfGAP concentration. For the analysis, one-site binding hyperbola model was fitted (N=2). NP= no addition of peptide. No k_D constant could be calculated for the sample containing ArfGAP2 and no peptide.

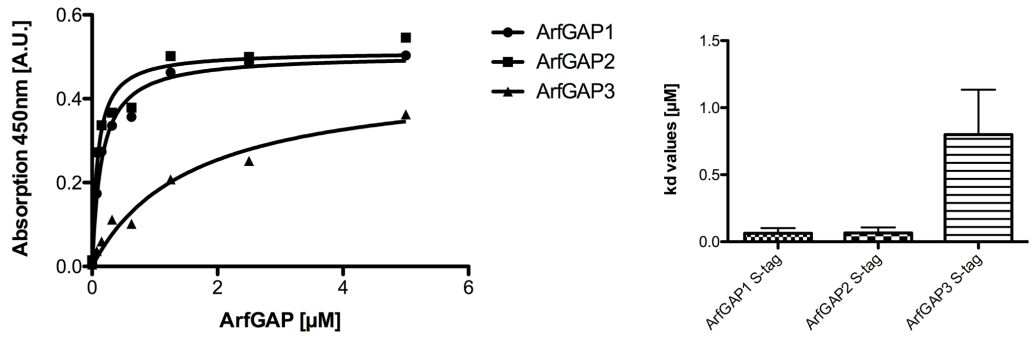

Figure 2.10: Affinity of S-tagged ArfGAPs for coatomer: direct coatomer immobilization. 96-well plates were coated overnight with 10pmol of purified coatomer of the γ1ζ1 isoform. Subsequently, the wells were incubated with the individual S-tagged ArfGAPs and in a second step with anti-ArfGAP antibodies. The detection and evaluation was performed as described in Figure 2.7. (N=2)

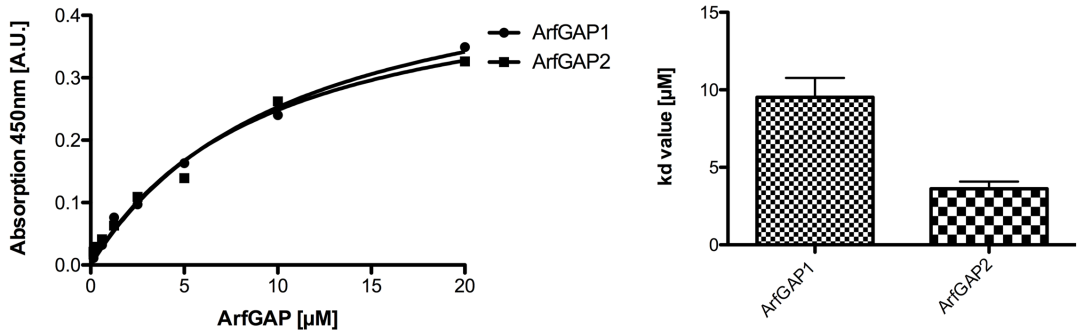

Figure 2.11: Affinity of S-tagged ArfGAPs for coatomer: coatomer immobilization via CM1. 96-well plates were coated overnight with 100µL of CM1 antibody generated from hybridoma supernatant. Subsequently, the wells were incubated with coatomer of the γ1ζ1 isoform and the three different ArfGAPs. Detection was performed with HRP substrate and the plate was measured at 450nm. The absorbance values were plotted against the ArfGAP concentration. For the analysis, one-site binding hyperbola model was fitted. (N=2)

2.3.3 Effect of coatomer conformation on ArfGAP affinity analysed in a pull down assay

Another approach to assess the interaction between the ArfGAPs and coatomer, depending on coatomer conformation state, was a conventional pull down set-up. Here, we used two independent experimental designs.

In the first set-up, One-STrEP-tag coatomer was immobilized on streptactin beads via its One-STrEP-tag located in α-COP and subsequently polymerized via the addition of dimeric p23. ArfGAP2 was added in the last step. To account for potential reversibility of the conformational change, we performed the experiment with and without washing away of the dimeric p23 meaning that the incubation with ArfGAP2 was performed either in the absence or presence of p23 dimer. The dimerized cytoplasmic tail of Wbp1 was used as a control. We did not detect a difference in the ArfGAP affinity for coatomer between the sample containing dimeric p23 and the sample containing the control peptide Wbp1 (Figure 2.12, upper panel). A possible drawback of this experimental set-up is that coatomer polymerization might not be as effective after binding to the beads as in solution. It was previously shown that the conformational change involves at least α-COP and γ-COP (Langer et al., 2007), and the One-STrEP-tag is located on the α-COP subunit, thus potentially preventing the interaction with the peptide.

In the second set-up, we tried to circumvent this potential limitation by first inducing the conformational change in coatomer in solution and then immobilizing the protein via its One-STrEP-tag on streptactin beads. Here, the incubation with ArfGAP was performed again either in the presence of dimeric p23 or after washing the peptide away. In this system, we observed a higher affinity of ArfGAP2 for coatomer in the absence of p23, however, only

under condition including p23 dimeric peptide throughout the entire experiment (Figure 2.12, lower panel). This result might be due to a reversible conformational change in coatomer as well as to a direct effect of the p23 cytoplasmic tail with ArfGAP2. One further possibility is that the polymerization in solution and the subsequent immobilization on the streptactin beads compromises coatomer functionality and thus its affinity for ArfGAP.

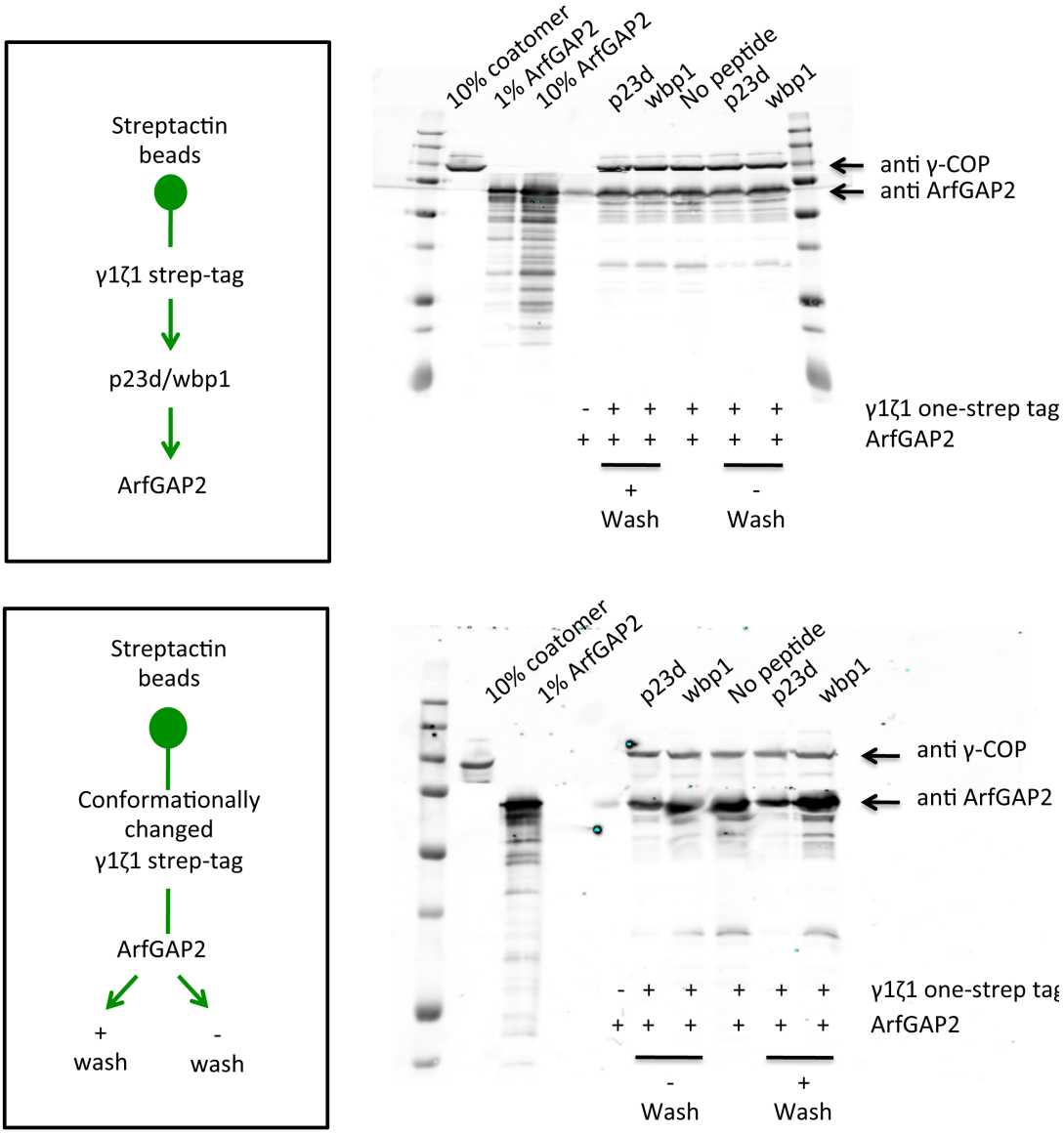

Figure 2.12: Affinity of ArfGAPs for polymerized versus soluble coatomer.
Upper panel: One-STrEP-tagged coatomer was immobilized via the OneStrepTag on streptactin beads. The conformation of coatomer was altered to the polymerized form via the addition of dimeric p23. Wbp1 in its dimeric form was used as a control. Incubation with ArfGAP2 was performed either in the absence or presence of the peptides.
Lower panel: Polymerization of coatomer was induced in solution via the addition of dimeric p23. The control sample was treated with dimeric Wbp1. Coatomer was then coupled to streptactin beads via its OneStrepTag. The incubation with ArfGAPs was performed either in the presence or absence of excessive peptide. Proteins bound to the beads were analysed by SDS PAGE and western blot. N=3

2.4 Effect of p23 on the activities of ArfGAP1 and ArfGAP2

2.4.1 Effect of p23 on ArfGAP activity assessed by Tryptophan Fluorescence and SLS

Previous studies reported an inhibiting role of both p23 and p24 on ArfGAP1 (Lanoix et al., 2001). In order to investigate if the cytoplasmic tail of p23 acts directly on the Arf1 activation/deactivation cycle, we performed tryptophane fluorescence assays. This liposome-based system utilizes the increase/decrease in tryptophane fluorescence in order to monitor the nucleotide-dependent conformational change in Arf1.

Here, we investigated the effect of p23 lipopeptide on the rate of ArfGAP-mediated GTP hydrolysis in Arf1. For this purpose, we extruded liposomes with a Golgi-like composition through polystyrene filters with a pore size of 100nm. This pore size was chosen due to the curvature sensitivity of ArfGAP1 (Bigay et al., 2003). In the first step, we compared the absolute activities of ArfGAP1 and ArfGAP2 on GTP hydrolysis within Arf1. 100nm liposomes with a Golgi-like composition were incubated with Arf1, coatomer and GTP. Nucleotide exchange was triggered by the addition of EDTA, which chelates the Mg^{2+} ions stabilizing the phosphate groups, and thus allows GDP release and binding of the more abundant GTP, which then results in an increase in tryptophane fluorescence. Once a plateau was reached, the GTP state was locked by the addition of excess Mg^{2+}. Subsequently, ArfGAP was added and the rate of hydrolysis was monitored by the decrease in tryptophane fluorescence (for more details see Materials and Methods). As shown in Figure 2.13, ArfGAP2 displayed higher activity than ArfGAP1 under these conditions. Still, 100nm liposomes were used for further experiments.

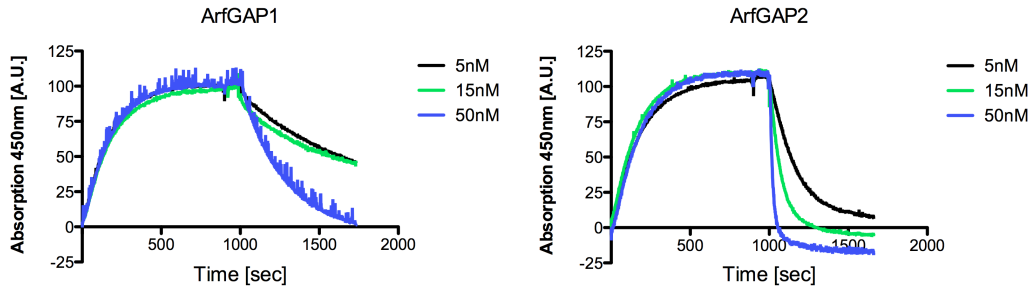

Figure 2.13: Activities of ArfGAP1 and ArfGAP2 on GTP hydrolysis within Arf1. An optical tryptophane fluorescence assay allows monitoring of the activities of ArfGAP1 and ArfGAP2 on GTP hydrolysis within Arf1. The increase in tryptophane fluorescence corresponds to exchange of GDP with GTP, which was chemically triggered by the addition of EDTA. The decrease in fluorescence reflects the extent of GTP hydrolysis triggered by ArfGAP1 or ArfGAP2.

In order to test if the cytoplasmic tail of p23 exhibits an effect on the ArfGAP mediated GTP hydrolysis, Golgi-like liposomes were prepared in the presence of p23 lipopeptide. As p23 is a transmembrane protein, this approach is closer to the *in vivo* situation than the set-up utilizing soluble peptide. The experiment was performed in the presence of ArfGAP2 as described above. Here, the activity of ArfGAP2 seemed to be enhanced in the presence of p23 lipopeptide (Figure 2.14). However, the GDP to GTP exchange was also reduced in the absence of the lipopeptide, which makes it difficult to interpret these results.

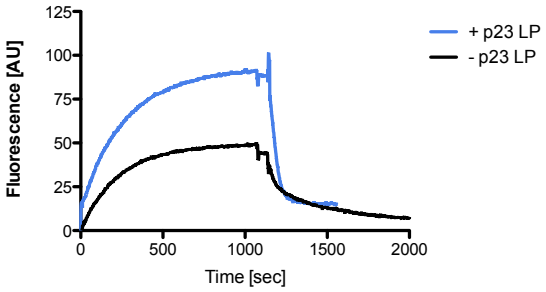

Figure 2.14: Activity of ArfGAP2 in the presence of p23 lipopetide. The activity of ArfGAP2 depending on the presence of p23 lipopetide was assessed in a tryptophan fluorescence assay in the presence of coatomer. Liposomes with Golgi-like composition were prepared in the presence or absence of p23 lipopeptide, extruded through 100nm polystyrene filters and loaded with Arf1 in the presence of EDTA. After addition of $MgCl_2$, which stabilizes the GTP-bound state of Arf1, GTP hydrolysis induced by ArfGAP2 was followed by the decrease in thryptophane fluorescence. N=2.

In order to test the effect of the p23 cytoplasmic tail on ArfGAP mediated COPI vesicle uncoating, we utilized a static light scattering assay. For this purpose, liposomes, Arf1, coatomer and GTP were incubated at 37°C and GDP to GTP exchange was triggered chemically by the addition of EDTA. Arf1-GTP was stabilized by the addition of $MgCl_2$, and GTP hydrolysis was induced by the addition of ArfGAP1 or ArfGAP2. Light scattering (excitation at 350nm, emission at 350nm) allows monitoring of an increase in mass, corresponding to coating, and subsequent decrease in mass during uncoating. Golgi-like liposomes were prepared in the presence of p23 lipopetide as described above. Uncoating was triggered either by 1nM ArfGAP1 or 1nM ArfGAP2. As shown in Figure 2.15, the addition of p23 lipopeptide affected both the coating and the uncoating step. Coat recruitment was increased in the presence of p23 lipopetide. The activities of ArfGAP1 and ArfGAP2 were influenced in a different manner. Whereas the activity of ArfGAP1 was slightly inhibited by p23 lipopeptide, the activity of ArfGAP2 was strongly enhanced.

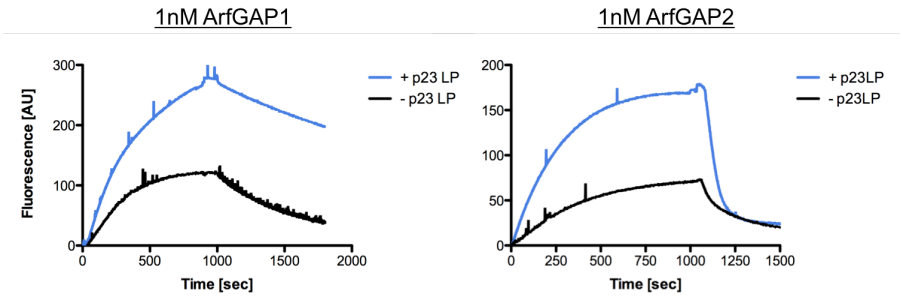

Figure 2.15: Uncoating activities of ArfGAP1 and ArfGAP2 in the presence of p23 lipopeptide. Uncoating activities of ArfGAP1 and ArfGAP2 depending on the presence of p23 were assessed in a static light scattering assay. Liposomes (100nm) with Golgi-like composition were prepared in the presence or absence of p23 lipopeptide and loaded with Arf1 and coatomer in the presence of EDTA. After addition of $MgCl_2$, GTP hydrolysis induced by ArfGAP1 or ArfGAP2 was followed by the decrease in static light scattering. N≤ 5, here is shown one representative concentration for ArfGAP1 and ArfGAP2.

The presence of p23 lipopeptide resulted in a three times higher mass recruitment. To test if this effect is due to more efficient recruitment of coatomer resulting from the increased nucleotide exchange within Arf1, we utilized the tryptophane fluorescence set up described above. We performed the experiment either in the absence or in the presence of coatomer. In samples not containing coatomer, the difference in the plateau in the presence or absence of p23 lipopeptide decreased from 3 to 1.4 (Figure 2.16).

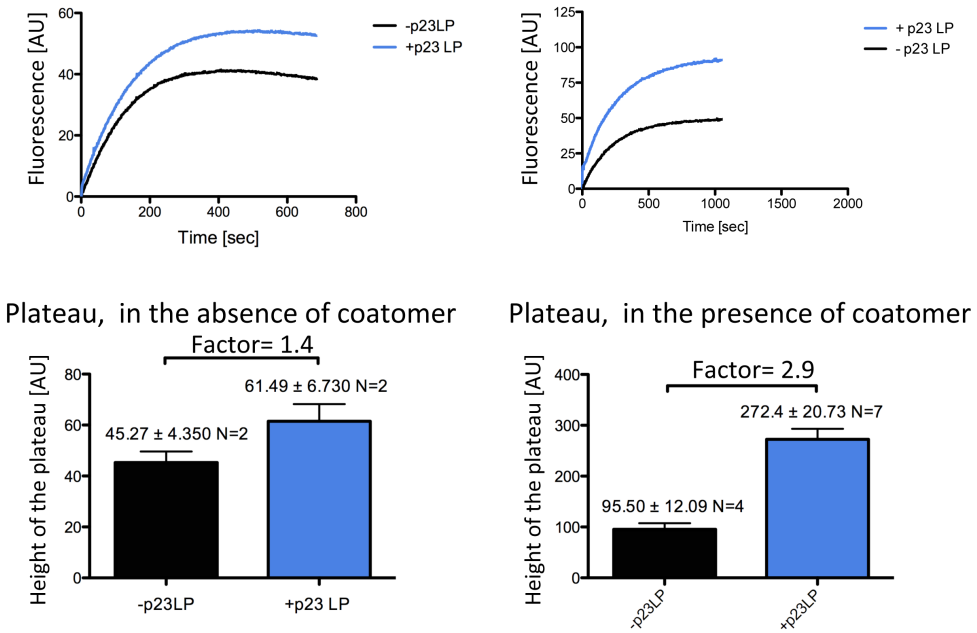

Figure 2.16: Nucleotide exchange is increased in the presence of p23 lipopetide. Liposomes (100nm) with Golgi-like composition were prepared in the presence or absence of p23 lipopeptide and loaded with Arf1 (left panels) or Arf1 and coatomer (right panels) in the presence of EDTA. The height of the plateau was quantified and the obtained absolute values were plotted as a bar diagram. (N≤2).

The experimental results shown in Figure 2.16 indicate that there might be a less efficient recruitment of coatomer to the liposomes in the absence of p23 lipopetide. To test this possibility, we performed a float up experiment. To this end, we incubated liposomes, Arf1, coatomer, GTP and EDTA for 10min at 37°C and subsequently stabilized the GTP loaded state of Arf1 by the addition of $MgCl_2$. These samples were then adjusted to 47 % sucrose and transferred at the bottom of SW60 tubes. The 47 % bottom layer was overlayed with 44 % weight per weight (w/w) sucrose, followed by 41 % w/w sucrose and then HKM buffer (for details see Materials and Methods). Liposomes together with the membrane-bound material were floated up by a 90-min spin in a SW60 rotor at 50 000rpm (Figure 2.17, upper panel). The amount of bound material was quantified in a western blot. A 1.5 times increase with respect to both Arf1 and coatomer recruitment was detected.

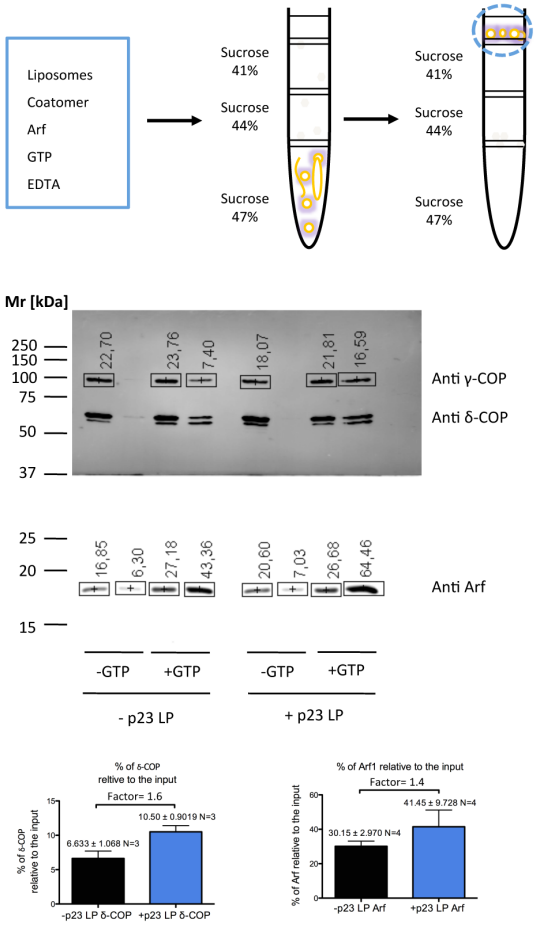

Figure 2.17: Recruitment of coatomer to liposomes of Golgi-like composition in the presence or absence of p23 lipopeptide. Liposomes (100nm) of Golgi-like composition were coated with Arf1 and coatomer. The bound material was then isolated on a sucrose gradient, shown schematically in the upper pannel. Amount of Arf1 and coatomer recruited to the liposomes in the presence or absence of the p23 lipopeptide was quantified and shown as a percentage of the input (lower panel, N≤3).

2.4.2 Effect of p23 on ArfGAP activity assessed by a radioactivity assay

Since the presence of p23 lipopeptide leads to a difference in the efficiency of Arf1 and coatomer recruitment to the liposomes, as found in both the tryptophane fluorescence and the light scattering assays, we attempted to establish a fluorescence-independent assay. For this purpose, we used radiolabeled nucleotide, which allows direct monitoring of GTP hydrolysis on Arf1. We applied a float up assay with radioactively labeled GTP. Golgi-like liposomes were prepared either in the presence or absence of p23 lipopeptide and extruded either through 30nm or through 100nm polystyrene filters. Upon recruitment of Arf1 and coatomer to the membrane in a 3H-GTP dependent manner, we isolated the membrane bound material via a sucrose gradient (see Figure 2.17 and Materials and Methods). The coated liposomes were then subjected to an incubation with ArfGAP1 or ArfGAP2 at 37°C, and samples were taken at 0, 2.5, 5, 10 and 15min. 3H-GTP was separated from 3H-GDP via thin layer chromatography and the radioactive signal was quantified in a ß-Imager. In this set-up, ArfGAP2 hydrolyzed higher amounts of GTP in the presence of the p23 lipopeptide than in the absence of the lipopeptide (Figure 2.18, middle and lower right panel). In contrast, the activity of ArfGAP1 was reduced in the presence of p23 lipopeptide (Figure 2.18, upper and lower left panel).

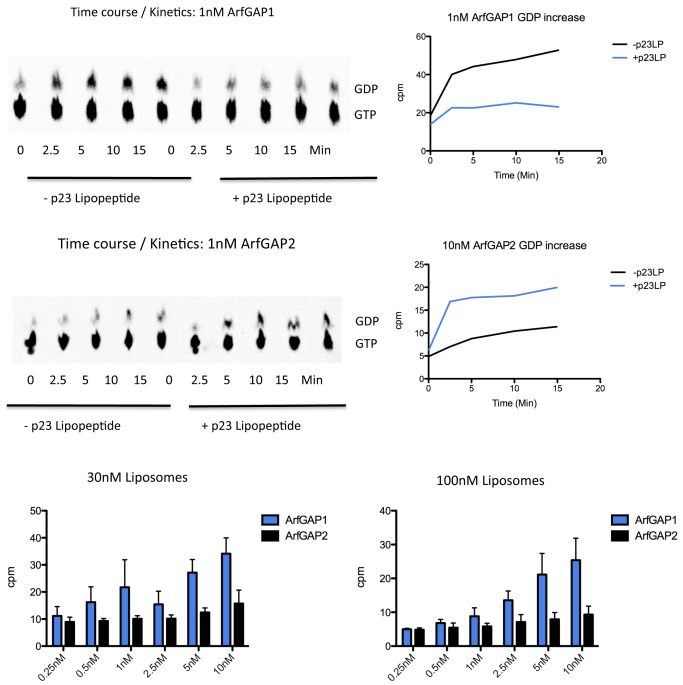

Figure 2.18: Analysis of the effect of p23 lipopetide on the activity of ArfGAP1 and ArfGAP2 in a radioactivity based assay. Liposomes of Golgi-like composition were extruded through a 30nm or 100nm filter, here a representative experiment performed with 100nm liposomes. Liposomes were subsequently coated with Arf1 and coatomer in the presence of 3H-GTP. The bound material was then isolated on a sucrose gradient. The degree of GTP hydrolysis exhibited by ArfGAP1 (upper panel) and ArfGAP2 (middle panel) was assessed via thin layer chromatography. The amount of GDP (cpm) dependent on the ArfGAP concentration added was plotted as a bar diagram (lower panel). N=2

To study the mechanism behind these differential effects, we tested if the higher activity is due to higher ArfGAP2 recruitment to the liposomes in the presence of p23 lipopeptide. To this end, we coated Golgi-like liposomes with Arf1 and coatomer. To prevent premature hydrolysis and potential ArfGAP2 disassembly, we performed the experiment in the presence of the non-hydrolyzable GTP analogue, GMP-PNP. Once coating was completed, ArfGAP2 was added to the samples for 10min at 37°C. The bound material was then isolated via the sucrose gradient described above. Only a slight difference in the efficiency of ArfGAP2 recruitment was observed depending on the absence or presence of p23 lipopeptide (Figure 2.19).

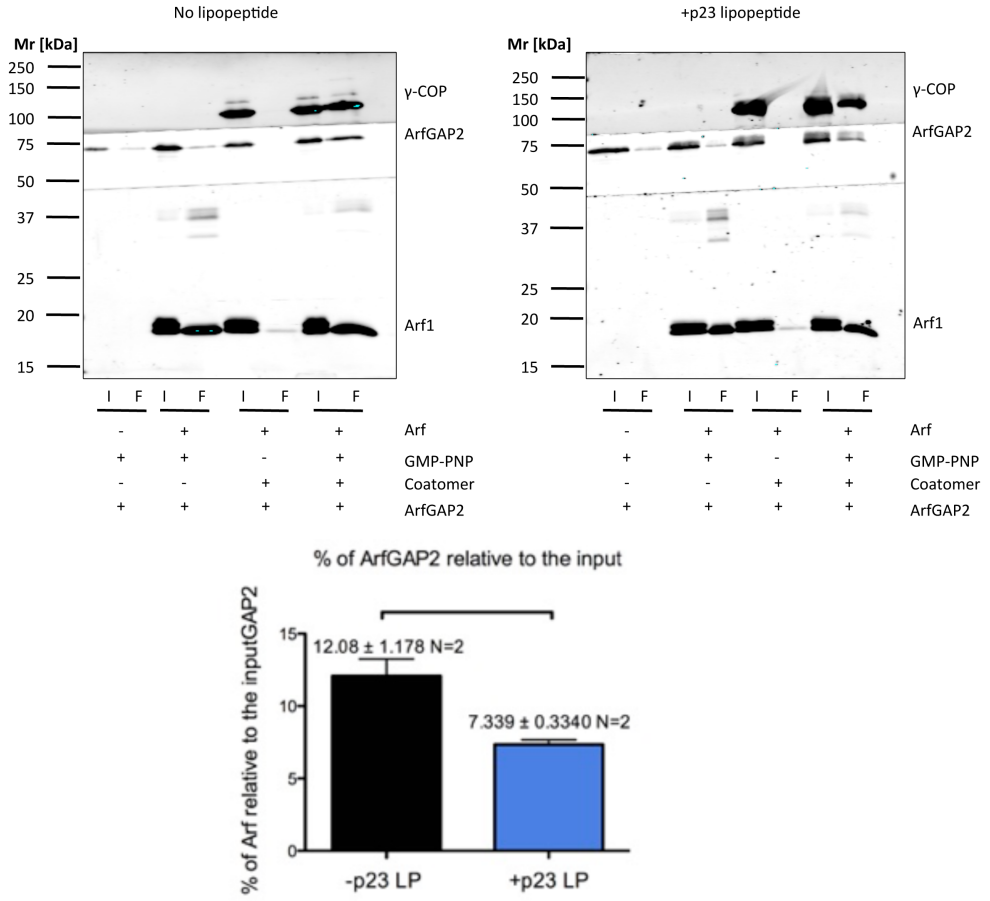

Figure 2.19: Recruitment of ArfGAP2 to liposomes of Golgi-like composition in the presence or absence of p23 lipoptide. Liposomes of Golgi-like composition were coated with Arf1 and coatomer in the presence of the non-hydrolyzable GTP analogue GMP-PNP. In a second step, the liposomes were incubated with ArfGAP2. The bound material was then isolated on a sucrose gradient. The degree of ArfGAP2 recruitment was quantified via western blot. N=2. I= Input, F= floated fraction, corresponding to liposomes and bound proteins.

2.5 ArfGAP1 and ArfGAP2 inhibit the formation of COPI vesicles in vitro

As some studies propose a role of ArfGAP1 as coat components (Lewis et al., 2004; Yang et al., 2002), we first tested the effect of the ArfGAPs on the yield of COPI vesicle. For this

purpose, we employed an *in vitro* vesicle preparation assay based on differential centrifugation using semi-intact cells as donor membranes (Adolf et al., 2013; Adolf and Wieland, 2013). Vesicle preparation was performed either in the presence or in the absence of ArfGAP1 and ArfGAP2. Vesicle yield was assessed by quantifying the amount of the membrane COPI markers Sec22b and p24, and controlled by blotting for the ER resident protein Calnexin, which is excluded from COPI vesicles. The amount of ArfGAP was titrated in a stochiometry of 0.05:1, 0.1:1 and 1:1 (molar ratio) to coatomer.

In contrast to previous reports (Lewis et al., 2004; Yang et al., 2002), we observed a decrease in the overall yield of COPI vesicles formed in the presence of ArfGAP1 or ArfGAP2 (Figure 2.20). This decrease displays a concentration-dependence and is more pronounced in the case of ArfGAP2 than in the case of ArfGAP1. These findings argue against a possible role of both ArfGAP1 and ArfGAP2 as coat components.

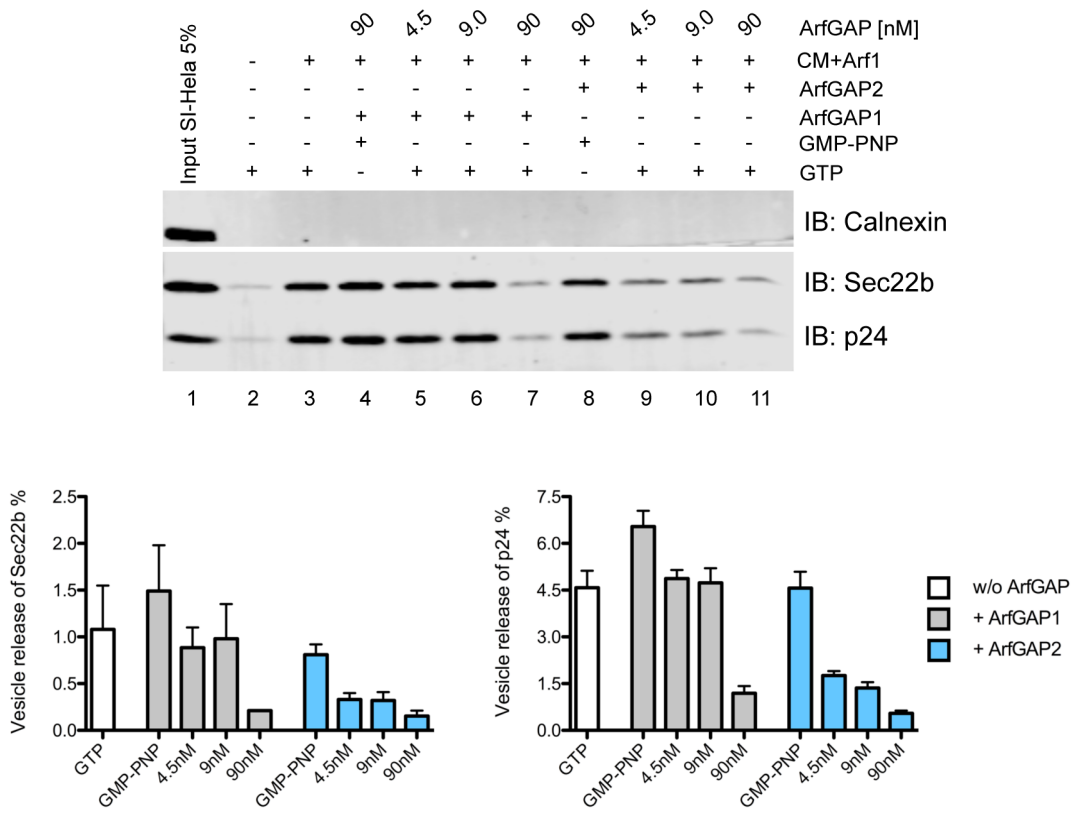

Figure 2.20: ArfGAP1 and ArfGAP2 inhibit the formation of COPI vesicles *in vitro*. COPI vesicle were formed in the presence of ArfGAP1 or ArfGAP2 by incubation of semi-intact cells with Arf1, coatomer and GTP as indicated. Newly formed vesicles were separated from donor membranes by differential centrifugation. 100 % of the vesicle fraction and 5 % of the semi-intact cells used for reconstitution (Input) were analyzed by western blotting for the presence of the non-cargo marker Calnexin and the two COPI cargo proteins Sec22b and p24 (upper panel). Vesicle yield was assessed by quantifying the COPI cargo proteins Sec22b and p24 utilizing the Li-Cor image studio (lower panels). Coat= Arf1 and coatomer. (N≤2, mean ± SD).

When ArfGAP was introduced from the beginning of the incubation, the number of the vesicles formed decreased with higher concentrations of ArfGAP. This could be due either to the GAP activity inhibiting vesicle formation, or to fusion of vesicles with endomembranes within the semi-intact cells, once they were formed and uncoated,. To assess a possible contribution of the latter mechanism to the yield of recovered vesicles, experiments in which ArfGAP was present during the formation of vesicles (time= 0-30min, Figure 2.21) were compared to conditions, in which ArfGAP was added after the initial formation of the vesicles (time= 30-60min, Figure 2.20). No significant change was observed between the two approaches (compare Figure 2.21, lane 10 with lane 7 (60min) and lane 3 (30min)), arguing against vesicle fusion playing a substantial role in the loss of vesicles observed in the presence of ArfGAP.

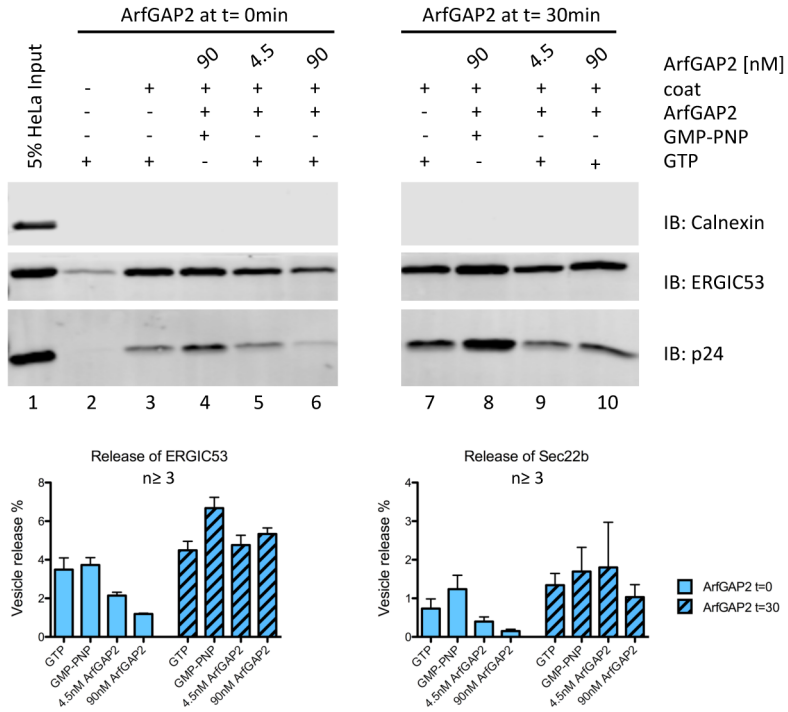

Figure 2.21: Formation of COPI vesicles *in vitro* in the presence of ArfGAP1 or ArfGAP2. Upper panel: COPI vesicle were generated *in vitro* from semi-intact cells in the presence of ArfGAP1 or ArfGAP2, and isolated by differential centrifugation. 100 % of the vesicle fractions and 5 % of the semi-intact cells used for reconstitution (Input) were analyzed by western blotting for the presence of the non-COPI marker calnexin and the COPI membrane proteins Sec22b and p24.
Lower panels: Vesicle yield was assessed by quantifying the intensities of the Sec22b (N=2) and p24 (N=3) bands. Coat= Arf1 and coatomer.

2.6 Role of ArfGAP1 and ArfGAP2 in COPI coat disassembly

Previous studies have reported that the ArfGAPs are involved in uncoating (Reinhard et al., 2003; Tanigawa et al., 1993). However, it still remains controversial to what extent the

ArfGAPs are determinants of completing coat disassembly. A series of open questions still remains to be answered 1) Does GTP hydrolysis in Arf1 trigger coat disassembly?; 2) Are additional factors required for uncoating?; and 3) Do the coat components leave the membrane simultaneously?.

2.6.1 Experimental set up

In an attempt to answer the above-mentioned questions, we established an ensemble measurement with single molecule sensitivity, which is based on fluorescence cross correlation set-up. This system allows real time monitoring of COPI coat disassembly. Previous studies of the uncoating reaction have mostly utilized artificial membranes (Bigay and Antonny, 2005; Bigay et al., 2003; Rawet et al., 2010; Reinhard et al., 2003). Liposomes, however, do not provide the multiple interactions that the COPI coat undergoes with the variety of transmembrane proteins present in an endogenous vesicle. Although coatomer is recruited by an interaction with Arf1-GTP, once at the membrane coatomer can interact with the cytoplasmic tails of cargo receptors and cargo proteins. Furthermore, membrane-bound coatomer polymerizes and thereby coatomer-coatomer interactions contribute to coat stabilization. To take into account all these determinants of coat stability, we prepared COPI vesicles from endogenous membranes. For this purpose, Golgi-enriched fractions were isolated from rat liver (for details see Materials and Methods) and used them as donor membranes for COPI vesicle formation. In order to monitor the individual kinetics of Arf1 and coatomer, we coupled the two proteins to different fluorescent dyes.

To allow efficient labeling, Arf1 was first recloned in such a way that its unique cystein at position 159 was mutated to a serine residue and the C-terminal lysin (Position 181) was exchanged for a cystein (Beck et al., 2011a). The protein was then coupled to a maleimide reactive Alexa647. Coatomer was labeled with NHS-reactive ATTO488.

The single molecule set-up was based on a confocal microscope suited for fluorescence cross correlation spectroscopy (Figure 2.22). The emitted photons were first collected by the same objective, passed through a pinhole and then separated by a dichroic mirror. After filtering, the detection was performed in each channel on avalanche photo diodes (APDs). This allows monitoring of vesicle populations diffusing in and out of the focus. Each vesicle passing through the confocal volume generates a peak in the fluorescence trace (Figure 2.23). The height of this peak is mainly determined by four different factors: 1) the exact path of the fluoresce molecule through the focus; 2) the concentration of coat protein on the membrane; 3) the degree of labeling of the protein and 4) the brightness of the dye. Thus, a vesicle passing through the center of the excitation volume will give a higher signal than the same vesicle passing through the rim.

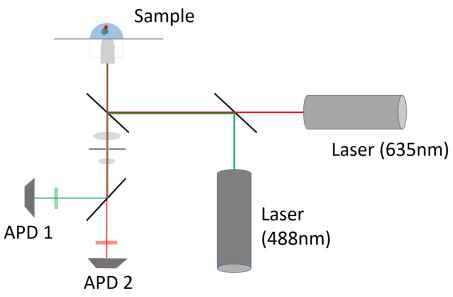

Figure 2.22: Confocal single molecule set-up. Fluorescence intensity traces were recorded with ms resolution with a LSM 710 microscope equipped with a confocor 3 and 488nm and 633 nm laser lines. Emitted photons were collected with the same objective, passed through a pinhole, separated by a dichroic mirror, and detected after filtering in each channel on avalanche photo diodes (APDs).

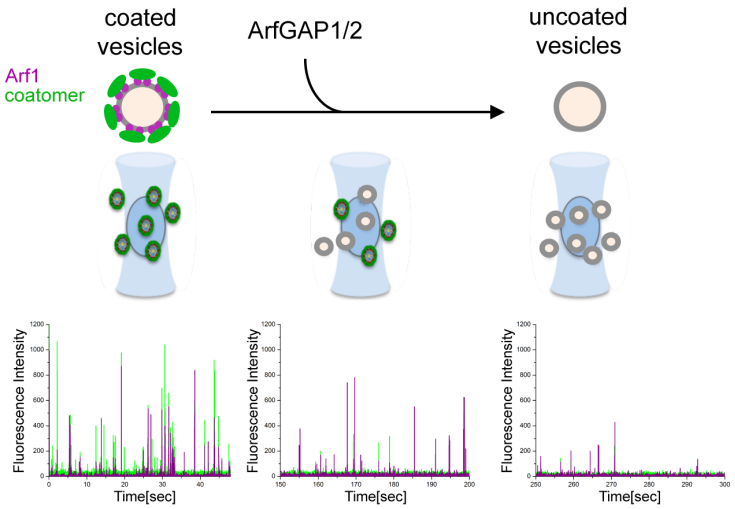

Figure 2.23: Experimental set up for the analysis of coat release. Schematic view of assessment of coat release from COPI coated vesicles. Fluorescent coat components are imaged with a confocal microscope equipped with avalanche photo diodes (APDs). Hour-glassed confocal volume is shaded in blue. Depending on their degree of coating, vesicles passing through the focus generate fluorescence intensity peaks.

In order to assess kinetics of coat disassembly, the raw data was subjected to a burst analysis (Figure 2.24). Burst analysis for all experiments was conducted utilizing custom scripts written in Matlab. Intensity traces were binned in 20 equally spaced time windows (length 15 seconds). A 0.9 percentile of the intensity values was chosen as a threshold to distinguish bursts (= vesicles containing bound coat proteins) from fluorescence background (= free proteis). The number of intensity values above the threshold was used as a measure for the number of peaks. As a second analysis approach, the average intensity above the threshold for both Arf1 and coatomer in each bin was calculated and used as a measure for the amount of vesicle-bound fluorophores. From this, we calculated for each bin the intensity ratio between red and green channels, which reports the relative abundance of both proteins

on the vesicles. The half-times for each component were calculated from a robust exponential decay fit and were displayed as decay constants.

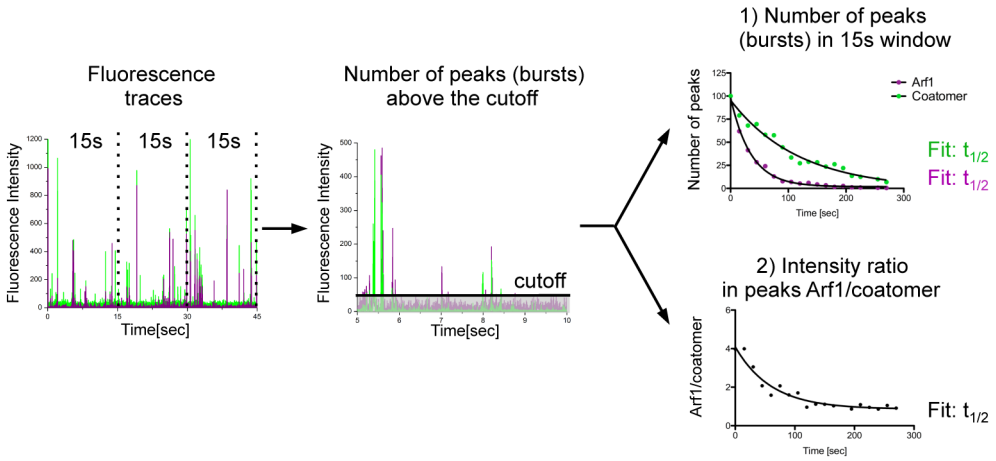

Figure 2.24: Scheme of data evaluation. After binning of the fluorescence trace in 15s time windows, the number of peaks in each bin above a 0.9 quantile (= cut-off) is determined. Results are displayed either as number of peaks (bursts) per bin for Arf1 and for coatomer, or as the intensity ratio in these peaks (IntArf1/Intcoatomer). Half-times were calculated from robust exponential decay fits.

2.6.2 GTP hydrolysis induced by ArfGAP1

COPI vesicles were prepared from rat liver Golgi membranes in the presence of Arf1-Alexa647, coatomer-ATTO488 and GTP, and stored at -80°C until shortly before the measurement. The vesicles were then imaged in a LSM 710 microscope equipped with a confocor 3 and 488nm and 633 nm laser lines. As shown in Figure 2.25 (upper panels) only a very slight change in fluorescence intensity was observed when the vesicles were imaged in the absence of ArfGAPs. This minor effect might be due to the internal GAP activity of the Golgi membranes as it was not the case in the vesicle sample generated with the non-hydrolysable GTP analogue, GMP-PNP (Figure 2.25, lower panels). After addition of full-length ArfGAP1, the fluorescence signal for both Arf1 and coatomer was reduced (Figure 2.25, left panels). This resulted in a decrease of the number of peaks (bursts) per time interval for Arf1 and for coatomer (Figure 2.26 middle panels) as well as in a decrease in the intensity ratio on the vesicles of Arf1 to coatomer (Figure 2.26 right panels). In incubations of COPI vesicles with 10nM ArfGAP1, Arf1 was fully released from the membrane after 150s, whereas coatomer was almost completely dissociated only after 250s. The faster release of Arf1 in comparison to coatomer might be explained by interactions, which coatomer undergoes in additional to those with Arf1 that keep coatomer membrane-associated. With increasing ArfGAP1 concentration, the rate of coat release increased accordingly (Figure 2.27). This data taken together shows that full length ArfGAP1 mediated GTP-hydrolysis in Arf1 is sufficient for complete COPI vesicle uncoating.

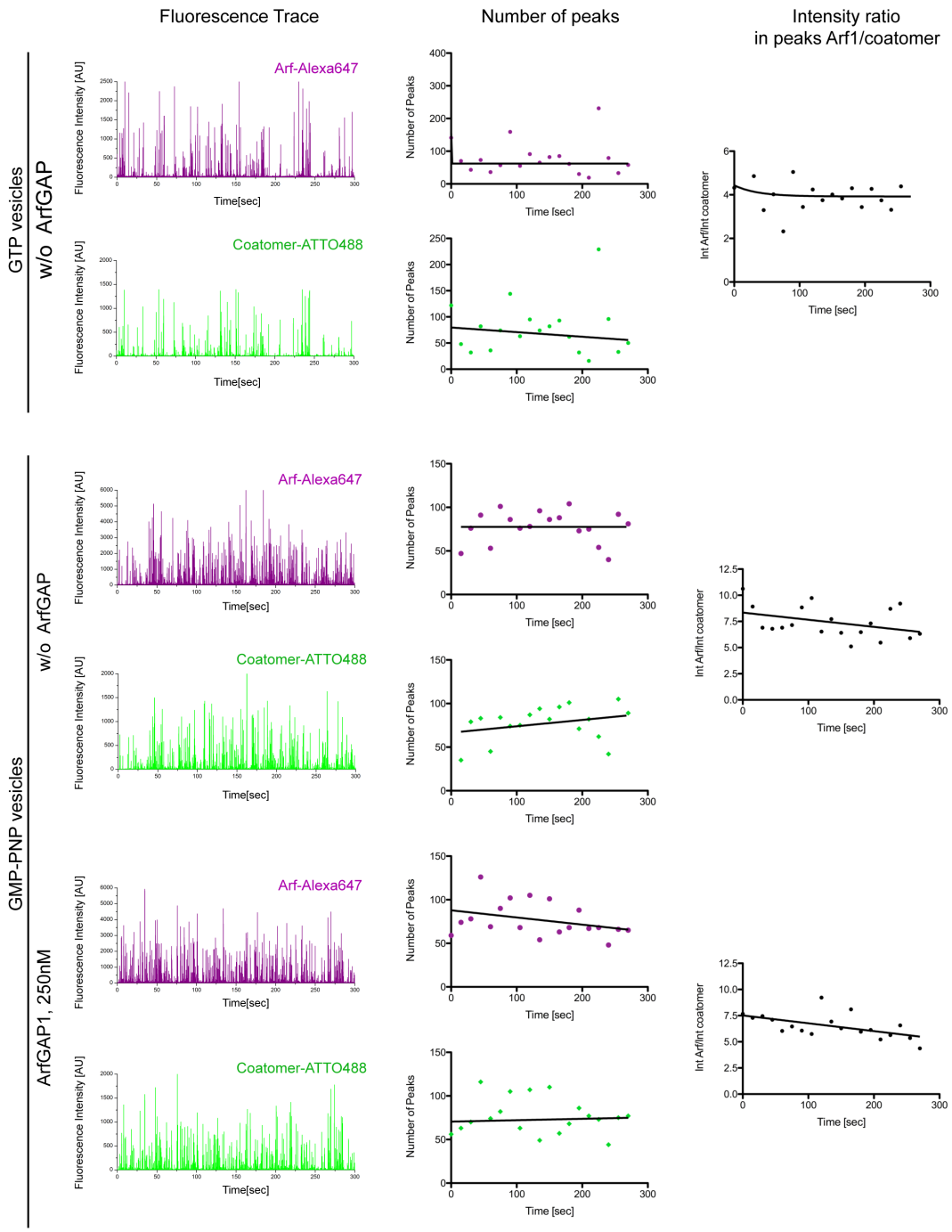

Figure 2.25: Release of the COPI coat: control experiments. Golgi-derived vesicles, coated with Arf1-Alexa647 and coatomer-ATTO488, prepared either with GTP or GMP-PNP, were imaged for 5 minutes in the absence or presence of ArfGAP1. Left panels show the fluorescence trace and middle panels the number of bursts per time interval for Arf1 and coatomer. Right panels show the relative intensity of Arf1-Alexa647 and coatomer-ATTO488 in the bursts, which reflects the relative abundance of both proteins on the vesicles.

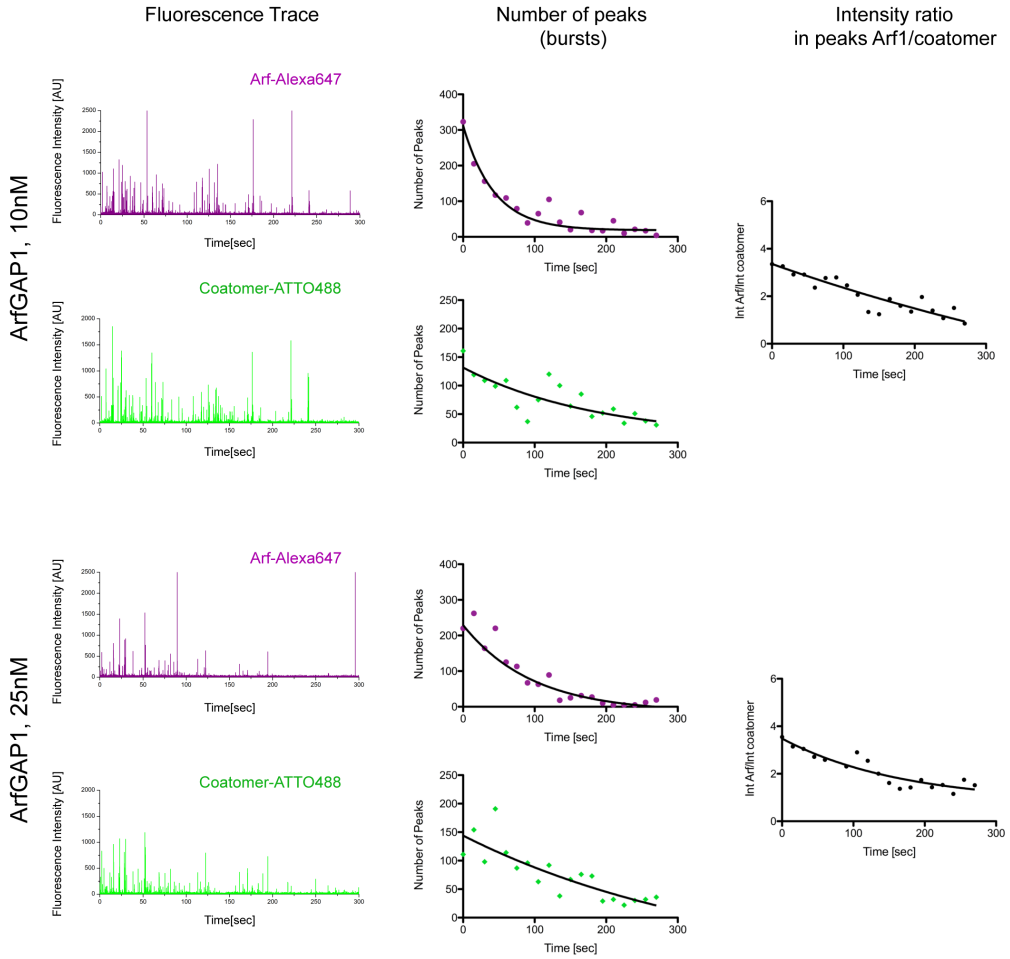

Figure 2.26: Release of the COPI coat by ArfGAP1. Golgi-derived vesicles, coated with Arf1-Alexa647 and coatomer-ATTO488, were imaged for 5 minutes in the presence of 10nM or 25nM ArfGAP1. Left panels fluorescence traces, middle panels number of bursts per time interval for Arf1 and coatomer and right panels relative intensity of Arf1-Alexa647 and coatomer-ATTO488 in the peaks.

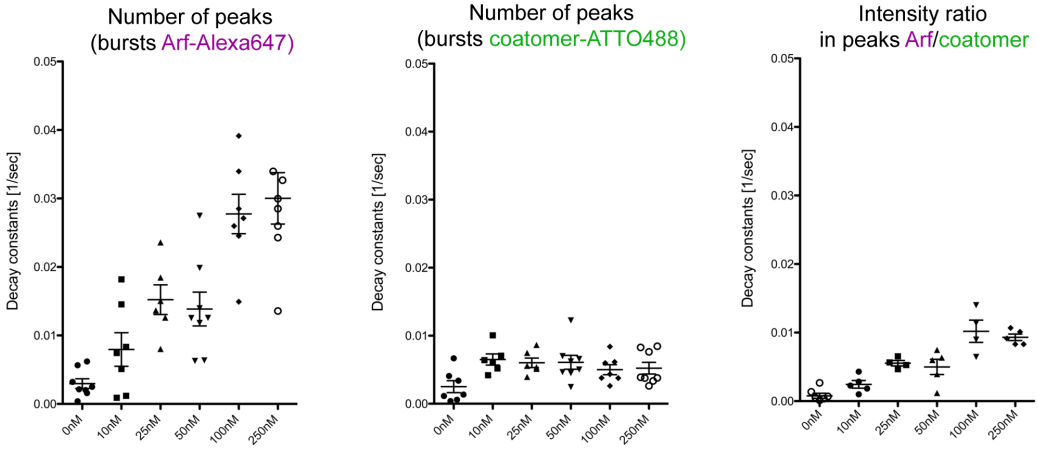

Figure 2.27: Release of the COPI coat by ArfGAP1: decay constants. Scatter plots of decay constants were calculated by fitting the curves for both the number of bursts for Arf1-Alexa647 and coatomer-ATTO488 (left and middle panel) and the relative intensity of Arf1-Alexa647 and coatomer-ATTO488 in the bursts with a single-exponential decay model and displayed as scatter plots. (N≥ 4, mean ± SEM).

2.6.3 GTP hydrolysis induced by ArfGAP2

Apart from ArfGAP1 also ArfGAP2 plays a role in COPI vesicle turnover. Recruitment to the membrane of ArfGAP1 and ArfGAP2 underlies different mechanisms. While ArfGAP1 interacts with the C-terminal domain of coatomer subunit δ-COP (Rawet et al., 2010) and is recruited mainly by the interactions of its ALPS-motifs with curved membranes, ArfGAP2 binds the appendage domain of γ-COP (Kliouchnikov et al., 2009; Watson et al., 2004) and is exclusively recruited by a direct interaction with coatomer. To investigate if ArfGAP2 mediated GTP-hydrolysis in Arf1 likewise leads to COPI coat disassembly, essentially the same experiments as described above were performed in the presence of ArfGAP2 full length (Figure 2.28). In our in vitro set up, we observed very similar uncoating kinetics for both ArfGAP1 and ArfGAP2 (compare Figure 2.27 and Figure 2.29).

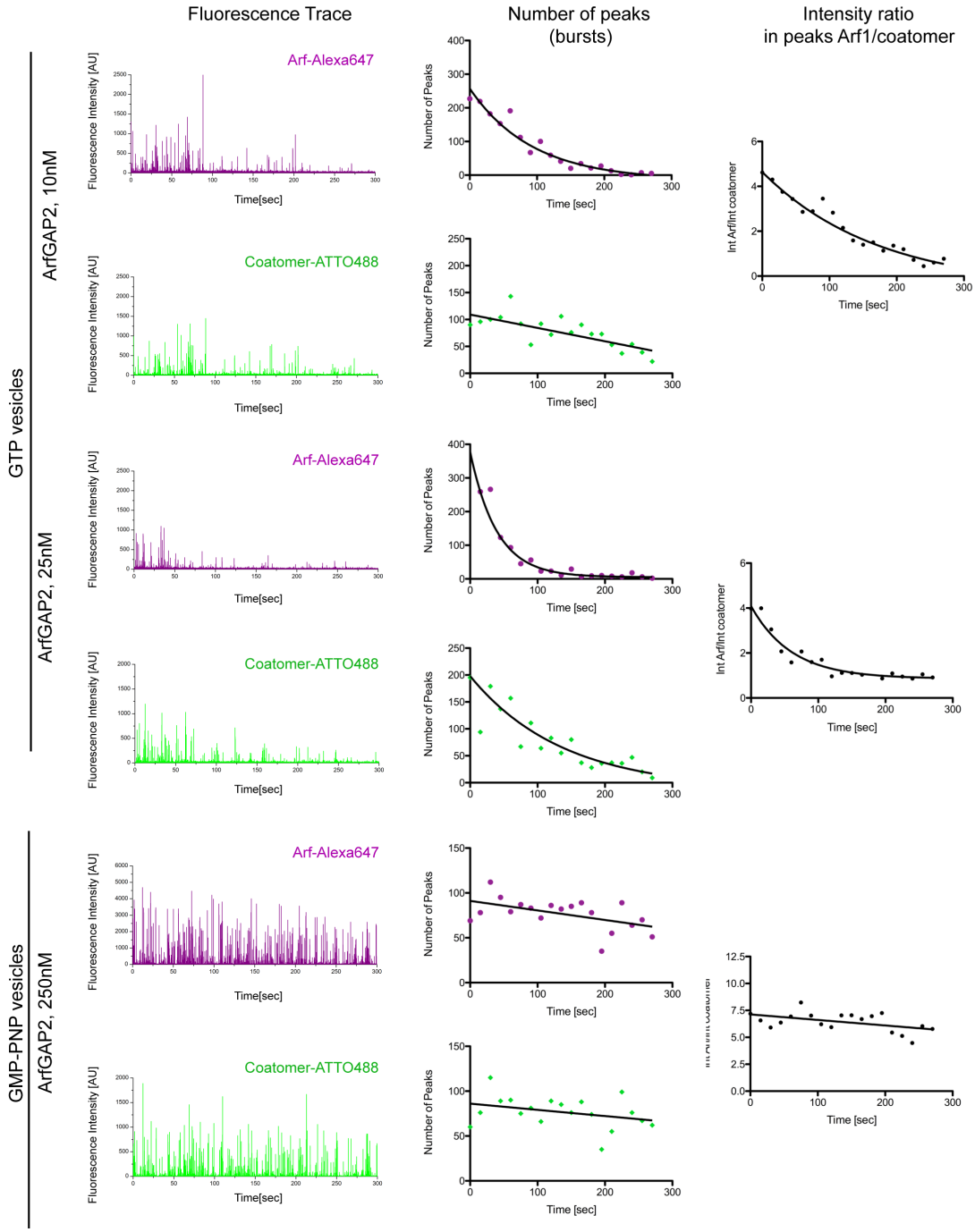

Figure 2.28: Release of the COPI coat mediated by ArfGAP2. Golgi-derived vesicles, coated with Arf1-Alexa647 and coatomer-ATTO488, were imaged for 5 minutes in the presence of ArfGAP2. Left panels fluorescence traces, middle panels number of bursts per time interval for Arf1 and coatomer and right panels relative intensity of Arf1-Alexa647 and coatomer-ATTO488 in the peaks.

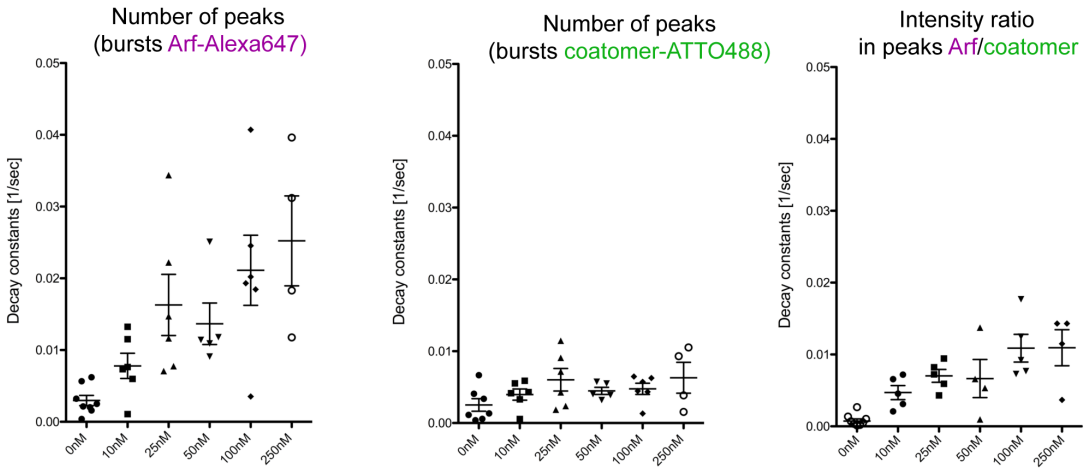

Figure 2.29: Release of the COPI coat by ArfGAP2: decay constants. Scatter plots of decay constants were calculated by fitting the curves for both the number of bursts (left and middle panel) and the relative intensity of Arf1-Alexa647 and coatomer-ATTO488 in the bursts with a single-exponential decay model and displayed as scatter plots. (N≥ 4, mean ± SEM).

2.6.4 GTP hydrolysis induced by the catalytic domain of ArfGAP1

To address contributions of individual domains of ArfGAP1 to coat disassembly, we investigated the activity of its recombinant catalytic domain (amino acid 1 to 137). As this constructs lacks the ALPS motifs, required for membrane recruitment, a twenty five- to hundred-fold higher protein concentration, compared to the full-length protein, was analysed. As shown in Figure 2.30, GTP hydrolysis within Arf1 induced by the catalytic domain of ArfGAP1 was sufficient to fully release Arf1 but not coatomer from the membrane. Coatomer remained mostly bound to the vesicles (Figure 2.30, lower middle panel), indicating a role of the non-catalytic domain in coat disassembly. Consistently, the intensity ratio of Arf1 to coatomer on the vesicles was reduced over time (Figure 2.29, right panel). The decay constant of Arf1 release depends on the concentration of the catalytic domain added to the reaction (Figure 2.31) whereas the decay constant of coatomer, even at the highest concentration of the catalytic domain analyzed, remains comparable to the one in the absence of ArfGAP (Figure 2.31, middle panel). Furthermore, the catalytic domain-induced dissociation of Arf1 but not of coatomer is evident when the curves obtained for the ratio of the intensities of the two proteins on the vesicles are fitted and the corresponding decay constants are calculated (Figure 2.31, right panel).

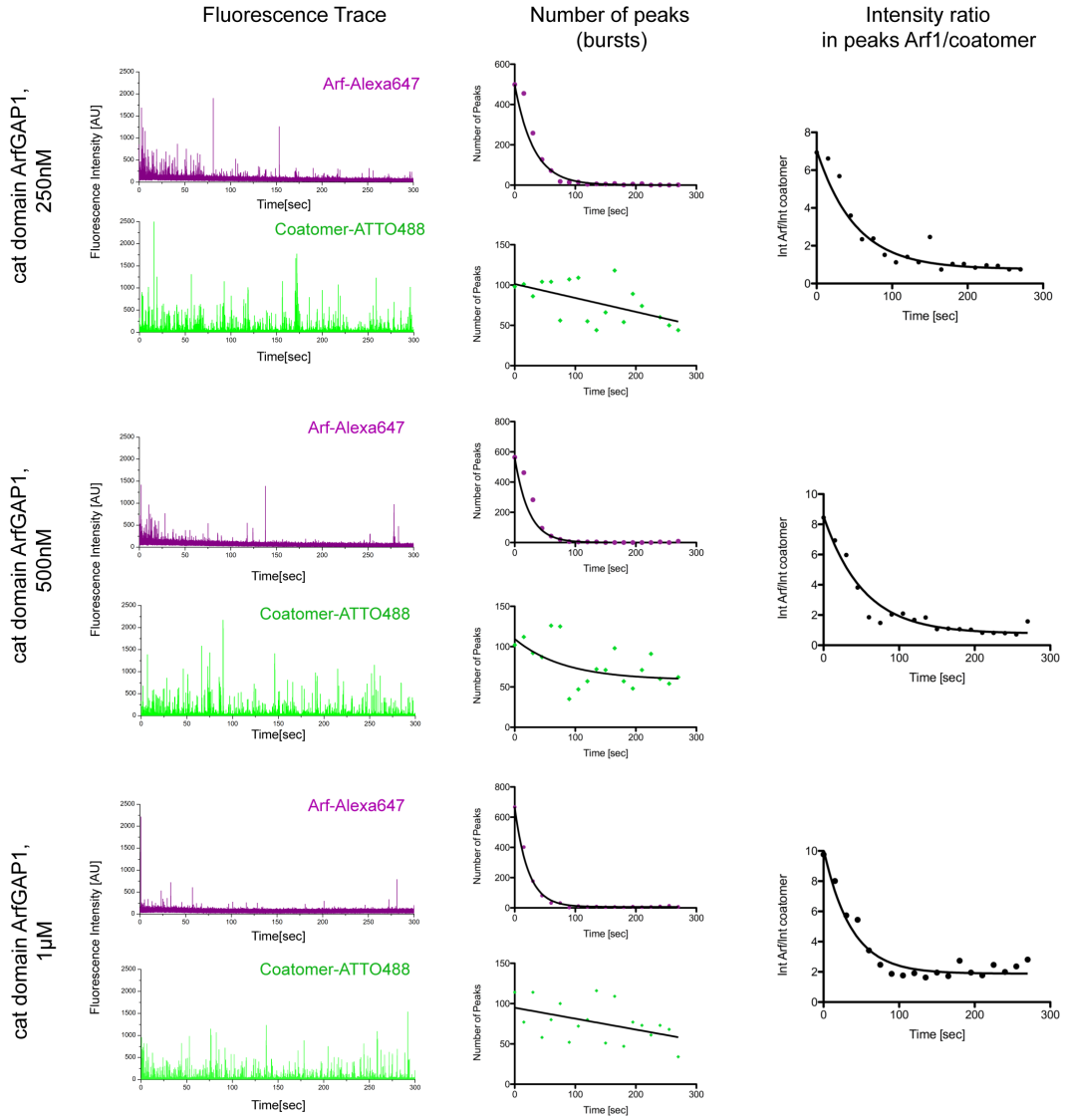

Figure 2.30: Release of COPI coat components triggered by the catalytic domain of ArfGAP1. Golgi-derived vesicles, coated with Arf1-Alexa647 and coatomer-ATTO488, were imaged for 5 minutes in the presence of ArfGAP1 catalytic domain. Left panels fluorescence traces, middle panels number of bursts per time interval for Arf1 and coatomer and right panels relative intensity of Arf1-Alexa647 and coatomer-ATTO488.

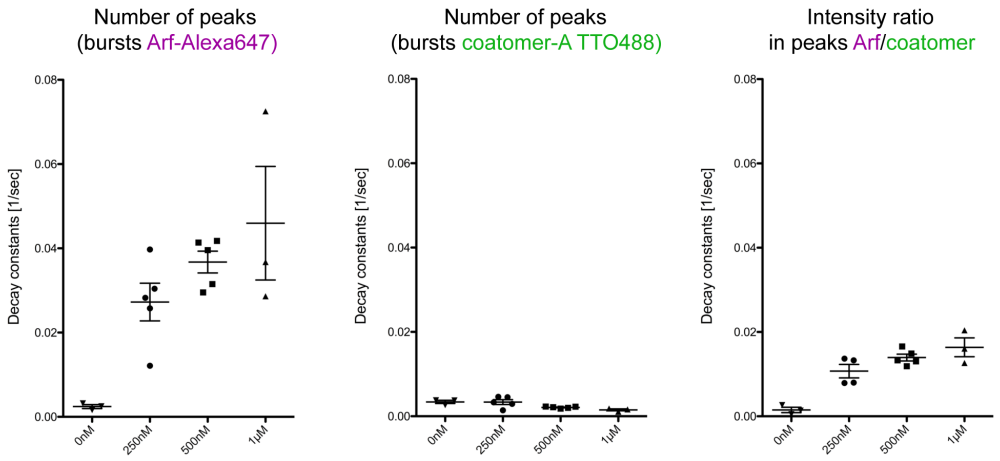

Figure 2.31: Release of COPI coat components triggered by the catalytic domain of ArfGAP1: decay constants. Scatter plots of decay constants were calculated by fitting the curves for both the number of bursts (left and middle panel) and the relative intensity of Arf1-Alexa647 and coatomer-ATTO488 in the bursts with a single-exponential decay model and displayed as scatter plots. (N≥ 4, mean ± SEM).

To further explore the requirement for the non-catalytic part of ArfGAP1 for uncoating, we performed rescue experiments. In a first step COPI vesicles were incubated with the catalytic domain of ArfGAP1 alone. Consistent with the previous experiments, Arf1 was released from the membrane while coatomer remained bound (Figure 2.32, middle panels). In a second step, either full length ArfGAP1 (Figure 2.32A, right panel) or full length ArfGAP2 was added (Figure 2.33A, right panel), or the non-catalytic part of ArfGAP1 or ArfGAP2 (Figure 2.32B and Figure 2.33B, right panels) was added. After 150s, coatomer was to a large extent still associated with the membrane. These results show that coat disassembly requires GTP hydrolysis to occur concomitant with a direct interaction of ArfGAP1 with coatomer.

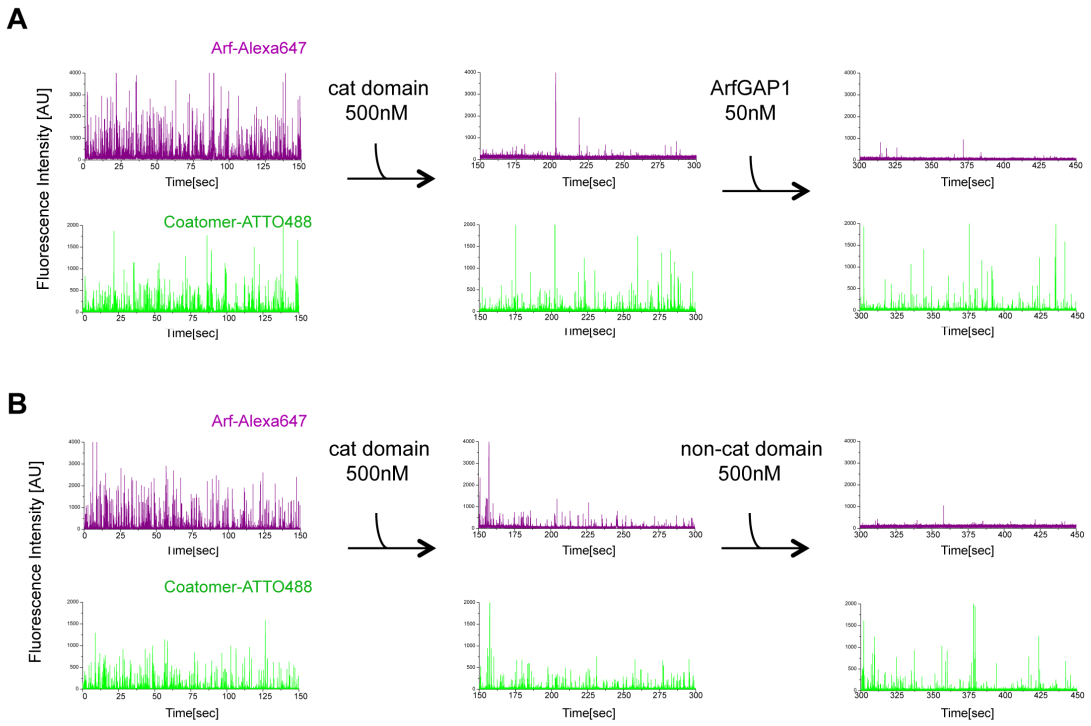

Figure 2.32: Sequential incubation of COPI coated vesicles with ArfGAP1 catalytic domain and non-catalytic domain or full length ArfGAP1. COPI vesicles were generated *in vitro* with Arf1-Alexa647 and coatomer-ATTO488 and analysed for a total time of 450s: 0-150s without ArfGAP, 150-300s after the addition of 500nM catalytic domain, 300-450s after the addition of A) 50nM full length ArfGAP1 or B) 500nM non-catalytic domain of ArfGAP1 (aa 137-337). The handling time for addition of the second and third component was less than 10s.

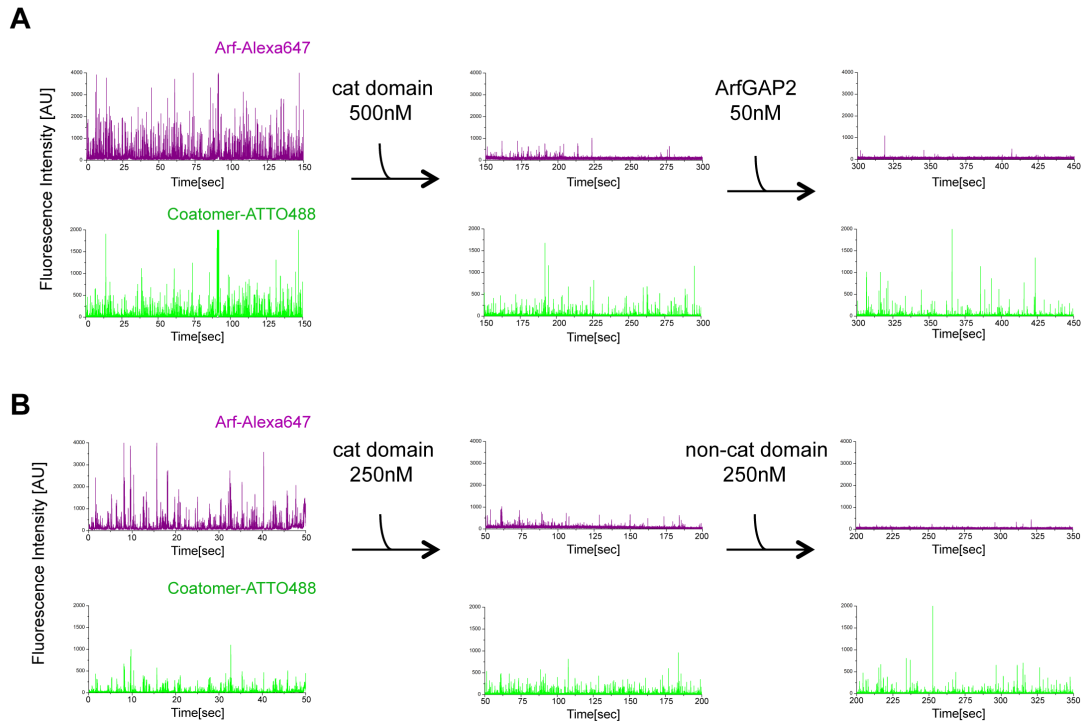

Figure 2.33: Sequential incubation of COPI coated vesicles with ArfGAP2 catalytic domain and non-catalytic domain or full length ArfGAP2. COPI vesicles were generated *in vitro* with Arf1-Alexa647 and coatomer-ATTO488 and analysed for a total time of 350s: 0-50s without ArfGAP2, 50-200s after the addition of A) 500nM and B) 250nM catalytic domain, 200-350s after the addition of A) 50nM full length ArfGAP2 or B) non-catalytic domain of ArfGAP2 (aa 204-362). Handling time for addition of the second and third component was less than 10s each.

In order to investigate if the overall loss in fluorescence is due to the presence of ArfGAP only, we determined the mean fluorescence intensity in each bin. A slight decrease in the signal, independent of ArfGAP activity, can be detected over time (Figure 2.34). However, a normalization of the curves and a direct comparison between the number of peaks (=bursts) for Arf1 and coatomer and the mean intensity shows that the decay is mainly due to ArfGAP activity.

Altogether, this data show that hydrolysis of GTP, mediated by full length ArfGAP1 or ArfGAP2, is sufficient to dissociate the coat components, Arf1 and coatomer, from COPI vesicles, with Arf1 being released faster than coatomer.

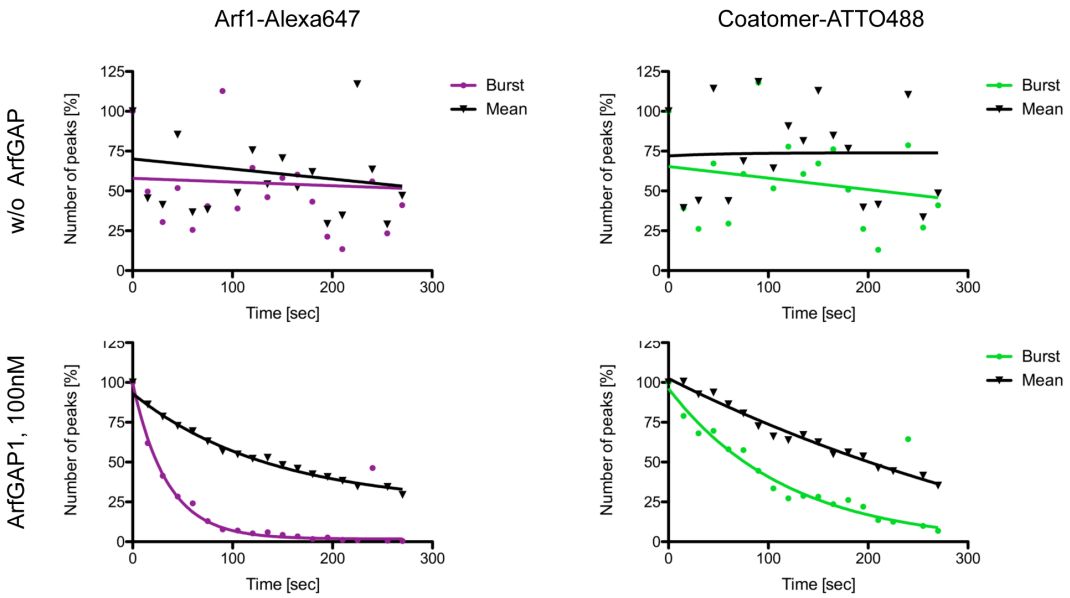

Figure 2.34: Quantification of mean fluorescence intensities. Vesicles were formed in the presence of GTP and traces of the measured intensities were split into 20 bins. The mean intensity for each bin was calculated and normalized. Mean intensity values for Arf1-Alexa647 and coatomer-ATTO488 are plotted against time (black triangles) and directly compared to the normalized number of bursts per time interval for Arf1 and coatomer (purple circles: Arf1, green circles: coatomer). A) in the absencence of ArfGAP and B) in the presence of 100nM ArfGAP1.

2.6.5 Assessing the metastability of the COPI coat after incubation with the catalytic domain of ArfGAP1

To obtain further insight into the mechanism of coat disassembly, the coat components of COPI vesicles that remain membrane bound after incubation with ArfGAP1 catalytic domain were characterized by chemical cross-linking. As the addition of ArfGAP1 catalytic domain to coated COPI vesicles led to Arf1 release, whereas coatomer remains membrane associated, we assumed that this remaining Arf1-free coat is metastable. Indeed, it was not stable enough to survive on the vesicle membranes during attempts to purify membranes and membrane-bound material by density gradient and differential centrifugation. In order to stabilize the coat on the membrane for the time necessary for isolation, a NHS-ester reactive, bifunctional cross linker (DTTSP), was applied to COPI vesicles. For this purpose, isolated coated COPI vesicles were initially treated with two sequential additions of various concentrations of DTTSP, twice 15min on ice. The cross-linked vesicles were adjusted to 40 % Opti-prep and overlaid with 30 % and 20 % Opti-prep. The membrane-bound material was then separated from the free proteins via an overnight centrifugation (for details see Materials and Methods). Prior to SDS-PAGE and western blot analysis, the cross linker was cleaved with ß-mercaptoethanol. As shown in Figure 2.35, 0.25mM DTTSP proved to be the optimal concentration for further experiments.

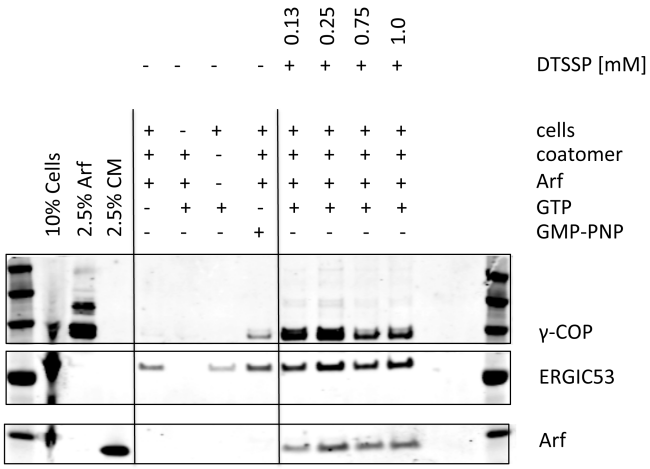

Figure 2.35: Titration of DTTSP crosslinker for stabilization of the COPI coat. Coated COPI vesicles, formed in the presence of GTP or GMP-PNP, were incubated with increasing concentrations of NHS-reactive DTTSP cross linker. The membrane bound material was then isolated via an Opti-prep gradient and analysed with SDS-PAGE and western blotting.

Once the necessary amount of the cross-linker was determined, isolated coated COPI vesicles were incubated for 5 min either with full length ArfGAP1 or ArfGAP1 catalytic domain and subjected to two two sequential incubations with 0.25mM DTTSP cross linker on ice. Membrane-bound material was then isolated on an OptiPrep gradient. As depicted in Figure 2.36, Arf1 and coatomer were found on the vesicular membrane only in the absence of both ArfGAP1 catalytic domain and ArfGAP1 full length. Thereby, the cross-linking reaction was not suitable to stabilize the metastable coatomer lattice after the release of Arf1.

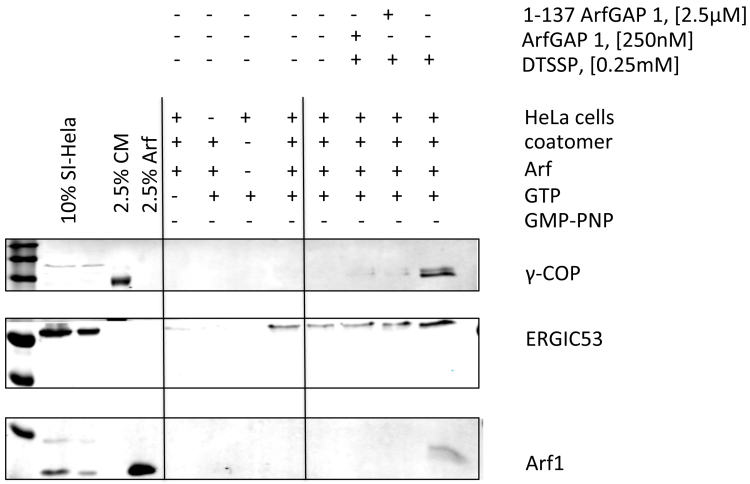

Figure 2.36: Cross linking of COPI vesicles with DTTSP. Coated COPI vesicles, formed in the presence of GTP or GMP-PNP, were incubated either with full length ArfGAP1 or ArfGAP1 catalytic domain. Membrane associated coat components were subsequently cross linked with 0.25mM NHS-reactive DTTSP. The membrane bound material was then isolated via an Opti-prep gradient and analysed with SDS-PAGE and western blotting.

In order to analyze the metastability of the coat in a system, which does not involve time consuming purification steps, we performed the single molecule assay described above with vesicles generated with a donor membrane labeled with Alexa647 and coatomer labeled with ATTO488. Thereby the signal of the vesicle itself (followed by the labeled membrane) should hardly be affected even if coat disassembly takes place, while coatomer release should be reflected by changes in both the number of peaks and the ratio of the intensity of the membrane to the intensity of Arf1. As shown in Figure 2.37A, in the absence of ArfGAP1 no coat disassembly took place. Addition of 50nM ArfGAP1 full length led to the disassembly of coatomer (Figure 2.37B) as observed for the vesicles with labelled Arf1 and labelled coatomer. Thus, labelling of the membrane did not compromise the functionality of the vesicles, at least with respect to coat disassembly. After incubation with the catalytic domain of ArfGAP1, both number of peaks and the ratio of the intensity of the membrane to the intensity of Arf1 remained to a large extent unchanged (Figure 2.37C). Thus, although the coatomer lattice is less stable in the absence of Arf1, coatomer still remains largely membrane-bound within the measured time window.

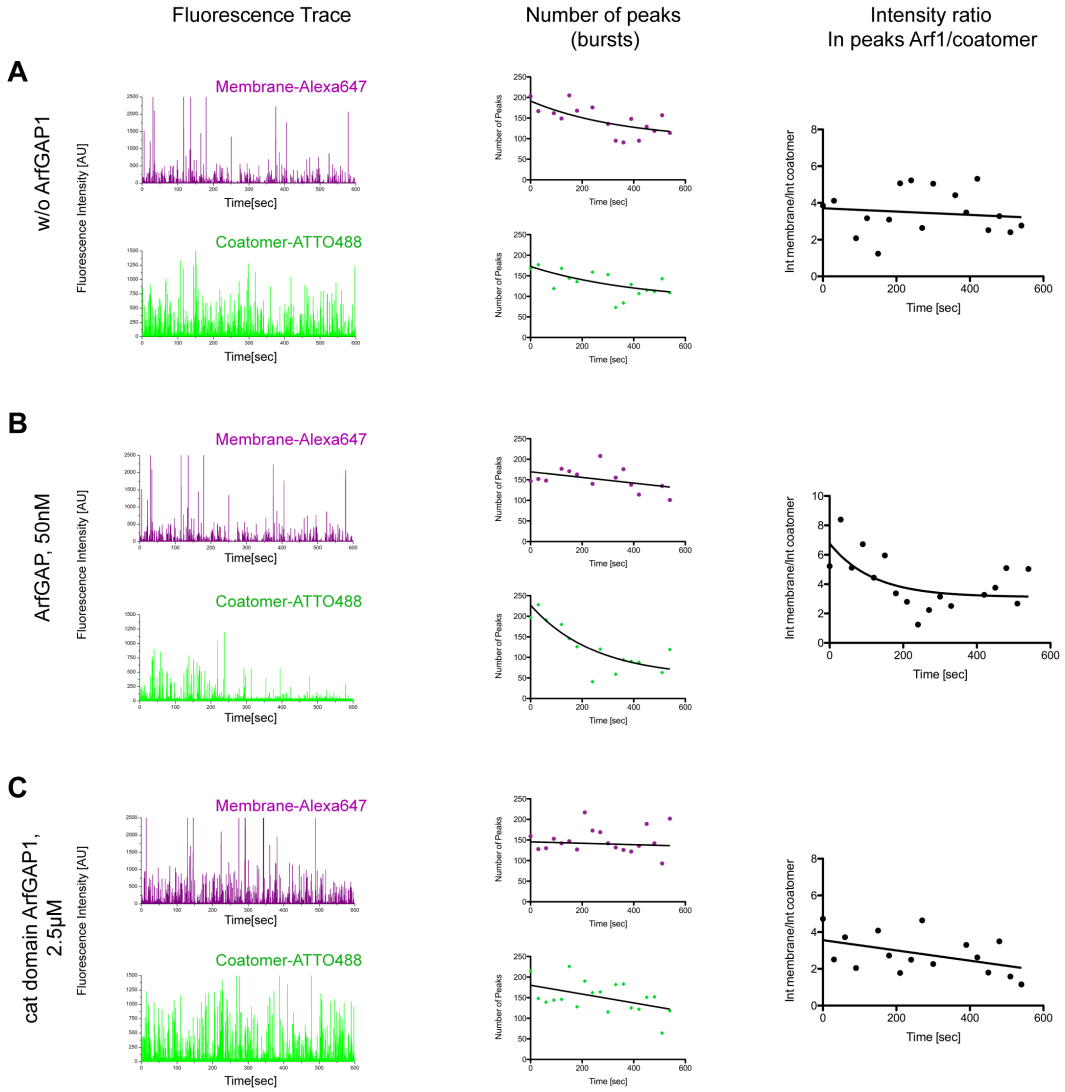

Figure 2.37: Burst analysis of vesicles generated with membrane-Alexa647 and coatomer-ATTO488. Golgi-derived vesicles, coated with Arf1 and coatomer-ATTO488, were imaged for 10 minutes (A) in the absence or in the presence of either (B) 50nM ArfGAP or (C) 2.5µM ArfGAP1 catalytic domain. Left panels fluorescence traces, middle panels number of bursts per time interval for membrane and coatomer and right panels relative intensity of Arf1-Alexa647 and coatomer-ATTO488 in the peaks. N=2.

In conclusion, the hydrolysis of GTP in Arf1 is a prerequisite for release not only of Arf1 but also of coatomer by full length ArfGAP1 or ArfGAP2. However, for dissociation of both components of the COPI coat, not only the catalytic and but also the non-catalytic domains of ArfGAP are to be present within the same molecule at the time of GTP-hydrolysis. Thus, we propose that GTP hydrolysis in Arf1 provides energy, which is transmitted to the coat by the non-catalytic domain of ArfGAP to release coatomer from vesicular membranes.

3 Discussion

3.1 Differential interactions of ArfGAP1/2/3 with coatomer isoforms

One of the goals of this thesis was characterizing the interaction between the coatomer isoforms and the ArfGAPs involved in COPI vesicle biogenesis in mammalians. Four different isoforms of the coat complex coatomer have been described in the literature: $\gamma_1\zeta_1$, $\gamma_1\zeta_2$, $\gamma_2\zeta_1$, and $\gamma_2\zeta_2$ (Futatsumori et al., 2000; Wegmann et al., 2004). Up to date no differences between the roles of the different coatomer isoforms were described in the literature. An immunoelectron microscopy study showed that the coatomer isoforms differ in their localisation within the Golgi apparatus: whereas γ_1- and ζ_2-COP are mainly located at the early Golgi and pre-Golgi compartment, the γ_2-COP isoform is found predominantly at the trans side of the organelle (Moelleken et al., 2007). In this study, it was probed if coatomer isoforms display preferences for a particular ArfGAP protein. Three ArfGAPs have been described to interact with the coat complex coatomer (Frigerio et al., 2007; Goldberg, 1999; Lee et al., 2005). Very early in evolution the family splits in two subfamilies: the ArfGAP1 and ArfGAP2 subfamily. In *S. cerevisiae*, Gcs1p is the ArfGAP1 homolog and Glo3p is the ArfGAP2/3 homologue (Poon et al., 1999). No difference in function could be attributed to ArfGAP2 and ArfGAP3 so far. The three ArfGAPs localize differently within the Golgi apparatus as found in immunogold labelling electron microscopy study (Weimer et al., 2008). ArfGAP1 was found equally distributed over the Golgi apparatus whereas both ArfGAP2 and ArfGAP3 localize predominantly at the cis-Golgi. Based on this localization of the coatomer isoforms, we hypothesized that ArfGAP2 and ArfGAP3 might display higher affinity for the γ_1-COP isoforms.

To quantitatively analyse the interactions between ArfGAPs and coatomer isoforms, we have adapted a previously described microtiter plate ligand-binding assay (Bethune et al., 2006). For this purpose, coatomer was immobilized on a polystyrene surface directly and subsequently incubated with ArfGAPs. We observed not only a preference of ArfGAP2/3 for $\gamma_1\zeta_1$ and $\gamma_1\zeta_2$ over $\gamma_2\zeta_1$, and $\gamma_2\zeta_2$ but also of ArfGAP1. Furthermore, ArfGAP1 displayed the highest affinity for all four coatomer isoforms followed by ArfGAP2. ArfGAP3 showed the weakest interaction with a statistically significant difference in the affinity for $\gamma_1\zeta_1$ and $\gamma_2\zeta_1$. As none of the three ArfGAPs localizes preferentially to the trans-Golgi apparatus (Weimer et al., 2008) and consequently none displayed a preference for the trans-Golgi localizing $\gamma_2\zeta_1$, and $\gamma_2\zeta_2$, one could speculate that an as yet not identified ArfGAP specifically interacts with $\gamma_2\zeta_1$ and $\gamma_2\zeta_2$ and localize to the trans-Golgi apparatus.

3.2 Effect of coatomer conformation on ArfGAP affinity

Another aspect studied in the course of this work focused on the mode of recruitment of ArfGAP1, 2 and 3 from the cytosol to Golgi membranes, and potentially differential roles of the three ArfGAPs in COPI biogenesis. ArfGAP1 and ArfGAP2/3 are recruited by different mechanisms to Golgi membrane. Whereas ArfGAP1 binds highly curved membranes via two amphipathic lipid packing sensor (ALPS) motifs (Bigay et al., 2003), ArfGAP2 and ArfGAP3 are recruited to Golgi membranes by a direct interaction with coatomer (Weimer et al., 2008). While it was clearly shown that ArfGAP2 and 3 depend on coatomer for their association with the Golgi membrane (Weimer et al., 2008), the spatial and temporal regulation of this process is yet unknown. One possibility is that ArfGAP2 and 3 bind to soluble coatomer already in the cytosol and are recruited as a complex with the heptameric complex to the Golgi membrane. Another possibility is that ArfGAP2 and 3 are recruited only once coatomer has polymerized on the donor membrane and the binding site for ArfGAP2/3 within coatomer is formed.

Based on the same experimental set of data, two opposing models about the roles of ArfGAP1, ArfGAP2 and ArfGAP3 in COPI vesicle biogenesis were forwarded.

According to the first model, ArfGAP1, which binds directly to curved membranes, and thus does not require the presence of coatomer on the Golgi membrane for its recruitment, was proposed to be involved in cargo sorting (Popoff et al., 2011a). As vesicle biogenesis is initiated at the rims of Golgi membranes, sites that feature high curvature, ArfGAP1 can be recruited and stimulate GTP hydrolysis within Arf1 when low amounts of cargo are available. Thereby, ArfGAP1 will ensure the efficiency of COPI vesicle transport by preventing budding of empty transport vesicles. ArfGAP2 and ArfGAP3, which are dependent on their interaction with coatomer for membrane recruitment, bind only to fully formed COPI vesicles featuring a polymerized coat and rather are involved in vesicle uncoating.

According to the second model, ArfGAP1 functions as the uncoating ArfGAP while ArfGAP2 and ArfGAP3 are involved in cargo sorting (Antonny, 2011). Due to its curvature sensitivity, ArfGAP1 is recruited to the loosely packed lipids of the highly curved COPI vesicles. ArfGAP2 and ArfGAP3 are recruited by their interaction with coatomer to sites of COPI vesicle formation and stimulate GTP hydrolysis in Arf1 thus leading to the disassembly of both Arf1 and coatomer from the Golgi membrane in the absence of cargo.

Assuming that a particular ArfGAP is involved in COPI coat disassembly rather than cargo sorting, this ArfGAP should display a higher affinity for polymerized coatomer than for soluble coatomer. In order to address this mechanistic question, we utilized both an ELISA-like binding assays as well as a conventional pull down assay. For the ELISA-like binding assay, coatomer was immobilized on a polystyrene surface either directly or via CM1A10, a

structure-specific monoclonal antibody against the heptameric coat complex coatomer. A conformational change was induced in the complex by the addition of a dimeric peptide mimicking the cytoplasmic tails of p23. The conformation obtained after binding to this peptide was previously shown to be similar to the one coatomer assumes when polymerized on COPI vesicles (Reinhard et al., 1999).

In the set-up based on a direct immobilization of coatomer, the k_D values for the interaction between ArfGAP and coatomer were determined to be in the low micromolar range. Here, no clear difference was detected between samples containing either p23 dimerized peptide, or the control peptide Wbp1, or no peptide. As the p23 induced conformational change in coatomer described in the literature was performed either in solution (Reinhard et al., 1999) or after coatomer immobilization via the antibody CM1A10 on a surface (Langer et al., 2008), it is possible that the reaction does not take place as efficiently when coatomer is directly immobilized on a polystyrene surface. To circumvent this drawback, existing ArfGAP baculo virus transfer vectors were recloned in order to introduce an S-tag upstream of the ArfGAP ORFs. With the modified constructs, we were able to perform a direct detection of ArfGAPs bound to coatomer with a S-protein-horseradish peroxidase (HRP) conjugate instead of detection via a secondary antibody coupled to HRP. Here, significantly higher k_D values were determined for the interaction between all three ArfGAPs and the coatomer isoform $\gamma_1\zeta_1$, which displays the highest abundance in cells and was thus used as a representative of all four coatomer isoforms. As the k_D values of S-tagged ArfGAPs for directly immobilized coatomer were comparable to the ones determined for His-tagged ArfGAPs, this effect is unlikely to be due to the S-tagged influencing the affinity of ArfGAPs for coatomer. Thus, presumably either the CM1A10 antibody masked the ArfGAP binding sites in coatomer or the concentration of immobilized coatomer in the set-ups involving CM1A10 antibody was lower than in the set-up relying on direct immobilization. Accordingly, this experimental design proved not to be suitable to address the question of interest.

Alternatively, we used a conventional pull down approach to measure interactions between the different ArfGAPs and coatomer, depending on the conformation of the coat protein. Here, we used two independent experimental set-ups. First, One-STrEP-tag coatomer was immobilized on streptactin beads and coatomer polymerization was triggered by the addition of dimeric p23 peptides. As a negative control, coatomer was incubated with the ER resident protein Wbp1. To avoid potential reversibility of the conformational change, we performed the incubation with the different ArfGAPs also in the presence or absence of the p23 peptide. In both cases, we were not able to detect any alteration in the affinity of ArfGAPs for coatomer. A possible drawback of this set-up could be that coatomer cannot be efficiently polymerized after binding to the beads. It was previously observed that the conformational change involves at least α-COP and γ-COP (Langer et al., 2008), and the One-STrEP-tag is located

on the C-terminus of α-COP subunit potentially preventing the conformational change. In a second setup, we tried to circumvent this limitation by first inducing the conformational change in coatomer in solution and then immobilizing the protein via its One-STrEP-tag on the streptactin beads. In the negative control sample, coatomer was treated with Wbp1. Here, we again either washed or did not wash away the peptide prior to the incubation with ArfGAP. In this system we unexpectedly observed a higher affinity of ArfGAP2 for soluble coatomer. This effect was visible only when the entire experiment was performed in the presence of the peptides pointing either to a reversible conformational change in coatomer or to a direct effect of the p23 cytoplasmic tail on ArfGAP2. Still, it cannot be excluded that the polymerization in solution and the subsequent immobilization on the streptactin beads compromises coatomer functionality and thereby its affinity for ArfGAP2.

One further possibility, which might allow determining the affinity of ArfGAP1 and ArfGAP2 for coatomer depending on its conformation, is establishing a float up assay where coatomer is recruited to the liposomal membrane either directly via its tag or via an interaction with Arf1. Coatomer recruited via the tag mimics the soluble form as found in the cytosol while coatomer recruited via an interaction with Arf1 and the cytoplasmic tail of p23 resembles polymerized coatomer as found on a fully formed COPI vesicle. Upon coatomer recruitment and subsequent ArfGAP incubation, the membrane-associated fraction can be isolated on a density gradient and the amount of bound ArfGAP can be assessed via SDS-PAGE and wetsren blot analysis.

3.3 Effect of p23 on the activity of ArfGAP1 and ArfGAP2

Another goal of this work was to analyse the effect of type I transmembrane proteins of the p24 family on the activity of ArfGAP1 and ArfGAP2 (as a representative of both ArfGAP2 and ArfGAP2). The literature points to an effect of p24 family proteins on the activity of ArfGAP1. It was reported that p23 and p24 inhibit ArfGAP1 mediated GTP hydrolysis in Arf1 (Lanoix et al., 2001).

In order to investigate if the cytoplasmic tail of p23 acts directly on the Arf1 activation/deactivation cycle, we performed tryptophane fluorescence assays. Here, we compared an effect of the p23 lipopeptide on the rate of GTP hydrolysis in Arf1, stimulated by either ArfGAP1 or ArfGAP2. The rate of GTP hydrolysis was altered in the presence of the p23 lipopeptide. The activity of ArfGAP1 was slightly inhibited by p23, whereas the activity of ArfGAP2 was significantly higher in the presence of p23. Furthermore, we utilized a static light scattering assay to test if ArfGAP1- and ArfGAP2-triggered uncoating of COPI coated liposomes is affected as well. The uncoating activities of the two enzymes were affected in the same way as observed in the tryptophan fluorescence assay: ArfGAP1 mediated a

slower disassembly in the presence of the lipopeptide while ArfGAP2 mediated a faster disassembly.

In order to challenge the results in a system not based on a fluorescence read-out, we utilized a float up assay with radioactively labeled GTP. For this purpose, Golgi-like liposomes were prepared either in the presence or absence of p23 lipopeptide. Upon recruitment of Arf1 and coatomer to the membrane in a 3H-GTP dependent manner, we analyzed the degree of GTP hydrolysis exhibited by ArfGAP1 and ArfGAP2. In agreement with the results from the fluorescence based kinetic measurements, we observed both a higher rate of GTP hydrolysis as well as a higher absolute amount of hydrolysed GTP by ArfGAP2 in the presence of the p23 lipopeptide. ArfGAP1 displayed an opposite effect: a higher rate of GTP hydrolysis and a higher total amount of hydrolyzed GTP in the absence of p23 lipopeptide.

It is important to note here that the two ArfGAPs interact with distinct subunits of coatomer (Kliouchnikov et al., 2009; Watson et al., 2004) and that these coatomer subunits contribute to COPI coat assembly in a different manner, as can be deduced from the structure of the COPI coat on a membrane (Dodonova et al., 2015; Faini et al., 2012) (for more details see 3.6). Furthermore, it could be speculated that the binding site for the respective ArfGAP is build only after polymerization of the coat lattice. It was reported earlier that p23 leads to a conformational change in coatomer (Langer et al., 2007; Reinhard et al., 1999) and that this conformation is likely to resemble the heptameric complex in the polymerized COPI coat on a transport vesicle (Reinhard et al., 1999). Thus, the higher activity of ArfGAP2 in the presence of p23 might result from a higher affinity of ArfGAP2 for polymerized coatomer as found on a transport vesicle, which in turn speaks for a role of ArfGAP2 in coat disassembly rather than in cargo sorting.

3.4 Effect of ArfGAP1 and ArfGAP2 on the yield of COPI vesicle formation

Another aspect analyzed in this study is the function of the ArfGAPs in coat assembly and disassembly. The role of the ArfGAPs in COPI vesicle biogenesis remains controversial. Earlier studies have proposed a mechanism, by which the ArfGAPs catalytically act on Arf1 and thereby induce GTP hydrolysis that is prerequisite for vesicle coat release (Tanigawa et al., 1993). Whereas originally, Arf1 was identified as a subunit of the COPI coat (Serafini et al., 1991a,), opposing reports suggest a model where, in analogy to the COPII system, ArfGAP1 is directly involved in coat formation. It was proposed that upon GTP hydrolysis (prerequisite for Arf1 release and COPI vesicle formation), ArfGAP1 together with coatomer remains associated with membranes to from the polymerized COPI coat (Yang et al., 2002). The amount of ArfGAP found on the vesicles was stoichiometric to the one of coatomer

whereas the level of Arf1 was reduced (Yang et al., 2002). Under GTPγS conditions, ArfGAP1 failed to induce COPI release from Golgi membranes. Isolation of the vesicles formed with GTPγS showed reduced labelling for ArfGAP1 pointing rather to an impairment of the GAP recruitment than to a direct inhibition of the GAP activity (Yang et al., 2002). Furthermore, others found the yeast orthologous of ArfGAP2/3, Glo3p on COPI vesicles generated in vitro from isolated yeast Golgi membranes (Lewis et al., 2004).

In order to address a potential role of ArfGAP1 and ArfGAP2 as stoichiometric coat components and to overcome the drawbacks of earlier studies using density gradients for the isolation of the vesicles (Beck et al., 2009), we established an assay based on semi-intact cells described both for COPII (Mancias and Goldberg, 2007) and COPI (Adolf and Wieland, 2013) reconstitutions. The major shortcoming of the density gradients is their selectivity for coated vesicles (vesicles formed and subsequently uncoated will not be taken into account, because these “naked” vesicles have a density different to coated vesicles and therefore would migrate to lower density in such gradients), which does not allow to tell apart formed vesicles that have subsequently undergone uncoating, or no vesicle formation having taken place to begin with (Hsu, 2011).

Isolation of COPI vesicles formed from semi-intact cells relies on a differential centrifugation where both coated and uncoated vesicles are assessed via the amount of cargo incorporated. In contrast to earlier studies pointing to a role of ArfGAP1 or ArfGAP2 as a coat component, we detected fewer COPI vesicles in the presence of ArfGAP1/2. This effect was more pronounced in the case of ArfGAP2. This difference could be explained by the use of semi-intact cells in our *in vitro* assay, which make accessible all the membranes in a cell and thus could enable ArfGAP1 to bind with its ALPS domains to sites additional to the ones at the *cis*-Golgi, as described previously, such that the actual concentration relevant for COPI sites would be reduced (Bai et al., 2011; Rawet et al., 2010; Zendeh-boodi et al., 2013). Thus, the physiological relevance of the potentially stronger effect of ArfGAP2 needs to be addressed in another system.

Results obtained from the semi-intact cell system argue strongly against a role of both ArfGAP1 and ArfGAP2 as stoichiometric coat components.

3.5 Role of ArfGAP1 and ArfGAP2 in COPI vesicle uncoating

It was proposed previously that the ArfGAP1 induced hydrolysis in Arf1 triggers uncoating of Golgi-derived COPI vesicles (Tanigawa et al., 1993). This hypothesis was based on a series of different studies. In early experiments, incorporation of GTPγS was found to block transport and led to an accumulation of coated vesicles (Melancon et al., 1987). Furthermore, an Arf1 variant, Arf1Q71L-GTP, which in its myristoylated form is competent to

bind membranes and recruit coatomer, but in contrast to wild type fails to hydrolyse GTP (Tanigawa et al., 1993), could mimic this effect. Cells expressing Arf1Q71L-GTP were shown by EM to feature vesicles with distinct electron-dense coats, which accumulated as they probably failed to fuse with the target membrane (Tanigawa et al., 1993). A similar effect was observed in cells expressing a defect Dsl/SNARE complex (Zink et al., 2009).

Here, we established an assay with single molecule sensitivity to study the process of COPI coat disassembly in real time. This system allows both analysing vesicles generated from endogenous membranes as well as following the kinetics of individual coat components. Purification of COPI vesicles from endogenous membranes has the advantage that all modes of interaction that keep coatomer on the membrane are present. Thus, we attempted to resolve the question if GTP hydrolysis induced by full length ArfGAP does not only trigger Arf1 disassembly but is also sufficient by itself to release all coat components from the vesicular membrane. Full length ArfGAP1 protein proved to be sufficient to trigger COPI coat disassembly. In our *in vitro* system Arf1 was released from the membrane faster than coatomer. This effect might be due to the various types of interactions that keep coatomer membrane-associated. On a membrane coatomer is not only bound to Arf1 but also to the cytoplasmic tails of cargo receptors and cargo proteins, and in addition undergoes coat-coat interactions. This data is in accordance with earlier studies performed in live cells. The dynamics of GFP-tagged Arf1 and coatomer membrane association and dissociation was studied by FRAP in living cells. The half time for the recovery of Arf1 was two times shorter than the one for coatomer implying that coatomer remains stabilized on the membrane after GTP hydrolysis and Arf1 dissociation (Presley et al., 2002).

To test if it is the ArfGAP induced hydrolysis of GTP in Arf1 that is sufficient for COPI coat disassembly; we performed experiments with only the catalytic part of ArfGAP1. Here, Arf1 was released from the membrane, whereas, surprisingly, coatomer remained to a large extent membrane-associated. Furthermore, incubating these resulting Arf1-free vesicles with full length ArfGAP1 did not lead to further COPI coat disassembly. These findings show a requirement for GTP hydrolysis concurring with a direct interaction between coatomer and ArfGAP1 for COPI coat release.

3.6 Comparison of the uncoating activities of ArfGAP1 and ArfGAP2

ArfGAP1 and ArfGAP2 display distinct mechanisms of recruitment to membranes. Whereas ArfGAP1 associates with the membrane by inserting its ALPS domains between loosely packed lipids on a curved membrane (Bigay et al., 2003), ArfGAP2 is recruited by a direct interaction with coatomer (Weimer et al., 2008). Furthermore, ArfGAP2/3 were isolated together with COPI vesicles formed *in vitro* while ArfGAP1 was mainly found associated with

donor Golgi membranes (Frigerio et al., 2007). In addition, overexpression of ArfGAP1 or ArfGAP2/3 leads to different phenotypes. Overexpression of ArfGAP1 causes coatomer dissociation from Golgi membranes as well as a relocalization of Golgi enzymes to the ER (Aoe et al., 1997). In contrast, overexpression of both ArfGAP2 and ArfGAP3 did not alter coatomer localization or Golgi structure (Kartberg et al., 2010). ArfGAP2/3 knockdown, on the other hand, leads to reduced Golgi-stacking and a decrease in the number of cisternae (Kartberg et al., 2010).

To address the question if these differences also result in distinctive coat disassembly efficiencies, we compared the efficiency of the two enzymes in our real time coat disassembly assay. To this end, we observed similar kinetics with respect to coat disassembly. As under our test conditions the composition of the components is not adapted to their *in vivo* ratios, more refined and subtle approaches will have to be taken in order to address such differences.

It is of note that the two ArfGAPs interact with coatomer at two different sites. ArfGAP1 binds δ-COP (Rawet et al., 2010), while ArfGAP2 interacts with γ-COP (Kliouchnikov et al., 2009; Watson et al., 2004). These two coatomer subunits contribute to COPI coat assembly in a different fashion, as can be delineated from the structure of the coat on a membrane (Dodonova et al., 2015; Faini et al., 2012). The COPI coat is built up of coatomer triads as minimal structural component (Faini et al., 2012). In a triad each of the three coatomer complexes binds to two Arf1 molecules: one Arf1 molecule interacts with the trunk domain of γ-COP and the other one simultaneously with β- and δ-COP. The C-termini of δ-COP are involved in inter-triad interactions whereas the γ-COP subunits play a role in assembly of the triad itself (Dodonova et al., 2015). These structural features suggest a hypothesis that ArfGAP1 and ArfGAP2 might act differentially and synergistically in order to release both types of interactions: hydrolysis of GTP in Arf1 bound to γ-COP would stimulate dissociation of triads from each other, whereas hydrolysis of GTP in Arf1 bound to β-and δ-COP would drive dissociation of triads to yield single coatomer complexes. As a result, coat dissociation would occur efficiently in spite of the fact that about 100 GTP molecules must be hydrolysed in two different structural environments within a single vesicle. Again based on the structure of the triads and their interactions, it is tempting to speculate that it is ArfGAP2 that stimulates GTP hydrolysis in the Arf1 molecules attached to γ-COP, whereas ArfGAP1 would stimulate GTP hydrolysis in β-δ-bound Arf1. To test this model in the future, a more subtle and technically simpler method will be needed to follow coat dissociation. Isolated COPI vesicles could be incubated with 1:1 mixtures of ArfGAP1 and ArfGAP2 and the kinetics of uncoating could be compared with the one of each enzyme alone when applied at the same concentration as the mixture. A very precise titration of the amount of ArfGAP added would be required as presumably once the ArfGAP concentration is high enough so many Arf1s in

one of the two chemical environments would be released, which in turn results in coatomer dissociation, that also the Arf1 molecules in the second chemical environment would become assessable for the ArfGAP.

3.7 A model of COPI coat disassembly

The precise mechanism of coat disassembly is not understood for any of the vesicular transport systems. The coat of endocytic vesicles consists of an inner scaffold, built of by the adaptor complex AP2, and an out layer comprising the clathrin triskelions (Fotin et al., 2004; Kirchhausen, 2000). Dissociation of the outer (clathrin) layer of an endocytic vesicle requires the heat-schock cognate protein-70 (Hsc 70) (Massol et al., 2006; Schlossman et al., 1984; Schmid et al., 1984; Ungewickell et al., 1995) The temporal regulation of the uncoating reaction is governed by the recruitment of auxillin, which in turn recruits Hsc70 (Massol et al., 2006). Auxilin binds with its three J-domains positioned in the vicinity of each vertex of the coat and brings about a conformational change, which allows Hsc70, recruited via a direct interaction with the J-domain of auxilin, to reach its target sequence QLMLT. As Hsc70 binds to this sequence in a groove on its substrate-binding domain, ATP hydrolysis occurs. This leads to two simultaneous events: the J-domain is released and the substrate becomes tightly clamped in the groove. In such a way, Hsc70 stabilizes the distorted conformation. Once a critical concentration of auxilin/Hsc70 is reached, the coat becomes irrevocably destabilized and falls apart in a all-or-none fashion (Bocking et al., 2011). It is still remains to be elucidated how and when the inner AP2 coat is released from the vesicular membrane.

GTP hydrolysis within the Arf1 analogue Sar1 is thought to contribute to the disassembly of the COPII coat (Antonny et al., 2001; Barlowe et al., 1994). COPII vesicles are incompetent to fuse with the target membrane when hydrolysis of GTP in Sar1 is blocked (Aridor et al., 1995; Barlowe et al., 1994). The GAP protein that stimulates GTP hydrolysis in Sar1 is the COPII inner coat component Sec23 (Yoshihisa et al., 1993), whose catalytic activity is further enhanced by its interaction with the COPII outer shell Sec13/31 complex (Antonny et al., 2001; Yoshihisa et al., 1993).

Here, I described a real-time assay to follow the fate of the COPI coat of purified COPI vesicles upon addition of ArfGAPs. Using this assay, I discovered an essential role of the non-catalytic domains of ArfGAPs. While GTP-hydrolysis within Arf1 by the catalytic domain of the ArfGAP alone released the small GTPase from the coat, the network of coatomer triads remained on the vesicle. Only with the non-catalytic part of ArfGAPs present within the ArfGAP molecule, the coat network was disassembled. We propose that the energy released upon GTP-hydrolysis in Arf1 is coupled by GAP-coatomer interactions to mediate conformational changes in coatomer that are required for COPI coat disassembly. This

mechanism is reminiscent of the activity of nucleotide dependent chaperones, e.g. Hsc70 and thus similar to the process of coat disassembly described for clathrin coated vesicles. In this model, ArfGTP together with the catalytic domain of ArfGAP would functionally resemble the ATP binding domain of Hsc70, and the non-catalytic domain of ArfGAP would resemble the substrate-binding domain of Hsc70.

4 Material and Methods

4.1 Materials

4.1.1 Chemicals and Equipment

4.1.1.1 Chemicals

Avanti Polar Lipids	Alabaster, USA
Agilent Technologies	Böblingen, Germany
Avantor	Center Vallley, USA
BD	Franklin Lakes, USA
Biochrom	Berlin, Germany
Biomers	Ulm, Germany
BioRad	München, Germany
Boehringer	Mannheim, Germany
Fermentas	Vilnius, Lithuania
Fluka	Taufkirchen, Germany
GE-Healthcare	Freiburg, Germany
Greiner Bio-One	Frickenhausen, Germany
Life Technologies/Invitrogen	Carlsbad, USA
Macherey-Nagel	Düren, Germany
Merck	Darmstadt, Germany
Millipore	Schwalbach, Germany
New England Biolabs	Frankfurt, Germany
PeqLab	Erlangen, Germany
Roche	Mannheim, Germany
Roth	Karlsruhe, Germany
Sarstedt	Nümbrecht, Germany
Sartorius	Goettingen, Germany
Serva	Heidelberg, Germany
Sigma-Aldrich	Taufkirchen, Germany
Source	BioScience Nottingham, UK
Thermo Fischer Scientific	Rockford, USA
Qiagen	Hilden, Germany

4.1.2 Materials for Biochemical Methods

4.1.2.1 Primary Antibodies

Antigen	Name	Species	Application	Dilution	Creator
ArfGAP1	GAP1 rab2	rabbit	WB	1:2500	Weimer et al., 2008
ArfGAP2	GAP2 rab2	rabbit	WB	1:5000	Weimer et al., 2008
ArfGAP3	GAP3 rab2	rabbit	WB	1:5000	Weimer et al., 2008
Arf 1 (C terminus)	Arf-C1 Emma	rabbit	WB	1:5000	Reinhard et al., 2003
α-COP	1409A	rabbit	WB	1:2000	Wieland lab
α-COP	alpha-COP1-10 rab3	rabbit	WB	1:500	Britta Brügger
β-COP	899	rabbit	WB	1:5000	Harter et al., 1993
δ-COP	877	rabbit	WB	1:5000	Faulstich et al., 1996
γ-COP 1/2	gamma-R	rabbit	WB	1:10000	Pavel et al., 1993
p23	Henriette	rabbit	WB	1:10000	Jenne et al., 2002
p24	Elfriede	rabbit	WB	1:5000	Gommel et al., 1999
p27	2087	rabbit	WB	1:1000	Jenne et al., 2002
ERGIC53	C6	mouse	WB	1:200	Santa Cruz
Mannosidase II	Rab1	rabbit	WB	1:1000	Wieland lab

Tab. 4.1: Primary Antibodies.

4.1.2.2 Secondary Antibodies

Fluorophore-conjugated secondary antibodies were used for detection in the LI-COR Odyssey System (LI-COR BioSciences, Lincol, USA).

Antigen	Name	Species	Application	Dilution	Manufacturer
anti-rabbit	Alexa680	goat	WB	1:10000	Invitrogen
anti-rabbit	Alexa800	goat	WB	1:10000	Invitrogen
anti-mouse	Alexa680	goat	WB	1:10000	Invitrogen
anti-mouse	Alexa800	goat	WB	1:10000	Invitrogen

Tab. 4.2: Secondary Antibodies.

4.1.2.3 Lipids

All of the following lipids were purchased from Avanti Polar Lipids (Alabaster, USA) and were stored as chloroform solutions under argon at -20 °C.

Phospholipids	Species	Molecular Weight	Order number
PC	Liver, Bovine	786.113	840055
PE	Liver, Bovine	768.005	840026
PS	Brain, Porcine	812.041	840032
PI	Liver, Bovine	909.110	840042
Liss Rhod PE (18:1)		1301.715	810150
Sphingolipids			
SM (18:0)	Brain, Porcine	731.081	860062
Sterols			
Cholesterol	Wool, Ovine	386.654	700000

Tab. 4.3: Lipids used for the preparation of the Golgi-like mix.

4.1.2.4 Protein Standard for SDS-PAGE

The Precision Plus Protein Standard All Blue was purchased from BioRad, Munich. The molecular weight size range is between 2 and 250 kDa and consists of highly purified recombinant proteins of the sizes 250, 150, 100, 75, 50, 37, 25, 20, 15 and 10 kDa.

4.1.2.5 Protein Standard for Size Exclusion Chromatography (SEC)

The SEC protein standard was purchased from BioRad, Munich. It contains thyreoglobulin (670 kDa), bovine gamma-globulin (158 kDa), chicken ovalbumin (44 kDa), equine myoglobulin (17 kDa), and vitamin B12 (1.35 kDa).

4.1.2.6 Chromatography Columns

The chromatography columns were purchased from GE Healthcare (Munich, Germany). Ni Sepharose 6 Fast flow (GE Healthcare, Munich, Germany) was used for affinity purification of His-tagged proteins. One-STrEP-tag proteins were purified via Strep-Tactin Sepharose (iba, Goettingen, Germany). Size exclusion chromatography was performed on Superdex75, Superdex200 and Superose6 columns of various sizes (GE Healthcare, Munich, Germany).

4.1.2.7 Nucleotides

All nucleotide stock solutions were prepared in 25 mM HEPES pH 7.4 (KOH) in a concentration of 25 mM and stored at -20 °C.

Name	Abbreviation	Purity	Manufacturer
Guanosine 5′-triphosphate	GTP	99 %	Sigma-Aldrich
Guanosine 5′-diphosphate	GDP	≥ 85 %	Sigma-Aldrich
Guanosine 5′-[γ-thio]-triphosphate	GTPγS	≥ 75 %	Sigma-Aldrich
Guanosine 5′-[β,γ-imido]-triphosphate	GMP-PNP	≥ 85 %	Sigma-Aldrich
Adenosine 5′-triphosphate	ATP	> 98 %	Roche

Tab. 4.4: Nucleotides.

4.1.2.8 ATP Regenerating System

The ATP regeneration system was prepared according to (Beckers et al., 1987) in assay buffer and utilized for the preparation of COPI vesicles in vitro.

10 mM ATP (Roche)
400 mM Sodium creatine phosphate (Sigma-Aldrich)
2000 µg/ml Creatine phosphokinase (Roche)

4.1.2.9 Protease Inhibitors

Complete Protease Inhibitor Cocktail Mix from Roche (Mannheim, Germany) was used for the purification of recombinant proteins.

4.1.3 Materials for Molecular Biology and Cell Culture Methods

4.1.3.1 Prokaryotic Strains

Strain	Species	Application	Manufacturer
DH5α	E.coli	subcloning	Invitrogen
Nova Blue	E.coli	subcloning	Novagen
BL21 star	E.coli	protein expression	Invitrogen
BL21 pLysS	E.coli	protein expression	Invitrogen
DH10MultiBac	E.coli	Bacmic production	I. Berger (Zürich)

Tab. 4.5: Prokaryotic Strains.

4.1.3.2 Eukaryotic strains

Strain	Species	Application	Manufacturer
HeLa	human	Semi-intact cells	ACC57 (DSMZ)
Sf9	Spodoptera frugiperda	Protein expression	Invitrogen

Tab. 4.6: Eukaryotic Strains.

4.1.3.3 Restriction Enzymes

All restriction enzymes were purchased from New England Biolabs (Frankfurt, Germany). T4 DNA ligase was purchased from Fermentas (Vilnius, Lithuania), Pfu turbo DNA polymerase from Agilent Technologies (Boeblingen, Germany), alkaline phosphatase from Roche (Mannheim, Germany).

4.1.3.4 Plasmids

Plasmid	Plasmids	Insert	Creator
pFB-rAG1#1	pFastBac HT B	Rat ArfGAP1	C. Weimer
pFB-rAG2#1	pFastBac HT B	Rat ArfGAP2	C. Weimer
pFB-rAG3#2	pFastBac HT B	Rat ArfGAP3	C. Weimer
pFB HT B ArfGAP1 S-tag	pFastBac HT B	S-tag	This thesis
pFB HT B ArfGAP2 S-tag	pFastBac HT B	S-tag	This thesis
pFB HT B ArfGAP3 S-tag	pFastBac HT B	S-tag	This thesis
pFBHTb 1-137 ArfGAP1	pFastBac HT B	1-137 ArfGAP1	This thesis

Tab. 4.7: Plasmids.

4.1.3.5 Oligonucleotide and PCR Primers

Primer	Sequenz	Manufacturer
S-tag Sfo	GCCAAAGAAACCGCTGCTGCTAAATTCGAACGCC AGCACATGGACAGCG	Biomers
S-tag BamHI	GATCCGCTGTCCATGTGCTGGCGTTCGAATTTAG CAGCAGCGGTTTCTTTGGC	Biomers

Tab. 4.8: Oligonucleotides.

Primer	Sequenz	Manufacturer
1-137 ArfGAP1 BamHI	GGAGGAGGATCCATGGCCAGC	Biomers
1-137 ArfGAP1 XhoI	GAAGAACTCGAGCTAAGGTGGGGTCCAGTT	Biomers

Tab. 4.9: PCR Primers.

4.1.3.6 Media for Prokaryotic Cell Culture

Medium	Ingredients	Concentration	Manufacturer
LB	Bacto-Trypton	10 g/L	BD
	Bacto Yeast Extract	5 g/L	BD
	Sodium chlorid	5 or 10 g/L	Roth
LB-Agar	Bacto-Trypton	10 g/L	BD
	Bacto Yeast Extract	5 g/L	BD
	Sodium chlorid	5 or 10 g/L	Roth
	Agar	15 g/L	Roth
SOC	Bacto-Trypton	20 g/L	BD
	Bacto Yeast Extract	5 g/L	BD
	Sodium chlorid	0.59 g/L	Carl Roth
	Potassium chlorid	0.19 g/L	Avantor
	Magnesium chlorid	10 mM	Carl Roth
	Glucose	20 mM	Merck
NZYM	Magnesium sulfate	2 g/L	Sigma-Aldrich
	Protein hydrolysate	10 g/L	
	N-Z-amine	5 g/L	
	Sodium chloride	5 g/L	
	Yeast extract		

Tab. 4.10: Media for prokaryotic cell culture.

4.1.3.7 Media for Eukaryotic Cell Culture

Medium	Additives	Manufacturer
DMEM	10 % (v/v) FCS 100 µg/ml Penicillin/Streptomyin	Sigma-Aldrich
Alpha-MEM	10 % (v/v) FCS 100 µg/ml Penicillin/Streptomyin	Sigma-Aldrich
GIBCO SF-900 II SFM	-	Invitrogen

Tab. 4.11: Media for eukaryotic cell culture.

4.1.3.8 DNA Ladder

1kb DNA ladder was purchased from New England Biolabs (Frankfurt, Germany).

4.1.3.9 Antibiotics

Antibiotic	Concentration (1000x)	Storage	Solvent
Ampicillin	100 mg/ml	-20 °C	Milli Q Water
Kanamycin	50 mg/ml	-20 °C	Milli Q Water
Gentamycin	7 mg/ml	Room temperature	Milli Q Water
Tetracyclin	10 mg/ml	-20 °C, light protection	Ethanol

Tab. 4.12: Antibiotics.

4.2 Methods

4.2.1 Biochemical Methods

4.2.1.1 Sodium Dodecyl Sulfate Polyacrylamide Gel Electrophoresis

- Acrylamid solution: Rotiphorese Gel 30 (Roth):
  30 % (w/v) Acrylamid
  0,8 % (w/v) N,N' -
  Methylenbisacrylamid

- 4 x Separating gel buffer: 1,5 M Tris-HCl, pH 8,8

- 4 x Stacking gel buffer: 0,5 M Tris-HCl, pH 6,8

- 1 x SDS running buffer: 25 mM Tris
  192 mM Glycin
  0,1 % (w/v) SDS

- 4 x Protein sample buffer: (reducing)
  200 mM Tris-HCl, pH 6,8
  40 % (v/v) Glycerol
  12 % (v/v) β-Mercaptoethanol
  8 % (w/v) SDS
  0,2 % (w/v) Bromphenolblue

- 4 x Protein sample buffer (non-reducing)
  200 mM Tris-HCl, pH 6,8
  40 % (v/v) Glycerol
  8 % (w/v) SDS
  0,2 % (w/v) Bromphenolblue

- Coomassie staining solution: 0,25 % (w/v) Coomassie Brilliant Blue
  40 % (v/v) Ethanol
  10 % (v/v) Acetic Acid

- Distaining solution: 20 % (v/v) Ethanol
  5 % (v/v) Acetic Acid

- PBS: 35,7 mM Na2HPO4
  14,3 mM KH2PO4
  136 mM NaCl
  3 mM KCl

- PBS-T: 0,05 % Tween 20 in PBS

4.2.1.2 Sample preparation for SDS-PAGE

The protein solution was diluted in a ratio of 3:4 in 4x protein sample buffer and incubated for 5 min at 95 °C. After a short centrifugation, the samples were loaded on a SDS gel.

4.2.1.3 Electrophoresis Conditions

Proteins, supplemented with protein sample buffer and denatured at 95 °C, were analysed using a BIORAD system, which is based on a modified, discontinuous gel system (Laemmli, 1970). The voltage was kept constant both in the stacking and the separation gel (200 V during the entire procedure).

4.2.1.4 Coomassie Staining

The gels were incubated for 20 min in Coomassie staining solution at room temperature. In order to visualise the protein bands, the gels were then washed in destaining solution for 1 h at room temperature.

For 2 Gels	4 %	12 %	15 %
Water	3.05 ml	3.35 ml	2.35 ml
4 x Stacking gel buffer	1.25 ml	-	-
4 x Separating gel buffer	-	2.50 ml	2.50 ml
Acrylamid solution	0.65 ml	4.00 ml	5.00 ml
10 % APS solution	0.05 ml	0.10 ml	0.10 ml
10 % SDS solution	0.05 ml	0.10 ml	0.10 ml
TEMED	0.01 ml	0.01 ml	0.01 ml
Total volume	5.06 ml	10.06 ml	10.06 ml

Tab. 4.13: Coomassie staining.

4.2.1.5 Western blot analysis

- PBS: 14.3 mM KH_2PO_4, 35.7 mM Na_2HPO_4, 137 mM NaCl, 3 mM KCl, pH 7.4
- PBS-T: PBS with 0.05 % Tween
- Blocking buffer: PBS containing 5 % non-fat dry milk
- Ponceau S staining solution: 0.8 % Ponceau S, 4 % TCA (Serva, Germany)

Proteins were transferred from SDS-PAGE gels onto PVDF membranes (Immobilon-P, Millipore, Eschborn) by the use of "wet" blot or "semi-dry" blot procedure in cells manufactured by BioRad (Munich, Germany).

4.2.1.6 Semi-dry Blot

- Blot buffer: 25 mM Tris base, 200 mM glycine, 20 % methanol

Per gel 7 filter papers (Whatman 3 mm) and one PVDF-membrane were cut 7 x 9 cm. The membrane was pre-activated in methanol. Four papers were soaked in the blot buffer and placed on the anode plate. On top of these was placed the PVDF membrane followed by the SDS gel. Finally, the 3 remaining filter papers were soaked in the blot buffer and applied on top. Proteins were then transferred onto the membrane at 18 V (constant voltage) for two hours.

4.2.1.7 Wet Blot

- Blot buffer: 25 mM Tris base, 200 mM glycine, 20 % methanol

Per gel four filter papers (Whatman 3mm) and one PVDF-membrane were cut 7 x 9 cm. The membrane was pre-activated in methanol. Two papers were soaked in the blot buffer and placed on a foam pad over the anode plate (white side of the BioRad holder cassette). On top of these was placed the PVDF membrane followed by the SDS gel. The two remaining filter papers were soaked in the blot buffer and applied above. Finally, a second foam pad was placed on top and the holder cassette was closed. Proteins were then transferred onto the membrane at 100 V (constant voltage) for two hours or at 30 V (constant voltage) over night.

4.2.1.8 Immunodetection of proteins on PVDF membranes

In order to block unspecific binding sites, the membranes with transferred proteins were first incubated for 1 h at room temperature with PBS containing 5 % (w/v) fat-free milk powder. Afterwards, the membranes were washed 3 times for 10 min in PBS-T and incubated for 1 h at room temperature/ overnight at 4 °C with the required

primary antibody diluted in PBS-T containing 2 % (w/v) bovine serum albumine. Subsequently, the blots were washed 3 times for 10 min with PBS-T and incubated with the secondary antibody, diluted in PBS-T containing 2 % (w/v) bovine serum albumine for 1h at room temperature. From this step on, the membrane was protected from light, as the fluorophores coupled to the secondary antibody are light sensitive. After three 10-min washes with PBS-T and one 5-min wash with PBS (for removal of the Tween), the membrane was exposed to the LI-COR Odyssey system manufactured by LI-COR Biosciences (Lincoln, USA). For detection, the protocol of the manufacturer was followed.

4.2.1.9 Bradford Assay

Protein concentrations were determined using a staining solution purchased from BioRad (Munich, Germany). The Bradford reagent was diluted 1:5 with water. All samples were prepared in a final volume of 1 ml with the pre-diluted Bradford reagent. A 1 mg/ml BSA standard solution was used as a reference. The BSA calibration curve consists of 7 points (BSA protein per sample): 0 µg/ml, 2.5 µg/ml, 5 µg/ml, 10 µg/ml, 15 µg/ml, 20 µg/ml and 25 µg/ml. The concentration of the protein of interest was measured in a triplicate. After 5-min incubation at room temperature, 200 µl of each sample were transferred into a 96-well plate and the optical density at 620 nm was measured in an ELISA reader.

4.2.1.10 Protein Expression

4.2.1.10.1 Expression of 1-137 ArfGAP1, 137-337 ArfGAP1, 204-362 ArfGAP2, 301-521 ArfGAP2, ArfGAP2 QKV and ArfGAP3 QKV in E.coli

- LB Medium: 20 g BactoTryptone, 10 g Yeast Extract, 20 g NaCl, 2 l of H_2O
- Ampicillin: 100 mg/ml stock solution, used in 1: 1000 dilution
- Kanamycin: 50 mg/ml stock solution, used in 1: 1000 dilution

A single *E. coli* colony was picked from an LB agar plate and used to inoculate 25 ml of LB medium containing the appropriate antibiotics. The pre-culture was incubated overnight at 37 °C with agitation. On the next day, 2 l of LB medium containing antibiotic were inoculated with 20 ml of the pre-culture and grown at 37 °C, 180 rpm until OD_{600} reached about 0.6. IPTG was then added to 1 mM final concentration and the incubation resumed at 37 °C for another 4 h.

After the end of the expression, the cells were recovered by centrifugation (4000 x g, 20 min) and the pellet was washed once in 50 ml PBS. The pellet was then snap frozen in liquid nitrogen and stored at -80 °C.

4.2.1.10.2 Expression of myrArf from E.coli

The two plasmids pHV738 (encodes hNMT1 and Met aminopeptidase), which has a kanamycin resistance, and pMON5840-Arf1wt, which has an ampicillin resistance, were cotransfected in BL21 (DE3) bacterial strain (for the transfection protocol see below). A pre-culture was prepared overnight at 37 °C from a single colony in NZYM medium supplied with 100 µg/ml ampicillin and 30 µg/ml kanamycin. On the next day, a main culture was prepared by inoculating 2 l of NZYM medium containing 100 µg/ml ampicillin and 30 µg/ml kanamycin with 20 ml of the overnight culture. The bacteria was grown at 37 °C until OD_{600}=0.6 was reached. The flasks were cooled down to 27 °C for 30 min in the cold room (4 °C). From here on, expression was performed at 27 °C. In the meantime, the sodium myristate solution/fat-free BSA mixture was prepared. Per one liter of culture, 21 mg of sodium myristate were dissolved in 1,25 ml of ddH_2O by heating up the solution in the microwave. Subsequently, 9.1 ml of prewarmed ddH_2O and 1.5 ml of 30 % fat-free BSA were added. After a ten-minute incubation of the bacterial culture with the sodium myristate solution/fat-free BSA mixture, 1 nM IPTG was added to induce the expression of the hNMT1 and the Met aminopeptidase, which increases the efficiency of the expression by facilitating the myristoylation. After one-hour incubation, the bacterial culture was supplied with 30 µg/ml of nalidixic acid dissolved in 300 mM NaOH in order to induce the Arf expression. The culture was incubated for further four hours at 27 °C and then the bacteria were harvested via a centrifugation at 4000 rpm for 20 min. After, a wash with PBS, the pellet was snap-frozen in liquid nitrogen and stored at -80 °C.

4.2.1.10.3 Expression of ArfGAP1, ArfGAP2, ArfGAP3, His-tagged coatomer, and One-STrEP-tag coatomer from Sf9 Cells

In order to express ArfGAP1, ArfGAP2 and ArfGAP3, His-tagged coatomer, and One-STrEP-tag coatomer from Sf9 Cells, 500 ml of 2 x 10^6 SF9 cells/ml were infected with the corresponding amount of P2 virus (for the preparation of the virus see Cell Culture Methods). The insect cells were then incubated for 72 h at 27 °C while stirred at 140 rpm. Subsequently, the cells were spun down at 2000 rpm for 5min. The obtained pellet was washed once with 30 ml of cold PBS, snap-frozen in liquid nitrogen and stored at -80 °C.

4.2.1.10.4 Cell Lysis

Cell pellets were thawed in a 20 °C water bath, resuspended in lysis buffer (content dependent on the protein preparation, see below) and disrupted by multiple passages through a high pressure cell homogeniser (Microfluidizer M-110L, 2010219, Microfluidics International Corporation, Westwoos, MA, USA): two passages for the Sf9 cell lysates and 5 passages for the *E.coli* bacterial lysates. Lysates were then centrifuged at 100 000 x g, 4 °C for 1 h. The obtained supernatant was used as a starting material for the purification.

4.2.1.11 Protein Purification

4.2.1.11.1 Purification of myrArf1 Wild Type from E.coli

- Lysis Buffer: 50 mM Tris, 1 mM DTT, 1 mM $MgCl_2$, 1 mM GDP, 40 µl Pepstatin A, 1 mM PMSF, 1 tablet of Roche Protease Inhibitor, pH 8
- Buffer B: 50 mM Tris, 1 mM DTT, 1 mM $MgCl_2$, pH 8
- Resuspension Buffer C: 20 mM Tris, 1 mM DTT, 1 mM $MgCl_2$, 200 µl GDP, 1 tablet of Roche Protease Inhibitor, pH 8
- PD-10 Buffer D: 10 mM Tris, 1 mM DTT, 1 mM $MgCl_2$, pH 8
- Equilibration Buffer E: 250 mM Tris, 1 mM DTT, 5 mM $MgCl_2$, pH 8
- Elution Buffer F: 10 mM Tris, 1 M KCl, 1 mM DTT, 5 mM $MgCl_2$, pH 8

All buffers were sterile filtrated and adjusted to the corresponding pH at 4°C. Afterwards, they were stored at 4°C.

After cell lysis in Lysis buffer and ultracentrifugation, the protein extract was adjusted to a final volume of 200 ml with Buffer B and subjected to a 35 % ammonium sulfate precipitation by addition of 38 g of ammonium sulfate powder. myrArf1 was enriched into the precipitate, subsequently centrifuged at 8000x g for 20 min and then resuspended in Resuspension Buffer C. Following desalting by a PD-10 gelfiltration column (GE Healthcare, Munich) using PD-10 Buffer, the proteins were subjected to DEAE anion exchange chromatography with PD-10 Buffer. The column was previously equilibrated with: 5x column volumes Equilibration buffer E, 5x column volumes PD-10 buffer D, 5x column volumes elution buffer F and 5x column volumes PD-10 buffer D. The sample was loaded by a 10 ml Superloop (GE Healthcare, Munich) and the column was washed with PD-10 buffer D until a baseline for UV280 and conductivity was reached. Bound proteins were eluted with a linear gradient from 0 to 1 M potassium chloride (0 to 100 % Elution buffer F) in 10 column volumes by

0.5 ml/min (100 min). 0.5 ml fractions were collected. Normally, Arf1 elutes at relatively low conductivity which corresponds to the first peak in the elution profile. By this procedure, a 90 % enrichment for the myristoylated form was yielded. Fractions were collected and further analysed by SDS-PAGE on a 15 % gel.

4.2.1.11.2 Purification of His-tagged/ S-tagged + His-tagged ArfGAP1/2/3 from Sf9 cells

- Lysis Buffer: 50 mM HEPES, 0.02 % (v/v) MTG, 300 mM KCl, 30 mM Imidazole, 1 tablet of Roche Protease Inhibitor, pH 7.4
- Washing Buffer: 50 mM HEPES, 0.02 % (v/v) MTG, 300 mM KCl, 50 mM Imidazole, pH 7.4
- Elution Buffer: 50 mM HEPES, 0.02 % (v/v) MTG, 300 mM KCl, 250 mM Imidazole, pH 7.4
- Gel Filtration Buffer: 50 mM HEPES, 0.02 % (v/v) MTG, 150 mM KCl, 1mM $MgCl_2$ 10 % (w/v) Glycerol, pH 7.4

All buffers were sterile filtered and the pH was adjusted at 4°C.

The purifcation was performed with one pellet obtained from 500ml of Sf9 culture. The cells were resuspended in lysis buffer and lysis was done as described above. Upon centrifugation of the cell lysate at 100000 x g for 1h in a 50.2Ti rotor (Beckmann Coulter, Krefeld, Germany), the supernatant was subjected to a one-hour incubation with 3 ml dry volume of Ni Sepharose Fast Flow beads (GE Healthcare, Munich, Germany). The beads were prequilibrated by two washes with water and one wash with washing buffer. The protein was eluted by gravity flow in steps of 0.5 ml. The fractions with the highest concentration were pooled and concentrated in a ultra centrifugation units from Sartorius (MWCO= 20 kDa) to a volume of 3 ml. The pool was then loaded on a Superdex 200 HighLoad 16/60 prep grade gel filtration column from GE Healthcare (Munich, Germany) connected to an Ettan FPLC System (GE Healthcare). The fractions containing the protein of interest were pooled and the quality of the protein was analysed by SDS-PAGE. Subsequently, the pool was aliquoted, snap-frozen in liquid nitrogen and stored at -80 °C.

4.2.1.11.3 Purification of His-tagged coatomer from Sf9 cells

- Lysis Buffer: 25 mM HEPES, 0.02 % (v/v) MTG, 200 mM KCl, 30 mM Imidazole, 1 tablet of Roche Protease Inhibitor, pH 7.4
- Washing Buffer: 25 mM HEPES, 0.02 % (v/v) MTG, 200 mM KCl, 50 mM Imidazole, pH 7.4
- Elution Buffer: 25 mM HEPES, 0.02 % (v/v) MTG, 200 mM KCl, 250 mM Imidazole, pH 7.4

- Gel Filtration Buffer: 25 mM HEPES, 0.02 % (v/v) MTG, 200 mM KCl, 10 % (w/v) Glycerol, pH 7.4

The purifcation was performed with one pellet obtained from 250ml of Sf9 culture according to the procedure described in 4.2.1.11.2 The fractions with the highest concentration after the elution from the Ni beads were pooled and concentrated in a ultracentrifugation units from Sartorius (MWCO= 100 kDa) to a volume of 0.5ml. The pool was then loaded on a Superose 6 HighLoad 10/300 GL column from GE Healthcare (Munich, Germany) connected to an Ettan FPLC System (GE Healthcare). The fractions containing the protein of interest were pooled, analysed by SDS-PAGE and aliquoted. After a snap-freezing in liquid nitrogen, the fractions were stored at -80 °C.

4.2.1.11.4 Purification of One-STrEP-tag coatomer from Sf9 cells

- Column Buffer: 25 mM HEPES, 10 % w/v Glycerol, 200 mM KCl, 1 mM DTT, 1 tablet of Roche Protease Inhibitor, pH 7.4
- Elution Buffer: 25 mM HEPES, 10 % w/v Glycerol, 200 mM KCl, 1 mM DTT, 2.5 mM D-desthiobiotin, 1 tablet of Roche Protease Inhibitor, pH 7.4
- Buffer W: 100 mM Tris-HCl, 150 mM NaCl, 1 mM EDTA, pH 8.0
- Buffer R: 100 mM Tris-HCl, 150 mM NaCl, 1 mM EDTA, 1 mM HABA (2-(4-hydroxyphenylazo)-benzoic acid), pH 8.0

All buffers were sterile filtered and the pH was adjusted at 4 °C for the buffers for the purification and at room temperature for the buffers for the regeneration.
The purifcation was performed with one pellet obtained from 500 ml of Sf9 culture. The cells were resuspended in lysis buffer and lysis was done as described above. Upon centrifugation of the cell lysate at 100000 x g for 1h in a 50.2Ti rotor (Beckmann, Krefeld, Germany), the supernatant was subjected to a two-hour incubation with 2 ml dry volume of StrepTactin Sepharose (IBA GmbH, Goettingen, Germany). The beads were prequilibrated by two washes with 25ml of Lysis buffer in a 25 ml Econo-Pac disposable chromatography column from BioRad (Munich, Germany). The protein was eluted by gravity flow in steps of 0.5 ml with 2 min of incubation time between the steps. The individual fractions were analysed by SDS-PAGE and subsequently, the ones with the highest purity, were pooled. Prior to a snap-freezing in liquid nitrogen and storage at -80 °C, the buffer was exchanged back to the Column buffer via PD-10 desalting coulumns (GE Healthcare, Munich, Germany) according to the protocol of the manufacturer.

After the purification, the StrepTactin Sepharose was regenerated and used multiple times. For the regeneration, the beads were washed twice with 5 column volumns of elution buffer, twice with 5 column volumns of buffer W and three times with 5 column volumns of buffer R. The beads were stored at 4 °C until the next purification.

4.2.1.11.5 Purification of 1-137 ArfGAP1 , 137-337 ArfGAP1, 204-362 ArfGAP2, 301-521 ArfGAP2, ArfGAP2 QKV and ArfGAP3 QKV from E.coli

- Resuspension Buffer 1: 20 mM Tris, 2mM MTG, 6 M guanidine hydrochloride, 1 tablet of Roche Protease Inhibitor, pH 8
- Resuspension Buffer 2: 20 mM Tris, 2mM MTG, 5 M guanidine hydrochloride, pH 8
- Elution Buffer: 20 mM Tris, 2mM MTG, 5 M Guanidine hydrochloride, 200mM Imidazole, pH 8
- Dialysis Buffer 1: 25 mM HEPES, 1 mM DTT, 300 mM NaCl, pH 7.4
- Dialysis Buffer 2: 25 mM HEPES, 1 mM DTT, 150 mM NaCl, pH 7.4

All buffers were sterile filtered and the pH was adjusted at 4 °C.

One pellet obtained from 2 L bacterial culture was thawn on ice. At the harvesting step, it was taken care that the pellet was as much depleted from the PBS used for washing as possible. Then, the pellet was mixed with 250 ml of Resuspension Buffer 1. In order to remove the released DNA, 1 µl of Benzonase Nuclease from Sigma Aldrich (Steinheim, Germany) was added. The suspension was placed in a glass beaker at 4 °C and stirred with a magnetic stirrer for 30 min. Subsequently, the bacteria was disrupted by five passages through a high pressure cell homogeniser (Microfluidizer M-110L, 2010219, Microfluidics International Corporation, Westwoos, MA, USA). The lysate was then subjected to a centrifugation at 14 000 rpm for 20 min in SLC 1400, Sorval rotor. 3ml of Ni Sepharose Fast Flow beads (GE Healthcare) per pellet were pre-equlibrated by two washes in ddH_2O and one wash in Resuspension Buffer 1. The supernatant from the centrifugation was incubated with the pre-equilibrated Ni beads for 1 h on a rotary wheel at 4 °C. Afterwards, the lysate/beads mixture was transffered in a Econo-Pac disposable chromatography column from BioRad (Munich, Germany) and the unbound protein was removed via two washes with 25 ml of Resuspension buffer 2. The protein was eluted with Elution buffer in 0.5 ml fractions by gravity flow. The individual fractions were analyzed by SDS-PAGE and the fractions containing the protein of interest were pooled. The pool was transferred in 3 ml Slide-A-Lyzer Dialysis Cassette (Thermo Scientific, Rockfor, USA) and dialysed at 4 °C twice for 1 h against 1 L of Dialysis buffer 1, and once overnight against 1 L of Dialysis buffer 2. The sample was removed with a syringe

from the Slide-A-Lyzer Dialysis Cassette, aliquoted, snap-frozen in liquid nitrogen and stored at -80°C. For the handling of the Slide-A-Lyzer Dialysis Cassette see protocol of the manufacturer.

4.2.1.11.6 Affinity Purification of anti-ArfGAP1/2/3 antibody

- PBS: 14.3 mM KH_2PO_4, 35.7 mM Na_2HPO_4, 137 mM NaCl, 3 mM KCl, pH 7.4

ArfGAP1 peptide was previously immobilzed on Thiopropylsepharose beads. 2 ml of the Thiopropylsepharose beads were transferred on a 5 ml disposable column with frit (Bio-Rad, Munich). The Sepharose was washed 4x with 5 ml PBS. Subsequently, 3 ml of antisera obtained from a rabbit immunised with ArfGAP1 peptide to produce antibodies against ArfGAP1 were loaded on the column. The mixture was incubated for 1 hour and 30 min at room temperature on a rotary wheel. Afterwards, the sepharose was washed 4x with 5 ml PBS. The antibody was eluted with 0.1 M Glycin adjusted to pH 2.8. Before the start of the fraction collection, 8 µl of 1.5 M Tris/HCl pH 8.8 were added in each 1.5 ml reaction tube prepared for the elution. 15 fractions, 250 µl each, were collected. The Sepharose was washed with 5 ml PBS and stored in PBS containing 0.02 % Na-azid. The protein concentration was measured on a UV/ visible specrofluorometer (Ultraspec 2000, Pharmacia Biotech) at OD_{280}. The fractions with the highest concentration were pooled and dialysed twice 1 h and subsequently overnight in 500 ml PBS with 10 % Glycin. After the dialysis the antibody concentration was measured by Nanodrop, the protein was aliquoted, snap frozen in liquid nitrogen and stored at -80 °C.

4.2.1.12 Preparation of Liposomes

- HKM Buffer: 25 mM HEPES, 150 mM KCl, 1 mM $MgCl_2$, pH 7.4
- Lipid Mix (Bigay, 2003): 50 mol % PC, 19 mol % PE, 5 mol % PS, 10 mol % PI, 10 mol % Cholesterol

All phospholipids and cholesterol were purchased from Avanti Polar Lipids (see Tab. 4.3). The lipid composition of interest was generated by transferring the desired concentrations of different lipid stocks, dissolved in chloroform, (for the Golgi-like composition see Materials) to a 1.5ml Eppendorf tube (Eppendorf, Hamburg, Germany) to a final total lipid concentration of 3 mM in a volume of 300µl. Depending on the experimental set-up 30nmol of lyophilized MPB-PE-C-p23 or 1 % of PiP2 (brain) or Liss Rhod PE (18:1) were added to the reaction mixture. The lipid stock was overlaid immediately with Argon in order to prevent oxidation. The lipids were dried using a stream of nitrogen until the chloroform was completely evaporated and the lipids formed a film on the walls of the tube. The tube was covered with

(perforated) parafilm and put under a vacuum for 30 min to remove any residual chloroform. Then, lipid film was resuspended in 900 µl of HKM buffer and vortexed until the solution appeared to be homogeneous. In order that unilaminar vesicles were formed, the lipids were subjected to ten freeze-thaw cycles: the suspension was first immersed into liquid nitrogen until it froze completely, then thawed in a water bath prewarmed to 37 °C. Liposomes were either stored frozen at -80 °C or extruded directly through a filter (Nuclepore Track-Etch Membrane, Whatman, Maidstone, United Kingdom, for the pore size see Results) and used immediately.

4.2.1.13 Tryptophan Fluorescence Measurements (Bigay et al., 2003)

- HKM Buffer: 25 mM HEPES, 150 mM KCl, 1 mM $MgCl_2$, pH 7.4

This fluorometric assay was used to monitor Arf1 nucleotide exchange *in vitro*. Tryptophane fluorescence was measured at 340 nm (bandwidth 20 nm) upon excitation at 297.5 nm (bandwidth 3 nm) in a Jasco spectrofluorometer equipped with a stirring device and injection platform. All assays were performed at 37 °C and 450 rpm in a final volume of 600 µl.

First of all, extruded liposomes (100 µM) were placed into a cylindrical quartz cuvette containing HKM buffer. Recombinantly expressed and purified myr-Arf (1 µM) was added and activated by the sequential addition of 100 µM GTP and 2 mM EDTA. After 10 min, the reaction mixture was supplied with 4 mM $MgCl_2$. GTP hydrolysis was initiated by the addition of different concentrations of ArfGAP1/2. For simplicity, the fluorescence level of Arf1-GDP was set to zero and the fluorescence level after the GTP loading step was set to 100 AU (arbitrary units). Therefore, the fluorescence scale shown in the figures directly reflects the fraction of Arf1 that undergoes GTP hydrolysis.

4.2.1.14 Static Light Scattering Measurements (Bigay et al., 2003)

- HKM Buffer: 25 mM HEPES, 150 mM KCl, 1 mM $MgCl_2$, pH 7.4

This fluorometric assay was used to monitor coating and uncoating of COPI vesicles *in vitro*. Static light scattering was measured at 340 nm (bandwidth 20 nm) in a Jasco spectrofluorometer equipped with a stirring device and injection platform. All assays were performed at 37 °C and 450 rpm in a final volume of 600 µl.

First of all, extruded liposomes (100 µM) were placed into a cylindrical quartz cuvette, which already contained HKM buffer. Recombinantly expressed and purified myr-Arf (1 µM) and coatomer (0.2 µM) were added and activated by the sequential

addition of 100 µM GTP and 2 mM EDTA. After 10 min, the reaction mixture was supplied with 4 mM $MgCl_2$. Uncoating was initiated by the addition of different concentrations of ArfGAP1/2. For simplicity, the fluorescence level of Arf1-GDP was set to zero and the fluorescence level after the GTP loading step was set to 100 AU (arbitrary units). Therefore, the fluorescence scale shown in the figures directly reflects the fraction of the coat, which dissociates from the membrane.

4.2.1.15 Preparation from Golgi-enriched Membranes from Rabbit Liver

- Homogenization buffer: 10 mM Tris/HCL pH 7.4, 0.5 M Sucrose, 5 mM DTT, 5 mM EDTA, 1 Tablette/50ml Roche Protease Inhibitor
- Assay buffer: 25 mM HEPES, 2.5 mM MgOAc, pH 7.2

Per membrane preparation, eleven male Wistar rats were subjected to a narcosis with diethylether, sacrificed and left shortly to bleed out. The livers were instantly excised and placed in cold homogenization buffer on ice. Subsequently, the liver was cut into small pieces, weight and washed once with homogenization buffer. Three volumes of homogenization buffer were added and the liver was homogenized with Ultra Thorax (IKA T18 basic, IKA Works, Inc., Wilmington, USA) three times for 20 sec each. The homogenate was then centrifuged at 2200 rpm for 10 min at 4°C. The post-nuclear supernatant was filtered through three layers of cheesecloth, transferred in ten SW32 tubes and overlaid with 20 ml of 1.25 M sucrose dissolved in 10 mM Tris-HCL, pH 7.4. The tubes were then subjected to a 100 000 x g centrifugation in SW32Ti rotor for 90 min at 4 °C. After removal of the top lipid layer with a vacuum pump, the sucrose interface was taken and the refractive index was determined. The sucrose final concentration was then adjusted to 1.215 M with sucrose powder. The interface was once again separated in ten fractions, transferred into SW32 tubes and overlaid with 10 ml of 1.1 M sucrose dissolved in 10 mM Tris-HCL, pH 7.4, 10 ml of 1.0 M sucrose dissolved in 10 mM Tris-HCL, pH 7.4 and 10 ml of 0.5M sucrose dissolved in 10 mM Tris-HCL, pH 7.4. After centrifugation at 100 000 x g in SW32Ti rotor for 150 min at 4 °C, the interface between 0.5 M and 1.0 M sucrose was collected. The refractive index of the Golgi-enriched fraction was determined and the sucrose final concentration was diluted to 250 mM by the addition of 10 mM Tris-HCL, pH 7.4. Subsequently, the solution was transferred into SW32 tubes and underplayed with 1.5 ml of 50 % sucrose solution dissolved in 10 mM Tris-HCL, pH 7.4. After centrifugation at 100 000 x g in SW32Ti rotor for 60 min at 4 °C, the interface was collected and homogenized by pipetting. The Golgi membranes were

then salt washed by an adjustment of the KCl concentration to 500 mM with 3 M KCl. The solution was transferred to SW32 tubes, underplayed with 3 ml 23 % sucrose dissolved in assay buffer and 0.2 ml 50 % sucrose dissolved in assay buffer, and subjected to a centrifugation at 100 000 x g in SW32Ti rotor for 60 min at 4 °C. The Golgi fraction was then collected. After a determination of the refractive index and the protein concentration, it was aliquoted, snap frozen and stored at -80 °C.

4.2.1.16 Vesicle Preparation from rat-liver Golgi modified from (Beck et al., 2008)

- Assay Buffer: 25 mM HEPES, 2.5 mM Mg_2Ac, pH 7.2

COPI vesicles were generated from endogenous Golgi membranes isolated from rat liver. 120 µg of the purified mebranes were mixed with 10 µg of recombinant myrArf1, 25 µg of recombinant coatomer mix (50 % γ1ζ2, 30 % γ2ζ1 and 20 % γ1ζ2), 1 mM GTP and 0.25 mM DTT in a final volume of 250 µl. The assay was performed in the assay buffer described above. The final concentration of KCl in the assay was adjusted to 50 mM and the one of sucrose to 200 mM, where the amounts added were back calculated dependent on the concentrations of the two components present in the Golgi membrane preparation. After a five-minute incubation at 37 °C, the tubes were transferred on ice and the KCl concentration was increased to 250 nM. 2 % of the reaction mixture were taken as input and the set-ups were allowed to incubate for further 10 min on ice. The donor membranes were separated from the formed vesicles by a seven-minute centrifugation at 13000 rpm in a table-top centrifuge. The supernatant was transferred in a SW60 tube and underlayed with two sucrose cushons: 50 µl of 37.5 % w/w sucrose and 5 µl of 50 % w/w sucrose. The gradients were then centrifuged for 50 min at 32000 rpm in a SW60 swing-rotor and the 16 µl vesicle fraction was isolated from the boarder between the 37.5 % w/w sucrose and the 50 % w/w sucrose. 50 % of the vesicle fraction and 1 % of the input fraction were loaded on a 12 % polyacrylamid gel and subjected to SDS-PAGE. The analysis of the membrane associated material was performed via Western blot with specific primary antibodies and secondary antibodies coupled to Alexa dyes. The fluorescent signals were quantified in a Li-CORE Odyssey system (Lincoln, USA).

4.2.1.17 Preparation of Semi Intact Cells

- Assay Buffer: 25 mM HEPES, 150 mM KOAc, 2 mM MgOAc, pH 7.2
- PBS: 35.7 mM Na_2HPO_4, 14.3 mM KH_2PO_4, 136 mM NaCl, 3 mM KCl, pH 7.4

The protocol for the semi-intact cell preparation was modified from Mancias and Goldberg, 2007 for COPI vesicle preparations (Adolf et al., 2013) (Adolf and Wieland, 2013). HeLa cells were cultured in 15cm cell culture dishes (Greiner Bio-One GmbH, Frickenhausen, Deutschland) until 90 % confluence. After one wash with 15 ml cold sterile PBS, the cells were detached by an incubation with 1.5 ml of Trypsin per plate for five minutes at 37 °C. Subsequently, 300 µl of 1 mg/ml Trypsin inhibitor (Sigma-Aldrich) were added per plate and the detached cells were collected in 15 ml/plate of cold PBS (cells from three plates in one 50 ml reaction tube). The cells were then centrifuged for 5 min at 300 x g and 4 °C, resuspended in 20 ml (per three plates= 1 50 ml reaction tube) of cold PBS and permeabilized by the addition of 20 µl of 40 mg/ml Digitonin (Sigma-Aldrich) for 5 min at 4°C. The volume of the cold PBS was increased to 50 ml and the permeabilized cells were centrifuged 5 min at 300 x g and 4 °C. The PBS was discarded, the pellet was resuspended in 50 ml of assay buffer, and incubated for 10 min at 4 °C. After a five-minute centrifugation at 300 x g and 4 °C, the buffer was discarded and the cell pellet from 6 plates was resuspended in 500 µl of assay buffer. The total protein concentration was determined via a Bradford test and the cells were directly used for a vesicle preparation.

4.2.1.18 Vesicle Preparation from Semi Intact Cells modified from (Adolf and Wieland, 2013)

- Assay Buffer: 25 mM HEPES, 150 mM KOAc, 2 mM MgOAc, pH 7.2

COPI vesicles were generated from freshly permeabilized semi-intact HeLa cells. For the COPI vesicle formation, 100 µg of semi-intact cells were incubated for 30 min at 37 °C with 2 µg of recombinant myrArf1, 10 µg of recombinant coatomer mix (50 % γ1ζ2, 30 % γ2ζ1 and 20 % γ1ζ2), 1 mM GTP and 0.25 mM DTT in a final volume of 200 µl. The assay was performed in the vesicle preparation buffer described above. 1 % of the reaction mixture were taken as input. The donor membranes were separated from the formed vesicles by a ten-minute centrifugation at 10000 x g in a table-top centrifuge. The supernatant was transferred in a SW60 tube and underlaid with two sucrose cushons: 50 µl of 37.5 % w/w sucrose and 5 µl of 50 % w/w sucrose. The gradients were then centrifuged for 50 min at 32000 rpm in a SW60 swing-rotor. The vesicle fraction was collected in 16 µl on the boarder between the

37.5 % w/w sucrose and the 50 % w/w sucrose. 50 % of the vesicle fraction and 1 % of the input fraction were loaded on a 12 % polyacrylamid gel and subjected to SDS-PAGE. The analysis of the membrane associated material was performed via Western blot with specific primary antibodies and secondary antibodies coupled to Alexa dyes. The fluorescent signals were quantified in a Li-CORE Odyssey system (Lincoln, USA).

4.2.1.19 Isolation of cross-linked COPI vesicles via an OptiPrep Gradient

COPI vesicles were essentially prepared from semi-intact cells according to the protocol described in 4.2.1.17 with the exception of the modifications described here. All the components of reaction mixture were doubled while the reaction volume was kept at 200 µl. After the low speed centrifugation step at 10 000 x g for 10 min, the supernatant was transferred to a new 1.5 ml reaction tube and incubated with ArfGAP1 full length, 1-137 ArfGAP1 or buffer as a negative control for 10 min at room temperature. The set-ups were then transferred on ice and cross-linked via 0.25 mM NHS-ester reactive, bifunctional cross linker DTTSP (Thermo Fischer Scientific Inc.) for twice 15 min (two sequential additions of DTTSP). The sample was then adjusted to 40 % Opti Prep (Sigma-Aldrich) in a final volume of 900 µl, transferred to a 2.4 ml SW60 tube and subsequently overlaid with 1000 µl of 30 % Opti Prep and 400 µl 20 % Opti Prep. All OptiPrep solutions were prepared in assay buffer. The reaction mixtures were centrifuged for 14 hours at 50 000 rpm, 4 °C in a SW60 rotor. 400 µl corresponding to the top fraction were removed. The next 500 µl fraction contains the COPI vesicles and was correspondingly harvested and pelleted by a one-hour centrifugation in a TLA45 rotor for 60 min, 4 °C. The supernatant was removed; the pellet was dissolved in 10 µl of 2xSDS buffer and subjected to SDS-PAGE and western blot analysis.

4.2.1.20 ELISA modified from (Bethune et al., 2006)

- Binding Buffer: 50 mM HEPES, 90 mM KCl, 300 mM NaCl, 1 mM EDTA, 1 % BSA, 0.5 % Triton X-100, pH 7.4

96-well microtiter plate (Corning, New York, USA) was coated with 10 pmol of isotypic coatomer dissolved in 100 µl of PBS per well. As a negativ control, the corresponding number of wells was coated with BSA dissolved in 100 µl of PBS. The coating of the microtiter plate was perfomed overnight at 4 °C. Subsequently, the wells were washed three times with PBS and blocked with 300 µl of PBS-T

containing 5 % BSA for 30min at room temperature. After three washes with PBS-T and one wash with binding buffer, different concentrations of ArfGAP1, ArfGAP2 and ArfGAP3 were added to the microtiter plate, and incubated for one hour at room temperature. Concentrations of 0 µM, 0.313 µM, 0.625 µM, 1.250 µM, 2.5 µM and 5 µM were used. Subsequent to the binding, the wells were washed three times with binding buffer and incubated for one hour at room temperature with primary antibody against ArfGAP1, ArfGAP2 and ArfGAP3, which was diluted 1: 1000 in binding buffer. The microtiter plate was then washed three times with binding buffer and incubated for further one hour at room temperature with secondary anti-rabbit antibody coupled to HRP, which was diluted 1: 1000 in binding buffer. After the antibody incubation, the plate was washed three times with binding buffer and once with binding buffer without BSA and Triton X-100. For the detection were added 100 µl of 0.1 mg/ml 3,3,´5,´5-Tetramethylbenzidine (TMD) from Sigma-Aldrich (Taufkirchen, Germany) dissolved in 50 mM phosphate citrate buffer, pH 5 supplemented with 0.02 % H_2O_2. The phosphate buffer containing the HRP substrate was prepared directly prior to use. The reaction was stopped with 50 µl of 0.5 M H_2O_2 and the absorbance was directly measured at 450 nm (reference filter= 620nm) in an Anthos 2001 microtiter plate reader (Anthos Lab Tec, Salzburg, Austria).

4.2.1.21 Labeling of Arf1 and coatomer

Myristoylated Arf1 was purified as described above. To allow optimal activity of labeled Arf1, its unique cysteine residue was exchanged with a serine residue (C159S) and its C-terminal lysine was exchanged for a cysteine (K181C). The purified protein was subsequently labeled with 10x molar excess of maleimide reactive Alexa647 dye (Life technologies) for 1 h on ice. The free dye was separated via gel filtration on a Superdex 75 10/300 column. Coatomer was purified by affinity purification as described above. After elution with 2.5 mM D-Desthiobiotin (iba, Goettingen, Germany), fractions of interest were pooled and the buffer was exchanged on PD10 desalting columns to remove D-Desthiobiotin. The purified protein was labeled with NHS-ester reactive ATTO488 dye (Life technologies) for 1 h on ice and the residual free dye was separated on a Superose 6 10/300 column.

4.2.1.22 Fluorescence Cross Correlation Spectroscopy Measurements

5 µl of COPI vesicles purified from endogenous rat liver Golgi membranes in the presence of Arf1-Alexa647 and coatomer-ATTO488, were mixed with PBS and

ArfGAP to a final volume of 20 µl. The reaction mixture was directly pipetted in a chamber and imaged with a LSM710 supplied with confocor 3 microscope (Zeiss, Oberkochen, Germany). The fluorescence traces were analysed using custom made scripts written in Mat Lab (Jonas Ries, EMBL, Heidelberg, Germany).
Intensity traces with a bin size of 20 µs were calculated and the 90 % percentile of the intensity values was chosen as a threshold to distinguish bursts from fluorescence background. In 20 equally spaced time windows (length 15 seconds) the number of intensity values above the threshold was used as a measure for the number of peaks. In addition, the average intensity of the values above the threshold was calculated as a measure for the amount of vesicle-bound fluorophores. From this, we calculated in each time window the intensity ratio between red and green channels, which reports the relative abundance of both proteins on the vesicles. The decay constants were calculated from a robust exponential decay fit. The final figures were plotted in GraphPadPrism.

4.2.1.23 Float Up

- Assay Buffer: 25 mM HEPES, 150 mM KCl, 1 mM $MgCl_2$, pH 7.2

For the floatation experiment, liposomes containing p23 lipopetide with a Golgi-like composition were generated as described above and extruded through a 100 nm track-etch membrane (Whatman, Maidstone, United Kingdom). In the first step, Arf1 and coatomer were recruited to the membrane. For this purpose, 4 µg Arf1, 29 µg coatomer, 400 µM liposomes, 0.19 mM DTT, 1.6 mM EDTA and 100 µM GTP were mixed in a final volume of 60 µL and incubated for 10 min at 37 °C. To stop the reaction, 4 mM $MgCl_2$ were added. In the second step, different concentrations of ArfGAP1 or ArfGAP2 were added and the set-ups were incubated for further 5 min at room temperature. 5 µl of the reaction were removed for the inputs and mixed with 55 µl HKM and 20 µl 4X SDS sample buffer. To the 55 µl of the reactions were added 160 µl cold solution of 59.5 % w/w sucrose (final concentration= 47 %w/w). The sample was mixed well, transferred carefully at the bottom of 0.7 ml SW60 tubes and overlaid with 200 µl 44 % w/w sucrose, 170 µl 41 % w/w sucrose, and 80 µl of HKM buffer. To isolate the coated liposomes, the sucrose gradients were centrifuged for 1 h 30 min at 50 000 rpm in a SW60 swing-rotor. The 80 µl top fraction was then carefully harvested and supplemented with 20 µl of 4xSDS sample buffer. 10 µl of the inputs and 10 µl of the float up fraction were loaded on a 12 % gel and analysed via SDS-PAGE and Western Blot.

4.2.1.24 Radioactivity assay

For the readioactivity experiments, the float-up was essentially performed as described in 4.2.1.23. For radioactive labelling of the nucleotide a mixture of 1 mM GTP and 1 pmol ^{3}H-GTP (Perkin Elmer) was used. After collecting the top fractions of the gradients, 20 µl of the samples were mixed with ArfGAP1 or ArfGAP2 at the concentrations indicated in the results part. The reaction was stopped by 1-minute incubation at 95 °C. 8µl of the samples were loaded on a Bis-Tris precasted NuPAGE gel and subjected to electrophoresis accoring to the instructions of the manufacturer. The rest of the sample was subjected to a 3-minute centrifugation at 13 000 rpm in order to separate the free nucleotide. The supernatant was transferred to a new tube. 2 µl of the suppernatant were mixed with 3 µl of szintigraphy solution and were subjected to a scintillation counting (cpm). According to the measured radioactivity, such a volume of the samples was choosen so that it corresponds to 4000 cpm. Samples were spotted on a PEI thin layer chromatography plate, 1 cm apart on a line, 2.5 cm from the bottom of the plate. Each plate was developed with 0.7 M freshly prepared $LiCl_2$ in a closed multiplate tank to a solvent front of 5 cm. The development required ca. 45 minutes. After drying of the plates with blow-dryer, they subjected to a counting with a ß-Imager (Biospace Lab) for 12 hours.

4.2.2 Molecular Biology Methods

4.2.2.1 Preparation of Chemically Competent Bacteria

- Buffer TFB 1: 50 mM $MnCl_2$, 100 mM RbCl, 10 mM $CaCl_2$, 30 mM Kaliumacetate, 15 % Glycerol
- Buffer TFB 2: 10 mM MOPS, 75 mM $CaCl_2$, 10 mM RbCl, 15 % Glycerol

To prepare the competent bacteria, 10 ml of LB medium were inoculated from a glycerol stock of *E. coli* DH5α (Invitrogen), which was prepared from a single clone. This overnight culture was incubated at 37 °C and 180 rpm for ca. 14 hours. For the day culture, two times of 200 ml of LB medium were inoculated each with 4 ml from the overnight culture. After the DH5α cells had reached OD_{600}= 0.4, they were harvested for 15 min at 4000 rpm and 4 °C in precooled 50 ml reaction tubes. The pellet was resuspended in 50 ml of TFB 1 buffer and the cells were spun down second time for 10 min at 3000 rpm and 4 °C. Subsequently, the pellet was resuspended in 5 ml of buffer TFB 2. Finally, the cells were aliquoted, shock frozen in liquid nitrogen and stored at -80 °C.

4.2.2.2 Determination of DNA-concentration

DNA concentration was determined by its absorption at 260 nm, using a ND-1000 Spectrophotometer (NanoDrop; Wilmington, USA). The absorption of the solution of interest is determined and the concentration of nucleic acid in the sample is automatically calculated applying the formula: c = OD_{260}· 0,05 · DF [µg/µl] (DF= dilution factor).

4.2.2.3 Agarose Gel Electrophoresis

- TAE buffer (50x): 2 M Tris-HCl, pH 8.0, 1 M acetic acid and 50 mM EDTA
- DNA sample buffer (5x): 50 mM Tris-HCl, pH 8.0, 4 M Urea, 25 % (w/v) Glycerol, 0.1 % (w/v) Bromphenol blue, 100 mM EDTA

Analytical and preparative agarose gel electrophoresis was performed on 1 % agarose gels prepared in TAE buffer supplied with 0.005 % (v/v) ethidium bromide. DNA samples were mixed with DNA sample buffer prior to loading (final concentration of the sample buffer= 1x) on the gel. The gel was run at 120 V until the desired separation. DNA bands were visualized on a GelDoc System (Biorad, Munich). DNA bands of interest were excised and purified from the gel using QIAquick Gel Extraction Kit (Qiagen, Hilden, Germany) according to the protocol of the manufacturer.

4.2.2.4 Ligation

Ligation of endonuclease treated DNA fragments (inserts) with the equivalently digested Vector-DNA was performed with T4-DNA-ligase (NEB, Ipswich, assachusetts, United States) using the corresponding T4-DNA-ligase buffer purchased from NEB. Vector and insert were mixed at a molar ratio of 1:3, 1:5 and 1:10 and were added to a ligation mix containing the T4-DNA-ligase and T4-DNA-ligase buffer. The ligation setup was incubated at 16°C over night and subsequently used for the transformation of chemically competent *E.coli* DH5α or stored until usage at -20°C.

4.2.2.5 Transformation of Chemically Competent Bacteria

- LB Agar: 3 g BactoTryptone, 1.5 g Yeast Extract, 3 g NaCl, 4.5 g Agar, 300 ml of H_2O
- Ampicillin: 100 mg/ml stock solution, used in 1: 1000 dilution
- Kanamycin: 50 mg/ml stoch solution, used in 1: 1000 dilution

- SOC medium: purchased from Invitrogen

100 µl BL21star/ Origami 2 (Invitrogen, Carlsbad, California, United States) *E. coli* competent cells were mixed with 0.5 µl of plasmid stock solution and incubated for 10 min on ice. The cells were then heat shocked at 42 °C for 30 sec and incubated at room temperature for 10 min. 80 µl of SOC medium were then added and the cells were allowed to grow for 1 h at 37 °C on an agitator. The cells were then plated on LB agar plates containing the appropriate antibiotics and incubated overnight at 37 °C.

4.2.2.6 Transformation of Electrically Competent Bacteria

For the tranformation, 10 ng of the plasmid of interest were transfected into 40 µl of electro-competent DH10B Bultibac bacteria. The bacteria was incubated with the plasmid for 10 to 15 min in a pre-cooled electroporation cuvette on ice. The electroporation was conducted at 1,8 KV, 25 µF, and 200 Ohm. The transformed bacteria was resuspended in 1 ml SOC-medium, transferred to a 1.5 ml reaction tube, and incubated for 6 hours at 37 °C and constant shaking at 180 rpm. The culture was then spun down for 1 min at 13000 rpm. 950 µl of the supernatant were discarded and the pellet was resuspenden into the remaining 50 µl of medium. The bacteria was plated on low-salt agar-plates containing: Ampicillin (100 mg/ml), Kanamycin (50 µg/ml), Gentamycin (7 µg/ml), Tetracyclin (10 µg/ml), Blougal (100 µg/ml), and IPTG (500 µM). The agar plates were incubated for 16 to 24 hours at 37 °C. Afterwards, the white colonies, corresponding to the ones containing the plasmid were picked, while the blue colonies, where the transfection failed, were discarded. Per construct 2 to 4 colonies were picked.

4.2.2.7 Restriction digest

A restriction digest of DNA fragments by endonucleases was performed in 1 x NEB reaction buffer (buffer type dependent on the enzyme) with/without 1 x BSA solution for 2 h at 37 °C.

4.2.2.8 Sequencing

All sequencing reactions were performed by GATC (Konstanz, Germany).

4.2.2.9 Polymerase Chain Reaction (PCR)

Pfu turbo DNA polymerase was used for the amplification of DNA fragments (Agilent Technology, Boeblingen, Germany). 50 ng of DNA template, 1 µl of both 10 µM forward and 10 µM reverse primer, 1 µl of 10 µM dNTP mix, 1 µl of 2.5 U/µl Pfu polymerase were mixed in a final volume of 40µl water. The reaction were performed in a thermo cycler (Thermo Fischer Scientific, Rockford, USA) at a temperature gradient for the annealing between 52 and 62°C.

4.2.2.10 Ethanol Precipitation

DNA was precipitated by the addition of 1/10 of a volume of 3 M sodium acetate and 2.5 volumes of Ethanol p.a. Following a 30-minute incubation at -20 °C, the samples were centrifuged at 12 000 x g for 10 min at 4 °C. Pellets were dissolved in 20 µl of MilliQ water.

4.2.2.11 Plasmid Preparation

Plasmids were prepared using Macherey-Nagel Nucleo Bond PC500 Kit (Dueren, Germany) according to the protocol of the manufacturer.

4.2.2.12 Bacmid Preparation

A single white colony, which corresponds to the colonies expressing the plasmid, was picked from the low-salt agar-plates containing: Ampicillin (100 mg/ml), Kanamycin (50 µg/ml), Gentamycin (7 µg/ml), Tetracyclin (10 µg/ml), Blougal (100 µg/ml), IPTG (500 µM/ml). For the details of the transformation procedure of electrically competent bacteria see above. Two to three colonies were choosen per construct and were inoculated in 3 ml of low-salt LB-medium containing the antibiotics above. This pre-culture was incubated overnight at 37 °C with a constant agitation at 180 rpm. 1.5 ml of the pre-culture were spun down for 1 min at 13000 rpm. The supernatant was discarded and the pellet was resuspended in 300 µl Resuspending buffer S1 from Nucleo-spin plasmid kit from Macherey Nagel (Dueren, Germany). 300 µl of Lysis buffer S2 were added carefully and the tube was inverted several times. Subsequently, 300 µl of Neutralisation buffer S3 were added and the tube was carefully inverted several times. The suspension was then centrifuged for 10 min at 13000 rpm, and 4 °C. The supernatant was transferred to a new 1,5 ml reaction tube and the DNA was precipitated by the addition of 700 µl of isopropanol.

After a centrifugation step for 10 min at 13000 rpm, and 4 °C, the supernatant was discarded. The pellet was washed with 1 of 70 % ethanol and centrifuged again for 10 min at 13000 rpm, and 4 °C. The supernatant was carefully removed and the pellet was spun down shortly again in order to remove the remainin ethanol. 50 µl of fresh ethanol were added and the tube was transferred to the sterile cell culture hood. The enthanol was then removed under the hood and the pellet was air-dried for 10 to 15 min under the hood directly prior to the transfection.

4.2.3 Cell Culture Methods

4.2.3.1 Adherent Cell Culture of HeLa Cells

Hela cells were cultured in alpha MEM supplemented with 10 % fetal calf serum (FCS) 100 µg/ml penicillin, 100 µg/µl streptomycin and 2 mM L-glutamine, at 5 % CO_2, 37 °C. Once the cells reached 80-90 % confluence, they were detached by the addition of Trypsin/EDTA (Sigma-Aldrich, Taufkirchen, Germany) and splitted either 1:3 or 1:8 in a new cell culture dish.

4.2.3.2 Cell Culture of Sf9 Insect Cells

Sf9 insect cells were cultured in GIBCO SF-900 II SFM medium either as an adherent culture in 10 -25 cm^2 flasks (Greiner Bio-One, Frickenhausen, Germany) at 27 °C or as a suspension culture in 2.5 l Cellmaster Roller Bottles (Greiner Bio-One, Frickenhausen, Germany) at 27 °C and 150 rpm. The cells were split twice per week to $1x10^6$ Cells/ml.

4.2.3.3 Transfection of Sf9 Insect Cells

Sf9 cells were counted and 0,7 -0,8$x10^6$ cells/well were seeded in a 6-well-plate (Costar, Corning, USA). Per construct were prepared two wells for the actual transfection and two wells for a mock transfection (no DNA addition to the transfection mixture). The cells were allowed to adhere to the surface for 10 min. In the meantime, the transfection mixture was prepared. The dried DNA pellet from the bacmid preparation (for details see above) was carefully resuspended in 20 µl of sterile filtered ddH_2O and then supplemented with 200µl of GIBCO SF-900 II SFM medium (tube A). 100 µl of GIBCO SF-900 II SFM medium were transferred in a sterile 1.5 ml reaction tube and 10 µl of FUGENE (Roche) were pipetted into the medium (tube B). Subsequently, 100 µl of the medium/FUGENE mixture (tube B)

were transferred into the tube containing the bacmid DNA (tube A). After a careful mixing, 150 µl of the Medium/FUGENE/DNA mixture were added dropwise to each well of the 6-well plate. Mock transfection was conducted by the addition of the same volume of Medium/FUGENE mixture in the absence of DNA. The 6-well plate was sealed with parafilm and incubated for 48 h at 27 °C.

5 References

Adolf, F., Herrmann, A., Hellwig, A., Beck, R., Brugger, B., and Wieland, F.T. (2013). Scission of COPI and COPII vesicles is independent of GTP hydrolysis. Traffic *14*, 922-932.

Adolf, F., and Wieland, F.T. (2013). Analysis of Golgi complex functions: in vitro reconstitution systems. Methods Cell Biol *118*, 3-14.

Aguilera-Romero, A., Kaminska, J., Spang, A., Riezman, H., and Muniz, M. (2008). The yeast p24 complex is required for the formation of COPI retrograde transport vesicles from the Golgi apparatus. J Cell Biol *180*, 713-720.

Ahle, S., Mann, A., Eichelsbacher, U., and Ungewickell, E. (1988). Structural relationships between clathrin assembly proteins from the Golgi and the plasma membrane. Embo J *7*, 919-929.

Anantharaman, V., and Aravind, L. (2002). The GOLD domain, a novel protein module involved in Golgi function and secretion. Genome Biol *3*, research0023.

Andag, U., and Schmitt, H.D. (2003). Dsl1p, an essential component of the Golgi-endoplasmic reticulum retrieval system in yeast, uses the same sequence motif to interact with different subunits of the COPI vesicle coat. J Biol Chem *278*, 51722-51734.

Andreev, J., Simon, J.P., Sabatini, D.D., Kam, J., Plowman, G., Randazzo, P.A., and Schlessinger, J. (1999). Identification of a new Pyk2 target protein with Arf-GAP activity. Mol Cell Biol *19*, 2338-2350.

Antonny, B. (2011). Mechanisms of membrane curvature sensing. Annu Rev Biochem *80*, 101-123.

Antonny, B., Huber, I., Paris, S., Chabre, M., and Cassel, D. (1997). Activation of ADP-ribosylation factor 1 GTPase-activating protein by phosphatidylcholine-derived diacylglycerols. J Biol Chem *272*, 30848-30851.

Antonny, B., Madden, D., Hamamoto, S., Orci, L., and Schekman, R. (2001). Dynamics of the COPII coat with GTP and stable analogues. Nature cell biology *3*, 531-537.

Aoe, T., Cukierman, E., Lee, A., Cassel, D., Peters, P.J., and Hsu, V.W. (1997). The KDEL receptor, ERD2, regulates intracellular traffic by recruiting a GTPase-activating protein for ARF1. EMBO J *16*, 7305-7316.

Appenzeller-Herzog, C., and Hauri, H.P. (2006). The ER-Golgi intermediate compartment (ERGIC): in search of its identity and function. Journal of cell science *119*, 2173-2183.

Arakel, E.C., Richter, K.P., Clancy, A., and Schwappach, B. (2016). delta-COP contains a helix C-terminal to its longin domain key to COPI dynamics and function. Proc Natl Acad Sci U S A *113*, 6916-6921.

Aridor, M., Bannykh, S.I., Rowe, T., and Balch, W.E. (1995). Sequential coupling between COPII and COPI vesicle coats in endoplasmic reticulum to Golgi transport. J Cell Biol *131*, 875-893.

Austin, C., Hinners, I., and Tooze, S.A. (2000). Direct and GTP-dependent interaction of ADP-ribosylation factor 1 with clathrin adaptor protein AP-1 on immature secretory granules. J Biol Chem *275*, 21862-21869.

Bai, M., Gad, H., Turacchio, G., Cocucci, E., Yang, J.S., Li, J., Beznoussenko, G.V., Nie, Z., Luo, R., Fu, L.*, et al.* (2011). ARFGAP1 promotes AP-2-dependent endocytosis. Nature cell biology *13*, 559-567.

Bannykh, S.I., Rowe, T., and Balch, W.E. (1996). The organization of endoplasmic reticulum export complexes. J Cell Biol *135*, 19-35.

Barlowe, C., d'Enfert, C., and Schekman, R. (1993). Purification and characterization of SAR1p, a small GTP-binding protein required for transport vesicle formation from the endoplasmic reticulum. J Biol Chem *268*, 873-879.
Barlowe, C., Orci, L., Yeung, T., Hosobuchi, M., Hamamoto, S., Salama, N., Rexach, M.F., Ravazzola, M., Amherdt, M., and Schekman, R. (1994). COPII: a membrane coat formed by Sec proteins that drive vesicle budding from the endoplasmic reticulum. Cell *77*, 895-907.
Barlowe, C., and Schekman, R. (1993). SEC12 encodes a guanine-nucleotide-exchange factor essential for transport vesicle budding from the ER. Nature *365*, 347-349.
Barlowe, C.K., and Miller, E.A. (2013). Secretory protein biogenesis and traffic in the early secretory pathway. Genetics *193*, 383-410.
Beck, R., Adolf, F., Weimer, C., Bruegger, B., and Wieland, F.T. (2009). ArfGAP1 activity and COPI vesicle biogenesis. Traffic *10*, 307-315.
Beck, R., Brugger, B., and Wieland, F. (2011a). GAPs in the context of COPI: Enzymes, coat components or both? Cell Logist *1*, 52-54.
Beck, R., Prinz, S., Diestelkotter-Bachert, P., Rohling, S., Adolf, F., Hoehner, K., Welsch, S., Ronchi, P., Brugger, B., Briggs, J.A.*, et al.* (2011b). Coatomer and dimeric ADP ribosylation factor 1 promote distinct steps in membrane scission. J Cell Biol *194*, 765-777.
Beck, R., Sun, Z., Adolf, F., Rutz, C., Bassler, J., Wild, C., Sinning, I., Hurt, E., Bruegger, B., Béthune, J.*, et al.* (2008). Membrane curvature induced by Arf1-GTP is essential for vesicle formation. Proc Natl Acad Sci U S A *In press.*
Beckers, C.J., Keller, D.S., and Balch, W.E. (1987). Semi-intact cells permeable to macromolecules: use in reconstitution of protein transport from the endoplasmic reticulum to the Golgi complex. Cell *50*, 523-534.
Belden, W.J., and Barlowe, C. (2001a). Deletion of yeast p24 genes activates the unfolded protein response. Mol Biol Cell *12*, 957-969.
Belden, W.J., and Barlowe, C. (2001b). Distinct roles for the cytoplasmic tail sequences of Emp24p and Erv25p in transport between the endoplasmic reticulum and Golgi complex. J Biol Chem *276*, 43040-43048.
Bethune, J., Kol, M., Hoffmann, J., Reckmann, I., Brugger, B., and Wieland, F. (2006). Coatomer, the Coat Protein of COPI Transport Vesicles, Discriminates Endoplasmic Reticulum Residents from p24 Proteins. Mol Cell Biol *26*, 8011-8021.
Bi, X., Corpina, R.A., and Goldberg, J. (2002). Structure of the Sec23/24-Sar1 pre-budding complex of the COPII vesicle coat. Nature *419*, 271-277.
Bigay, J., and Antonny, B. (2005). Real-time assays for the assembly-disassembly cycle of COP coats on liposomes of defined size. Methods in enzymology *404*, 95-107.
Bigay, J., Gounon, P., Robineau, S., and Antonny, B. (2003). Lipid packing sensed by ArfGAP1 couples COPI coat disassembly to membrane bilayer curvature. Nature *426*, 563-566.
Blum, R., Pfeiffer, F., Feick, P., Nastainczyk, W., Kohler, B., Schafer, K.H., and Schulz, I. (1999). Intracellular localization and in vivo trafficking of p24A and p23. Journal of cell science *112 (Pt 4)*, 537-548.
Bocking, T., Aguet, F., Harrison, S.C., and Kirchhausen, T. (2011). Single-molecule analysis of a molecular disassemblase reveals the mechanism of Hsc70-driven clathrin uncoating. Nat Struct Mol Biol *18*, 295-301.
Boehm, M., Aguilar, R.C., and Bonifacino, J.S. (2001). Functional and physical interactions of the adaptor protein complex AP-4 with ADP-ribosylation factors (ARFs). Embo J *20*, 6265-6276.
Boman, A.L., Zhang, C., Zhu, X., and Kahn, R.A. (2000). A family of ADP-ribosylation factor effectors that can alter membrane transport through the trans-Golgi. Mol Biol Cell *11*, 1241-1255.

Bonfanti, L., Mironov, A.A., Jr., Martinez-Menarguez, J.A., Martella, O., Fusella, A., Baldassarre, M., Buccione, R., Geuze, H.J., Mironov, A.A., and Luini, A. (1998). Procollagen traverses the Golgi stack without leaving the lumen of cisternae: evidence for cisternal maturation. Cell *95*, 993-1003.
Bonifacino, J.S., and Glick, B.S. (2004). The mechanisms of vesicle budding and fusion. Cell *116*, 153-166.
Borner, G.H., Antrobus, R., Hirst, J., Bhumbra, G.S., Kozik, P., Jackson, L.P., Sahlender, D.A., and Robinson, M.S. (2012). Multivariate proteomic profiling identifies novel accessory proteins of coated vesicles. J Cell Biol *197*, 141-160.
Braell, W.A., Schlossman, D.M., Schmid, S.L., and Rothman, J.E. (1984). Dissociation of clathrin coats coupled to the hydrolysis of ATP: role of an uncoating ATPase. J Cell Biol *99*, 734-741.
Bremser, M., Nickel, W., Schweikert, M., Ravazzola, M., Amherdt, M., Hughes, C.A., Sollner, T.H., Rothman, J.E., and Wieland, F.T. (1999). Coupling of coat assembly and vesicle budding to packaging of putative cargo receptors. Cell *96*, 495-506.
Brown, M.T., Andrade, J., Radhakrishna, H., Donaldson, J.G., Cooper, J.A., and Randazzo, P.A. (1998). ASAP1, a phospholipid-dependent arf GTPase-activating protein that associates with and is phosphorylated by Src. Mol Cell Biol *18*, 7038-7051.
Buchanan, R., Kaufman, A., Kung-Tran, L., and Miller, E.A. (2010). Genetic analysis of yeast Sec24p mutants suggests cargo binding is not co-operative during ER export. Traffic *11*, 1034-1043.
Caro, L.G., and Palade, G.E. (1964). Protein Synthesis, Storage, and Discharge in the Pancreatic Exocrine Cell. an Autoradiographic Study. J Cell Biol *20*, 473-495.
Casanova, J.E. (2007). Regulation of Arf activation: the Sec7 family of guanine nucleotide exchange factors. Traffic *8*, 1476-1485.
Cavenagh, M.M., Whitney, J.A., Carroll, K., Zhang, C., Boman, A.L., Rosenwald, A.G., Mellman, I., and Kahn, R.A. (1996). Intracellular distribution of Arf proteins in mammalian cells. Arf6 is uniquely localized to the plasma membrane. J Biol Chem *271*, 21767-21774.
Chen, S., Cai, H., Park, S.K., Menon, S., Jackson, C.L., and Ferro-Novick, S. (2011). Trs65p, a subunit of the Ypt1p GEF TRAPPII, interacts with the Arf1p exchange factor Gea2p to facilitate COPI-mediated vesicle traffic. Mol Biol Cell *22*, 3634-3644.
Chun, J., Shapovalova, Z., Dejgaard, S.Y., Presley, J.F., and Melancon, P. (2008). Characterization of class I and II ADP-ribosylation factors (Arfs) in live cells: GDP-bound class II Arfs associate with the ER-Golgi intermediate compartment independently of GBF1. Mol Biol Cell *19*, 3488-3500.
Ciufo, L.F., and Boyd, A. (2000). Identification of a lumenal sequence specifying the assembly of Emp24p into p24 complexes in the yeast secretory pathway. J Biol Chem *275*, 8382-8388.
Claing, A., Perry, S.J., Achiriloaie, M., Walker, J.K., Albanesi, J.P., Lefkowitz, R.J., and Premont, R.T. (2000). Multiple endocytic pathways of G protein-coupled receptors delineated by GIT1 sensitivity. Proc Natl Acad Sci U S A *97*, 1119-1124.
Claude, A., Zhao, B.P., Kuziemsky, C.E., Dahan, S., Berger, S.J., Yan, J.P., Armold, A.D., Sullivan, E.M., and Melancon, P. (1999). GBF1: A novel Golgi-associated BFA-resistant guanine nucleotide exchange factor that displays specificity for ADP-ribosylation factor 5. J Cell Biol *146*, 71-84.
Collins, B.M., McCoy, A.J., Kent, H.M., Evans, P.R., and Owen, D.J. (2002). Molecular architecture and functional model of the endocytic AP2 complex. Cell *109*, 523-535.
Cosson, P., and Letourneur, F. (1994). Coatomer interaction with di-lysine endoplasmic reticulum retention motifs. Science *263*, 1629-1631.

Cukierman, E., Huber, I., Rotman, M., and Cassel, D. (1995). The ARF1 GTPase-activating protein: zinc finger motif and Golgi complex localization. Science *270*, 1999-2002.
d'Enfert, C., Wuestehube, L.J., Lila, T., and Schekman, R. (1991). Sec12p-dependent membrane binding of the small GTP-binding protein Sar1p promotes formation of transport vesicles from the ER. J Cell Biol *114*, 663-670.
D'Souza-Schorey, C., van Donselaar, E., Hsu, V.W., Yang, C., Stahl, P.D., and Peters, P.J. (1998). ARF6 targets recycling vesicles to the plasma membrane: insights from an ultrastructural investigation. J Cell Biol *140*, 603-616.
de Graffenried, C.L., and Bertozzi, C.R. (2004). The roles of enzyme localisation and complex formation in glycan assembly within the Golgi apparatus. Curr Opin Cell Biol *16*, 356-363.
Dell'Angelica, E.C., Klumperman, J., Stoorvogel, W., and Bonifacino, J.S. (1998). Association of the AP-3 adaptor complex with clathrin. Science *280*, 431-434.
Dell'Angelica, E.C., Mullins, C., and Bonifacino, J.S. (1999). AP-4, a novel protein complex related to clathrin adaptors. J Biol Chem *274*, 7278-7285.
Dell'Angelica, E.C., Ohno, H., Ooi, C.E., Rabinovich, E., Roche, K.W., and Bonifacino, J.S. (1997). AP-3: an adaptor-like protein complex with ubiquitous expression. Embo J *16*, 917-928.
Dell'Angelica, E.C., Puertollano, R., Mullins, C., Aguilar, R.C., Vargas, J.D., Hartnell, L.M., and Bonifacino, J.S. (2000). GGAs: a family of ADP ribosylation factor-binding proteins related to adaptors and associated with the Golgi complex. J Cell Biol *149*, 81-94.
Deng, Y., Golinelli-Cohen, M.P., Smirnova, E., and Jackson, C.L. (2009). A COPI coat subunit interacts directly with an early-Golgi localized Arf exchange factor. EMBO reports *10*, 58-64.
Denzel, A., Otto, F., Girod, A., Pepperkok, R., Watson, R., Rosewell, I., Bergeron, J.J., Solari, R.C., and Owen, M.J. (2000). The p24 family member p23 is required for early embryonic development. Curr Biol *10*, 55-58.
Di Cesare, A., Paris, S., Albertinazzi, C., Dariozzi, S., Andersen, J., Mann, M., Longhi, R., and de Curtis, I. (2000). p95-APP1 links membrane transport to Rac-mediated reorganization of actin. Nature cell biology *2*, 521-530.
Dodonova, S.O., Diestelkoetter-Bachert, P., von Appen, A., Hagen, W.J., Beck, R., Beck, M., Wieland, F., and Briggs, J.A. (2015). VESICULAR TRANSPORT. A structure of the COPI coat and the role of coat proteins in membrane vesicle assembly. Science *349*, 195-198.
Dominguez, M., Dejgaard, K., Fullekrug, J., Dahan, S., Fazel, A., Paccaud, J.P., Thomas, D.Y., Bergeron, J.J., and Nilsson, T. (1998). gp25L/emp24/p24 protein family members of the cis-Golgi network bind both COP I and II coatomer. J Cell Biol *140*, 751-765.
Donaldson, J.G., Cassel, D., Kahn, R.A., and Klausner, R.D. (1992). ADP-ribosylation factor, a small GTP-binding protein, is required for binding of the coatomer protein beta-COP to Golgi membranes. Proc Natl Acad Sci U S A *89*, 6408-6412.
Duden, R., Griffiths, G., Frank, R., Argos, P., and Kreis, T.E. (1991). Beta-COP, a 110 kd protein associated with non-clathrin-coated vesicles and the Golgi complex, shows homology to beta-adaptin. Cell *64*, 649-665.
Dunphy, W.G., Fries, E., Urbani, L.J., and Rothman, J.E. (1981). Early and late functions associated with the Golgi apparatus reside in distinct compartments. Proc Natl Acad Sci U S A *78*, 7453-7457.
Dunphy, W.G., and Rothman, J.E. (1983). Compartmentation of asparagine-linked oligosaccharide processing in the Golgi apparatus. J Cell Biol *97*, 270-275.
Emery, G., Rojo, M., and Gruenberg, J. (2000). Coupled transport of p24 family members. Journal of cell science *113 (Pt 13)*, 2507-2516.

Espenshade, P., Gimeno, R.E., Holzmacher, E., Teung, P., and Kaiser, C.A. (1995). Yeast SEC16 gene encodes a multidomain vesicle coat protein that interacts with Sec23p. J Cell Biol *131*, 311-324.
Eugster, A., Frigerio, G., Dale, M., and Duden, R. (2000). COP I domains required for coatomer integrity, and novel interactions with ARF and ARF-GAP. Embo J *19*, 3905-3917.
Faini, M., Prinz, S., Beck, R., Schorb, M., Riches, J.D., Bacia, K., Brugger, B., Wieland, F.T., and Briggs, J.A. (2012). The structures of COPI-coated vesicles reveal alternate coatomer conformations and interactions. Science *336*, 1451-1454.
Forster, R., Weiss, M., Zimmermann, T., Reynaud, E.G., Verissimo, F., Stephens, D.J., and Pepperkok, R. (2006). Secretory cargo regulates the turnover of COPII subunits at single ER exit sites. Curr Biol *16*, 173-179.
Fotin, A., Cheng, Y., Sliz, P., Grigorieff, N., Harrison, S.C., Kirchhausen, T., and Walz, T. (2004). Molecular model for a complete clathrin lattice from electron cryomicroscopy. Nature *432*, 573-579.
Frigerio, G., Grimsey, N., Dale, M., Majoul, I., and Duden, R. (2007). Two human ARFGAPs associated with COP-I-coated vesicles. Traffic *8*, 1644-1655.
Fullekrug, J., Suganuma, T., Tang, B.L., Hong, W., Storrie, B., and Nilsson, T. (1999). Localization and recycling of gp27 (hp24gamma3): complex formation with other p24 family members. Mol Biol Cell *10*, 1939-1955.
Futai, E., Hamamoto, S., Orci, L., and Schekman, R. (2004). GTP/GDP exchange by Sec12p enables COPII vesicle bud formation on synthetic liposomes. EMBO J *23*, 4146-4155.
Futatsumori, M., Kasai, K., Takatsu, H., Shin, H.W., and Nakayama, K. (2000). Identification and characterization of novel isoforms of COP I subunits. Journal of biochemistry *128*, 793-801.
Gaidarov, I., Chen, Q., Falck, J.R., Reddy, K.K., and Keen, J.H. (1996). A functional phosphatidylinositol 3,4,5-trisphosphate/phosphoinositide binding domain in the clathrin adaptor AP-2 alpha subunit. Implications for the endocytic pathway. J Biol Chem *271*, 20922-20929.
Gaidarov, I., and Keen, J.H. (1999). Phosphoinositide-AP-2 interactions required for targeting to plasma membrane clathrin-coated pits. J Cell Biol *146*, 755-764.
Garcia-Mata, R., Szul, T., Alvarez, C., and Sztul, E. (2003). ADP-ribosylation factor/COPI-dependent events at the endoplasmic reticulum-Golgi interface are regulated by the guanine nucleotide exchange factor GBF1. Mol Biol Cell *14*, 2250-2261.
Gillingham, A.K., and Munro, S. (2007). The small G proteins of the Arf family and their regulators. Annu Rev Cell Dev Biol *23*, 579-611.
Gimeno, R.E., Espenshade, P., and Kaiser, C.A. (1996). COPII coat subunit interactions: Sec24p and Sec23p bind to adjacent regions of Sec16p. Mol Biol Cell *7*, 1815-1823.
Glick, B.S., and Luini, A. (2011). Models for Golgi traffic: a critical assessment. Cold Spring Harb Perspect Biol *3*, a005215.
Glick, B.S., and Malhotra, V. (1998). The curious status of the Golgi apparatus. Cell *95*, 883-889.
Glickman, J.N., Conibear, E., and Pearse, B.M. (1989). Specificity of binding of clathrin adaptors to signals on the mannose-6-phosphate/insulin-like growth factor II receptor. Embo J *8*, 1041-1047.
Goldberg, J. (1999). Structural and functional analysis of the ARF1-ARFGAP complex reveals a role for coatomer in GTP hydrolysis. Cell *96*, 893-902.
Gommel, D., Orci, L., Emig, E.M., Hannah, M.J., Ravazzola, M., Nickel, W., Helms, J.B., Wieland, F.T., and Sohn, K. (1999). p24 and p23, the major transmembrane proteins of COPI-coated transport vesicles, form hetero-oligomeric complexes and

cycle between the organelles of the early secretory pathway. FEBS Lett *447*, 179-185.
Gommel, D.U., Memon, A.R., Heiss, A., Lottspeich, F., Pfannstiel, J., Lechner, J., Reinhard, C., Helms, J.B., Nickel, W., and Wieland, F.T. (2001). Recruitment to Golgi membranes of ADP-ribosylation factor 1 is mediated by the cytoplasmic domain of p23. Embo J *20*, 6751-6760.
Goud, B., and Gleeson, P.A. (2010). TGN golgins, Rabs and cytoskeleton: regulating the Golgi trafficking highways. Trends in cell biology *20*, 329-336.
Griffiths, G., Quinn, P., and Warren, G. (1983). Dissection of the Golgi complex. I. Monensin inhibits the transport of viral membrane proteins from medial to trans Golgi cisternae in baby hamster kidney cells infected with Semliki Forest virus. J Cell Biol *96*, 835-850.
Gu, F., Crump, C.M., and Thomas, G. (2001). Trans-Golgi network sorting. Cell Mol Life Sci *58*, 1067-1084.
Hammond, A.T., and Glick, B.S. (2000). Dynamics of transitional endoplasmic reticulum sites in vertebrate cells. Mol Biol Cell *11*, 3013-3030.
Hara-Kuge, S., Kuge, O., Orci, L., Amherdt, M., Ravazzola, M., Wieland, F.T., and Rothman, J.E. (1994). En bloc incorporation of coatomer subunits during the assembly of COP-coated vesicles. J Cell Biol *124*, 883-892.
Harter, C., and Wieland, F.T. (1998). A single binding site for dilysine retrieval motifs and p23 within the gamma subunit of coatomer. Proc Natl Acad Sci U S A *95*, 11649-11654.
Hill, K., Li, Y., Bennett, M., McKay, M., Zhu, X., Shern, J., Torre, E., Lah, J.J., Levey, A.I., and Kahn, R.A. (2003). Munc18 interacting proteins: ADP-ribosylation factor-dependent coat proteins that regulate the traffic of beta-Alzheimer's precursor protein. J Biol Chem *278*, 36032-36040.
Hinners, I., and Tooze, S.A. (2003). Changing directions: clathrin-mediated transport between the Golgi and endosomes. Journal of cell science *116*, 763-771.
Hirst, J., Barlow, L.D., Francisco, G.C., Sahlender, D.A., Seaman, M.N., Dacks, J.B., and Robinson, M.S. (2011). The fifth adaptor protein complex. PLoS biology *9*, e1001170.
Hirst, J., Bright, N.A., Rous, B., and Robinson, M.S. (1999). Characterization of a fourth adaptor-related protein complex. Mol Biol Cell *10*, 2787-2802.
Hirst, J., Lui, W.W., Bright, N.A., Totty, N., Seaman, M.N., and Robinson, M.S. (2000). A family of proteins with gamma-adaptin and VHS domains that facilitate trafficking between the trans-Golgi network and the vacuole/lysosome. J Cell Biol *149*, 67-80.
Hsu, V.W. (2011). Role of ArfGAP1 in COPI vesicle biogenesis. Cell Logist *1*, 55-56.
Huang, M., Weissman, J.T., Beraud-Dufour, S., Luan, P., Wang, C., Chen, W., Aridor, M., Wilson, I.A., and Balch, W.E. (2001). Crystal structure of Sar1-GDP at 1.7 A resolution and the role of the NH2 terminus in ER export. J Cell Biol *155*, 937-948.
Hughes, H., Budnik, A., Schmidt, K., Palmer, K.J., Mantell, J., Noakes, C., Johnson, A., Carter, D.A., Verkade, P., Watson, P.*, et al.* (2009). Organisation of human ER-exit sites: requirements for the localisation of Sec16 to transitional ER. Journal of cell science *122*, 2924-2934.
I, S.T., Nie, Z., Stewart, A., Najdovska, M., Hall, N.E., He, H., Randazzo, P.A., and Lock, P. (2004). ARAP3 is transiently tyrosine phosphorylated in cells attaching to fibronectin and inhibits cell spreading in a RhoGAP-dependent manner. Journal of cell science *117*, 6071-6084.
Inoue, H., and Randazzo, P.A. (2007). Arf GAPs and their interacting proteins. Traffic *8*, 1465-1475.
Ivan, V., de Voer, G., Xanthakis, D., Spoorendonk, K.M., Kondylis, V., and Rabouille, C. (2008). Drosophila Sec16 mediates the biogenesis of tER sites upstream of Sar1 through an arginine-rich motif. Mol Biol Cell *19*, 4352-4365.

Jackson, L.P. (2014). Structure and mechanism of COPI vesicle biogenesis. Curr Opin Cell Biol *29*, 67-73.
Jackson, M.R., Nilsson, T., and Peterson, P.A. (1990). Identification of a consensus motif for retention of transmembrane proteins in the endoplasmic reticulum. EMBO J *9*, 3153-3162.
Jacques, K.M., Nie, Z., Stauffer, S., Hirsch, D.S., Chen, L.X., Stanley, K.T., and Randazzo, P.A. (2002). Arf1 dissociates from the clathrin adaptor GGA prior to being inactivated by Arf GTPase-activating proteins. J Biol Chem *277*, 47235-47241.
Jamieson, J.D., and Palade, G.E. (1967). Intracellular transport of secretory proteins in the pancreatic exocrine cell. I. Role of the peripheral elements of the Golgi complex. J Cell Biol *34*, 577-596.
Kahn, R.A., Cherfils, J., Elias, M., Lovering, R.C., Munro, S., and Schurmann, A. (2006). Nomenclature for the human Arf family of GTP-binding proteins: ARF, ARL, and SAR proteins. J Cell Biol *172*, 645-650.
Kaiser, C.A., and Schekman, R. (1990). Distinct sets of SEC genes govern transport vesicle formation and fusion early in the secretory pathway. Cell *61*, 723-733.
Karrenbauer, A., Jeckel, D., Just, W., Birk, R., Schmidt, R.R., Rothman, J.E., and Wieland, F.T. (1990). The rate of bulk flow from the Golgi to the plasma membrane. Cell *63*, 259-267.
Kartberg, F., Asp, L., Dejgaard, S.Y., Smedh, M., Fernandez-Rodriguez, J., Nilsson, T., and Presley, J.F. (2010). ARFGAP2 and ARFGAP3 are essential for COPI coat assembly on the Golgi membrane of living cells. J Biol Chem *285*, 36709-36720.
Kirchhausen, T. (2000). Clathrin. Annu Rev Biochem *69*, 699-727.
Kirchhausen, T., and Harrison, S.C. (1981). Protein organization in clathrin trimers. Cell *23*, 755-761.
Kirchhausen, T., Owen, D., and Harrison, S.C. (2014). Molecular structure, function, and dynamics of clathrin-mediated membrane traffic. Cold Spring Harb Perspect Biol *6*, a016725.
Kliouchnikov, L., Bigay, J., Mesmin, B., Parnis, A., Rawet, M., Goldfeder, N., Antonny, B., and Cassel, D. (2009). Discrete determinants in ArfGAP2/3 conferring Golgi localization and regulation by the COPI coat. Mol Biol Cell *20*, 859-869.
Krugmann, S., Anderson, K.E., Ridley, S.H., Risso, N., McGregor, A., Coadwell, J., Davidson, K., Eguinoa, A., Ellson, C.D., Lipp, P.*, et al.* (2002). Identification of ARAP3, a novel PI3K effector regulating both Arf and Rho GTPases, by selective capture on phosphoinositide affinity matrices. Molecular cell *9*, 95-108.
Kuehn, M.J., Herrmann, J.M., and Schekman, R. (1998). COPII-cargo interactions direct protein sorting into ER-derived transport vesicles. Nature *391*, 187-190.
Kung, L.F., Pagant, S., Futai, E., D'Arcangelo, J.G., Buchanan, R., Dittmar, J.C., Reid, R.J., Rothstein, R., Hamamoto, S., Snapp, E.L.*, et al.* (2012). Sec24p and Sec16p cooperate to regulate the GTP cycle of the COPII coat. EMBO J *31*, 1014-1027.
Langer, J.D., Roth, C.M., Bethune, J., Stoops, E.H., Brugger, B., Herten, D.P., and Wieland, F.T. (2008). A conformational change in the alpha-subunit of coatomer induced by ligand binding to gamma-COP revealed by single-pair FRET. Traffic *9*, 597-607.
Langer, J.D., Stoops, E.H., Bethune, J., and Wieland, F.T. (2007). Conformational changes of coat proteins during vesicle formation. FEBS Lett *581*, 2083-2088.
Lanoix, J., Ouwendijk, J., Lin, C.C., Stark, A., Love, H.D., Ostermann, J., and Nilsson, T. (1999). GTP hydrolysis by arf-1 mediates sorting and concentration of Golgi resident enzymes into functional COP I vesicles. Embo J *18*, 4935-4948.
Lanoix, J., Ouwendijk, J., Stark, A., Szafer, E., Cassel, D., Dejgaard, K., Weiss, M., and Nilsson, T. (2001). Sorting of Golgi resident proteins into different subpopulations of COPI vesicles: a role for ArfGAP1. J Cell Biol *155*, 1199-1212.

Lee, S.Y., Yang, J.S., Hong, W., Premont, R.T., and Hsu, V.W. (2005). ARFGAP1 plays a central role in coupling COPI cargo sorting with vesicle formation. J Cell Biol *168*, 281-290.
Lenhard, J.M., Kahn, R.A., and Stahl, P.D. (1992). Evidence for ADP-ribosylation factor (ARF) as a regulator of in vitro endosome-endosome fusion. J Biol Chem *267*, 13047-13052.
Letourneur, F., Gaynor, E.C., Hennecke, S., Demolliere, C., Duden, R., Emr, S.D., Riezman, H., and Cosson, P. (1994). Coatomer is essential for retrieval of dilysine-tagged proteins to the endoplasmic reticulum. Cell *79*, 1199-1207.
Levi, V., Villamil Giraldo, A.M., Castello, P.R., Rossi, J.P., and Gonzalez Flecha, F.L. (2008). Effects of phosphatidylethanolamine glycation on lipid-protein interactions and membrane protein thermal stability. The Biochemical journal *416*, 145-152.
Lewis, S.M., Poon, P.P., Singer, R.A., Johnston, G.C., and Spang, A. (2004). The ArfGAP Glo3 is required for the generation of COPI vesicles. Mol Biol Cell *15*, 4064-4072.
Li, J., Peters, P.J., Bai, M., Dai, J., Bos, E., Kirchhausen, T., Kandror, K.V., and Hsu, V.W. (2007). An ACAP1-containing clathrin coat complex for endocytic recycling. J Cell Biol *178*, 453-464.
Lord, C., Bhandari, D., Menon, S., Ghassemian, M., Nycz, D., Hay, J., Ghosh, P., and Ferro-Novick, S. (2011). Sequential interactions with Sec23 control the direction of vesicle traffic. Nature *473*, 181-186.
Love, H.D., Lin, C.C., Short, C.S., and Ostermann, J. (1998). Isolation of functional Golgi-derived vesicles with a possible role in retrograde transport. J Cell Biol *140*, 541-551.
Majoul, I., Straub, M., Hell, S.W., Duden, R., and Soling, H.D. (2001). KDEL-cargo regulates interactions between proteins involved in COPI vesicle traffic: measurements in living cells using FRET. Developmental cell *1*, 139-153.
Malsam, J., Gommel, D., Wieland, F.T., and Nickel, W. (1999). A role for ADP ribosylation factor in the control of cargo uptake during COPI-coated vesicle biogenesis. FEBS Lett *462*, 267-272.
Mancias, J.D., and Goldberg, J. (2007). The transport signal on Sec22 for packaging into COPII-coated vesicles is a conformational epitope. Molecular cell *26*, 403-414.
Marzioch, M., Henthorn, D.C., Herrmann, J.M., Wilson, R., Thomas, D.Y., Bergeron, J.J., Solari, R.C., and Rowley, A. (1999). Erp1p and Erp2p, partners for Emp24p and Erv25p in a yeast p24 complex. Mol Biol Cell *10*, 1923-1938.
Massol, R.H., Boll, W., Griffin, A.M., and Kirchhausen, T. (2006). A burst of auxilin recruitment determines the onset of clathrin-coated vesicle uncoating. Proc Natl Acad Sci U S A *103*, 10265-10270.
Matsuoka, K., Orci, L., Amherdt, M., Bednarek, S.Y., Hamamoto, S., Schekman, R., and Yeung, T. (1998). COPII-coated vesicle formation reconstituted with purified coat proteins and chemically defined liposomes. Cell *93*, 263-275.
McMahon, H.T., and Mills, I.G. (2004). COP and clathrin-coated vesicle budding: different pathways, common approaches. Curr Opin Cell Biol *16*, 379-391.
Melancon, P., Glick, B.S., Malhotra, V., Weidman, P.J., Serafini, T., Gleason, M.L., Orci, L., and Rothman, J.E. (1987). Involvement of GTP-binding "G" proteins in transport through the Golgi stack. Cell *51*, 1053-1062.
Mellman, I. (1996). Endocytosis and molecular sorting. Annu Rev Cell Dev Biol *12*, 575-625.
Mesmin, B., Drin, G., Levi, S., Rawet, M., Cassel, D., Bigay, J., and Antonny, B. (2007). Two lipid-packing sensor motifs contribute to the sensitivity of ArfGAP1 to membrane curvature. Biochemistry *46*, 1779-1790.
Miller, E., Antonny, B., Hamamoto, S., and Schekman, R. (2002). Cargo selection into COPII vesicles is driven by the Sec24p subunit. EMBO J *21*, 6105-6113.

Miller, E.A., and Barlowe, C. (2010). Regulation of coat assembly--sorting things out at the ER. Curr Opin Cell Biol *22*, 447-453.
Miller, E.A., Beilharz, T.H., Malkus, P.N., Lee, M.C., Hamamoto, S., Orci, L., and Schekman, R. (2003). Multiple cargo binding sites on the COPII subunit Sec24p ensure capture of diverse membrane proteins into transport vesicles. Cell *114*, 497-509.
Miller, E.A., and Schekman, R. (2013). COPII - a flexible vesicle formation system. Curr Opin Cell Biol *25*, 420-427.
Miura, K., Jacques, K.M., Stauffer, S., Kubosaki, A., Zhu, K., Hirsch, D.S., Resau, J., Zheng, Y., and Randazzo, P.A. (2002). ARAP1: a point of convergence for Arf and Rho signaling. Molecular cell *9*, 109-119.
Moelleken, J., Malsam, J., Betts, M.J., Movafeghi, A., Reckmann, I., Meissner, I., Hellwig, A., Russell, R.B., Sollner, T., Brugger, B.*, et al.* (2007). Differential localization of coatomer complex isoforms within the Golgi apparatus. Proc Natl Acad Sci U S A *104*, 4425-4430.
Mogelsvang, S., Gomez-Ospina, N., Soderholm, J., Glick, B.S., and Staehelin, L.A. (2003). Tomographic evidence for continuous turnover of Golgi cisternae in Pichia pastoris. Mol Biol Cell *14*, 2277-2291.
Montegna, E.A., Bhave, M., Liu, Y., Bhattacharyya, D., and Glick, B.S. (2012). Sec12 binds to Sec16 at transitional ER sites. PLoS One *7*, e31156.
Mossessova, E., Bickford, L.C., and Goldberg, J. (2003). SNARE selectivity of the COPII coat. Cell *114*, 483-495.
Muniz, M., Nuoffer, C., Hauri, H.P., and Riezman, H. (2000). The Emp24 complex recruits a specific cargo molecule into endoplasmic reticulum-derived vesicles. J Cell Biol *148*, 925-930.
Munro, S. (2001). What can yeast tell us about N-linked glycosylation in the Golgi apparatus? FEBS Lett *498*, 223-227.
Munro, S. (2011). The golgin coiled-coil proteins of the Golgi apparatus. Cold Spring Harb Perspect Biol *3*.
Nakano, A., and Muramatsu, M. (1989). A novel GTP-binding protein, Sar1p, is involved in transport from the endoplasmic reticulum to the Golgi apparatus. J Cell Biol *109*, 2677-2691.
Nakatsu, F., and Ohno, H. (2003). Adaptor protein complexes as the key regulators of protein sorting in the post-Golgi network. Cell Struct Funct *28*, 419-429.
Natsume, W., Tanabe, K., Kon, S., Yoshida, N., Watanabe, T., Torii, T., and Satake, M. (2006). SMAP2, a novel ARF GTPase-activating protein, interacts with clathrin and clathrin assembly protein and functions on the AP-1-positive early endosome/trans-Golgi network. Mol Biol Cell *17*, 2592-2603.
Nickel, W., Malsam, J., Gorgas, K., Ravazzola, M., Jenne, N., Helms, J.B., and Wieland, F.T. (1998). Uptake by COPI-coated vesicles of both anterograde and retrograde cargo is inhibited by GTPgammaS in vitro. Journal of cell science *111 (Pt 20)*, 3081-3090.
Nickel, W., Sohn, K., Bunning, C., and Wieland, F.T. (1997). p23, a major COPI-vesicle membrane protein, constitutively cycles through the early secretory pathway. Proc Natl Acad Sci U S A *94*, 11393-11398.
Nie, Z., Boehm, M., Boja, E.S., Vass, W.C., Bonifacino, J.S., Fales, H.M., and Randazzo, P.A. (2003a). Specific regulation of the adaptor protein complex AP-3 by the Arf GAP AGAP1. Developmental cell *5*, 513-521.
Nie, Z., Fei, J., Premont, R.T., and Randazzo, P.A. (2005). The Arf GAPs AGAP1 and AGAP2 distinguish between the adaptor protein complexes AP-1 and AP-3. Journal of cell science *118*, 3555-3566.
Nie, Z., Hirsch, D.S., Luo, R., Jian, X., Stauffer, S., Cremesti, A., Andrade, J., Lebowitz, J., Marino, M., Ahvazi, B.*, et al.* (2006). A BAR domain in the N terminus of

the Arf GAP ASAP1 affects membrane structure and trafficking of epidermal growth factor receptor. Curr Biol *16*, 130-139.
Nie, Z., Hirsch, D.S., and Randazzo, P.A. (2003b). Arf and its many interactors. Curr Opin Cell Biol *15*, 396-404.
Nilsson, T., Au, C.E., and Bergeron, J.J. (2009). Sorting out glycosylation enzymes in the Golgi apparatus. FEBS Lett *583*, 3764-3769.
Niu, T.K., Pfeifer, A.C., Lippincott-Schwartz, J., and Jackson, C.L. (2005). Dynamics of GBF1, a Brefeldin A-sensitive Arf1 exchange factor at the Golgi. Mol Biol Cell *16*, 1213-1222.
Novick, P., Field, C., and Schekman, R. (1980). Identification of 23 complementation groups required for post-translational events in the yeast secretory pathway. Cell *21*, 205-215.
Ooi, C.E., Dell'Angelica, E.C., and Bonifacino, J.S. (1998). ADP-Ribosylation factor 1 (ARF1) regulates recruitment of the AP-3 adaptor complex to membranes. J Cell Biol *142*, 391-402.
Opat, A.S., Houghton, F., and Gleeson, P.A. (2001). Steady-state localization of a medial-Golgi glycosyltransferase involves transit through the trans-Golgi network. The Biochemical journal *358*, 33-40.
Orci, L., Palmer, D.J., Ravazzola, M., Perrelet, A., Amherdt, M., and Rothman, J.E. (1993). Budding from Golgi membranes requires the coatomer complex of non-clathrin coat proteins. Nature *362*, 648-652.
Orci, L., Stamnes, M., Ravazzola, M., Amherdt, M., Perrelet, A., Sollner, T.H., and Rothman, J.E. (1997). Bidirectional transport by distinct populations of COPI-coated vesicles. Cell *90*, 335-349.
Ostermann, J., Orci, L., Tani, K., Amherdt, M., Ravazzola, M., Elazar, Z., and Rothman, J.E. (1993). Stepwise assembly of functionally active transport vesicles. Cell *75*, 1015-1025.
Owen, D.J., Collins, B.M., and Evans, P.R. (2004). Adaptors for clathrin coats: structure and function. Annu Rev Cell Dev Biol *20*, 153-191.
Paczkowski, J.E., Richardson, B.C., and Fromme, J.C. (2015). Cargo adaptors: structures illuminate mechanisms regulating vesicle biogenesis. Trends in cell biology *25*, 408-416.
Palade, G. (1975). Intracellular aspects of the process of protein synthesis. Science *189*, 347-358.
Palmer, D.J., Helms, J.B., Beckers, C.J., Orci, L., and Rothman, J.E. (1993). Binding of coatomer to Golgi membranes requires ADP-ribosylation factor. J Biol Chem *268*, 12083-12089.
Parlati, F., McNew, J.A., Fukuda, R., Miller, R., Sollner, T.H., and Rothman, J.E. (2000). Topological restriction of SNARE-dependent membrane fusion. Nature *407*, 194-198.
Pearse, B.M., and Robinson, M.S. (1990). Clathrin, adaptors, and sorting. Annu Rev Cell Biol *6*, 151-171.
Peden, A.A., Rudge, R.E., Lui, W.W., and Robinson, M.S. (2002). Assembly and function of AP-3 complexes in cells expressing mutant subunits. J Cell Biol *156*, 327-336.
Pepperkok, R., Whitney, J.A., Gomez, M., and Kreis, T.E. (2000). COPI vesicles accumulating in the presence of a GTP restricted arf1 mutant are depleted of anterograde and retrograde cargo. Journal of cell science *113 (Pt 1)*, 135-144.
Peters, P.J., Hsu, V.W., Ooi, C.E., Finazzi, D., Teal, S.B., Oorschot, V., Donaldson, J.G., and Klausner, R.D. (1995). Overexpression of wild-type and mutant ARF1 and ARF6: distinct perturbations of nonoverlapping membrane compartments. J Cell Biol *128*, 1003-1017.

Pevzner, I., Strating, J., Lifshitz, L., Parnis, A., Glaser, F., Herrmann, A., Brugger, B., Wieland, F., and Cassel, D. (2012). Distinct role of subcomplexes of the COPI coat in the regulation of ArfGAP2 activity. Traffic *13*, 849-856.
Pfeffer, S.R. (2010). How the Golgi works: a cisternal progenitor model. Proc Natl Acad Sci U S A *107*, 19614-19618.
Poon, P.P., Cassel, D., Spang, A., Rotman, M., Pick, E., Singer, R.A., and Johnston, G.C. (1999). Retrograde transport from the yeast Golgi is mediated by two ARF GAP proteins with overlapping function. EMBO J *18*, 555-564.
Popoff, V., Adolf, F., Brugger, B., and Wieland, F. (2011a). COPI budding within the Golgi stack. Cold Spring Harb Perspect Biol *3*, a005231.
Popoff, V., Langer, J.D., Reckmann, I., Hellwig, A., Kahn, R.A., Brugger, B., and Wieland, F.T. (2011b). Several ADP-ribosylation factor (Arf) isoforms support COPI vesicle formation. J Biol Chem *286*, 35634-35642.
Premont, R.T., Perry, S.J., Schmalzigaug, R., Roseman, J.T., Xing, Y., and Claing, A. (2004). The GIT/PIX complex: an oligomeric assembly of GIT family ARF GTPase-activating proteins and PIX family Rac1/Cdc42 guanine nucleotide exchange factors. Cell Signal *16*, 1001-1011.
Presley, J.F., Cole, N.B., Schroer, T.A., Hirschberg, K., Zaal, K.J., and Lippincott-Schwartz, J. (1997). ER-to-Golgi transport visualized in living cells. Nature *389*, 81-85.
Presley, J.F., Ward, T.H., Pfeifer, A.C., Siggia, E.D., Phair, R.D., and Lippincott-Schwartz, J. (2002). Dissection of COPI and Arf1 dynamics in vivo and role in Golgi membrane transport. Nature *417*, 187-193.
Puertollano, R., Randazzo, P.A., Presley, J.F., Hartnell, L.M., and Bonifacino, J.S. (2001). The GGAs promote ARF-dependent recruitment of clathrin to the TGN. Cell *105*, 93-102.
Quinn, P., Griffiths, G., and Warren, G. (1983). Dissection of the Golgi complex. II. Density separation of specific Golgi functions in virally infected cells treated with monensin. J Cell Biol *96*, 851-856.
Rambourg, A., and Clermont, Y. (1990). Three-dimensional electron microscopy: structure of the Golgi apparatus. Eur J Cell Biol *51*, 189-200.
Ramirez, I.B., and Lowe, M. (2009). Golgins and GRASPs: holding the Golgi together. Semin Cell Dev Biol *20*, 770-779.
Randazzo, P.A., and Hirsch, D.S. (2004). Arf GAPs: multifunctional proteins that regulate membrane traffic and actin remodelling. Cell Signal *16*, 401-413.
Rapoport, T.A. (2008). Protein transport across the endoplasmic reticulum membrane. FEBS J *275*, 4471-4478.
Rawet, M., Levi-Tal, S., Szafer-Glusman, E., Parnis, A., and Cassel, D. (2010). ArfGAP1 interacts with coat proteins through tryptophan-based motifs. Biochem Biophys Res Commun *394*, 553-557.
Rehling, P., Darsow, T., Katzmann, D.J., and Emr, S.D. (1999). Formation of AP-3 transport intermediates requires Vps41 function. Nature cell biology *1*, 346-353.
Reilly, B.A., Kraynack, B.A., VanRheenen, S.M., and Waters, M.G. (2001). Golgi-to-endoplasmic reticulum (ER) retrograde traffic in yeast requires Dsl1p, a component of the ER target site that interacts with a COPI coat subunit. Mol Biol Cell *12*, 3783-3796.
Reinhard, C., Harter, C., Bremser, M., Brugger, B., Sohn, K., Helms, J.B., and Wieland, F. (1999). Receptor-induced polymerization of coatomer. Proc Natl Acad Sci U S A *96*, 1224-1228.
Reinhard, C., Schweikert, M., Wieland, F.T., and Nickel, W. (2003). Functional reconstitution of COPI coat assembly and disassembly using chemically defined components. Proc Natl Acad Sci U S A *100*, 8253-8257.
Robinson, D.G., and Pimpl, P. (2014). Clathrin and post-Golgi trafficking: a very complicated issue. Trends Plant Sci *19*, 134-139.

Robinson, M.S. (2004). Adaptable adaptors for coated vesicles. Trends in cell biology *14*, 167-174.
Rodriguez-Boulan, E., and Musch, A. (2005). Protein sorting in the Golgi complex: shifting paradigms. Biochim Biophys Acta *1744*, 455-464.
Rohde, G., Wenzel, D., and Haucke, V. (2002). A phosphatidylinositol (4,5)-bisphosphate binding site within mu2-adaptin regulates clathrin-mediated endocytosis. J Cell Biol *158*, 209-214.
Rothman, J.E., and Wieland, F.T. (1996). Protein sorting by transport vesicles. Science *272*, 227-234.
Sanchez-Velar, N., Udofia, E.B., Yu, Z., and Zapp, M.L. (2004). hRIP, a cellular cofactor for Rev function, promotes release of HIV RNAs from the perinuclear region. Genes Dev *18*, 23-34.
Sato, K., and Nakano, A. (2005). Dissection of COPII subunit-cargo assembly and disassembly kinetics during Sar1p-GTP hydrolysis. Nat Struct Mol Biol *12*, 167-174.
Scheffzek, K., Ahmadian, M.R., and Wittinghofer, A. (1998). GTPase-activating proteins: helping hands to complement an active site. Trends Biochem Sci *23*, 257-262.
Schimmoller, F., Singer-Kruger, B., Schroder, S., Kruger, U., Barlowe, C., and Riezman, H. (1995). The absence of Emp24p, a component of ER-derived COPII-coated vesicles, causes a defect in transport of selected proteins to the Golgi. EMBO J *14*, 1329-1339.
Schledzewski, K., Brinkmann, H., and Mendel, R.R. (1999). Phylogenetic analysis of components of the eukaryotic vesicle transport system reveals a common origin of adaptor protein complexes 1, 2, and 3 and the F subcomplex of the coatomer COPI. J Mol Evol *48*, 770-778.
Schlossman, D.M., Schmid, S.L., Braell, W.A., and Rothman, J.E. (1984). An enzyme that removes clathrin coats: purification of an uncoating ATPase. J Cell Biol *99*, 723-733.
Schmalzigaug, R., Phee, H., Davidson, C.E., Weiss, A., and Premont, R.T. (2007). Differential expression of the ARF GAP genes GIT1 and GIT2 in mouse tissues. J Histochem Cytochem *55*, 1039-1048.
Schmid, S.L., Braell, W.A., Schlossman, D.M., and Rothman, J.E. (1984). A role for clathrin light chains in the recognition of clathrin cages by 'uncoating ATPase'. Nature *311*, 228-231.
Schoberer, J., and Strasser, R. (2011). Sub-compartmental organization of Golgi-resident N-glycan processing enzymes in plants. Mol Plant *4*, 220-228.
Serafini, T., Orci, L., Amherdt, M., Brunner, M., Kahn, R.A., and Rothman, J.E. (1991a). ADP-ribosylation factor is a subunit of the coat of Golgi-derived COP-coated vesicles: a novel role for a GTP-binding protein. Cell *67*, 239-253.
Serafini, T., Stenbeck, G., Brecht, A., Lottspeich, F., Orci, L., Rothman, J.E., and Wieland, F.T. (1991b). A coat subunit of Golgi-derived non-clathrin-coated vesicles with homology to the clathrin-coated vesicle coat protein beta-adaptin. Nature *349*, 215-220.
Simpson, F., Peden, A.A., Christopoulou, L., and Robinson, M.S. (1997). Characterization of the adaptor-related protein complex, AP-3. J Cell Biol *137*, 835-845.
Sohn, K., Orci, L., Ravazzola, M., Amherdt, M., Bremser, M., Lottspeich, F., Fiedler, K., Helms, J.B., and Wieland, F.T. (1996). A major transmembrane protein of Golgi-derived COPI-coated vesicles involved in coatomer binding. J Cell Biol *135*, 1239-1248.
Spang, A., Matsuoka, K., Hamamoto, S., Schekman, R., and Orci, L. (1998). Coatomer, Arf1p, and nucleotide are required to bud coat protein complex I-coated vesicles from large synthetic liposomes. Proc Natl Acad Sci U S A *95*, 11199-11204.

Springer, S., Chen, E., Duden, R., Marzioch, M., Rowley, A., Hamamoto, S., Merchant, S., and Schekman, R. (2000). The p24 proteins are not essential for vesicular transport in Saccharomyces cerevisiae. Proc Natl Acad Sci U S A *97*, 4034-4039.
Stamnes, M.A., Craighead, M.W., Hoe, M.H., Lampen, N., Geromanos, S., Tempst, P., and Rothman, J.E. (1995). An integral membrane component of coatomer-coated transport vesicles defines a family of proteins involved in budding. Proc Natl Acad Sci U S A *92*, 8011-8015.
Stamnes, M.A., and Rothman, J.E. (1993). The binding of AP-1 clathrin adaptor particles to Golgi membranes requires ADP-ribosylation factor, a small GTP-binding protein. Cell *73*, 999-1005.
Suda, Y., and Nakano, A. (2012). The yeast Golgi apparatus. Traffic *13*, 505-510.
Sun, Z., Anderl, F., Frohlich, K., Zhao, L., Hanke, S., Brugger, B., Wieland, F., and Bethune, J. (2007). Multiple and stepwise interactions between coatomer and ADP-ribosylation factor-1 (Arf1)-GTP. Traffic *8*, 582-593.
Supek, F., Madden, D.T., Hamamoto, S., Orci, L., and Schekman, R. (2002). Sec16p potentiates the action of COPII proteins to bud transport vesicles. J Cell Biol *158*, 1029-1038.
Szul, T., Garcia-Mata, R., Brandon, E., Shestopal, S., Alvarez, C., and Sztul, E. (2005). Dissection of membrane dynamics of the ARF-guanine nucleotide exchange factor GBF1. Traffic *6*, 374-385.
Szul, T., and Sztul, E. (2011). COPII and COPI traffic at the ER-Golgi interface. Physiology (Bethesda) *26*, 348-364.
Tanabe, K., Kon, S., Natsume, W., Torii, T., Watanabe, T., and Satake, M. (2006). Involvement of a novel ADP-ribosylation factor GTPase-activating protein, SMAP, in membrane trafficking: implications in cancer cell biology. Cancer Sci *97*, 801-806.
Tanabe, K., Torii, T., Natsume, W., Braesch-Andersen, S., Watanabe, T., and Satake, M. (2005). A novel GTPase-activating protein for ARF6 directly interacts with clathrin and regulates clathrin-dependent endocytosis. Mol Biol Cell *16*, 1617-1628.
Tanigawa, G., Orci, L., Amherdt, M., Ravazzola, M., Helms, J.B., and Rothman, J.E. (1993). Hydrolysis of bound GTP by ARF protein triggers uncoating of Golgi-derived COP-coated vesicles. J Cell Biol *123*, 1365-1371.
Thacker, E., Kearns, B., Chapman, C., Hammond, J., Howell, A., and Theibert, A. (2004). The arf6 GAP centaurin alpha-1 is a neuronal actin-binding protein which also functions via GAP-independent activity to regulate the actin cytoskeleton. Eur J Cell Biol *83*, 541-554.
Thor, F., Gautschi, M., Geiger, R., and Helenius, A. (2009). Bulk flow revisited: transport of a soluble protein in the secretory pathway. Traffic *10*, 1819-1830.
Traub, L.M., Ostrom, J.A., and Kornfeld, S. (1993). Biochemical dissection of AP-1 recruitment onto Golgi membranes. J Cell Biol *123*, 561-573.
Tu, L., and Banfield, D.K. (2010). Localization of Golgi-resident glycosyltransferases. Cell Mol Life Sci *67*, 29-41.
Ungewickell, E., and Branton, D. (1981). Assembly units of clathrin coats. Nature *289*, 420-422.
Ungewickell, E., Ungewickell, H., Holstein, S.E., Lindner, R., Prasad, K., Barouch, W., Martin, B., Greene, L.E., and Eisenberg, E. (1995). Role of auxilin in uncoating clathrin-coated vesicles. Nature *378*, 632-635.
Venkateswarlu, K., Brandom, K.G., and Lawrence, J.L. (2004). Centaurin-alpha1 is an in vivo phosphatidylinositol 3,4,5-trisphosphate-dependent GTPase-activating protein for ARF6 that is involved in actin cytoskeleton organization. J Biol Chem *279*, 6205-6208.
Vetter, I.R., and Wittinghofer, A. (2001). The guanine nucleotide-binding switch in three dimensions. Science *294*, 1299-1304.

Vitale, N., Patton, W.A., Moss, J., Vaughan, M., Lefkowitz, R.J., and Premont, R.T. (2000). GIT proteins, A novel family of phosphatidylinositol 3,4, 5-trisphosphate-stimulated GTPase-activating proteins for ARF6. J Biol Chem *275*, 13901-13906.
Volpicelli-Daley, L.A., Li, Y., Zhang, C.J., and Kahn, R.A. (2005). Isoform-selective effects of the depletion of ADP-ribosylation factors 1-5 on membrane traffic. Mol Biol Cell *16*, 4495-4508.
Waters, M.G., Serafini, T., and Rothman, J.E. (1991). 'Coatomer': a cytosolic protein complex containing subunits of non-clathrin-coated Golgi transport vesicles. Nature *349*, 248-251.
Watson, P., Townley, A.K., Koka, P., Palmer, K.J., and Stephens, D.J. (2006). Sec16 defines endoplasmic reticulum exit sites and is required for secretory cargo export in mammalian cells. Traffic *7*, 1678-1687.
Watson, P.J., Frigerio, G., Collins, B.M., Duden, R., and Owen, D.J. (2004). Gamma-COP appendage domain - structure and function. Traffic *5*, 79-88.
Weber, T., Zemelman, B.V., McNew, J.A., Westermann, B., Gmachl, M., Parlati, F., Sollner, T.H., and Rothman, J.E. (1998). SNAREpins: minimal machinery for membrane fusion. Cell *92*, 759-772.
Wegmann, D., Hess, P., Baier, C., Wieland, F.T., and Reinhard, C. (2004). Novel isotypic gamma/zeta subunits reveal three coatomer complexes in mammals. Mol Cell Biol *24*, 1070-1080.
Weidler, M., Reinhard, C., Friedrich, G., Wieland, F.T., and Rosch, P. (2000). Structure of the cytoplasmic domain of p23 in solution: implications for the formation of COPI vesicles. Biochem Biophys Res Commun *271*, 401-408.
Weimer, C., Beck, R., Eckert, P., Reckmann, I., Moelleken, J., Brugger, B., and Wieland, F. (2008). Differential roles of ArfGAP1, ArfGAP2, and ArfGAP3 in COPI trafficking. J Cell Biol *183*, 725-735.
Whittle, J.R., and Schwartz, T.U. (2010). Structure of the Sec13-Sec16 edge element, a template for assembly of the COPII vesicle coat. J Cell Biol *190*, 347-361.
Wieland, F.T., Gleason, M.L., Serafini, T.A., and Rothman, J.E. (1987). The rate of bulk flow from the endoplasmic reticulum to the cell surface. Cell *50*, 289-300.
Xing, Y., Bocking, T., Wolf, M., Grigorieff, N., Kirchhausen, T., and Harrison, S.C. (2010). Structure of clathrin coat with bound Hsc70 and auxilin: mechanism of Hsc70-facilitated disassembly. EMBO J *29*, 655-665.
Xu, D., and Hay, J.C. (2004). Reconstitution of COPII vesicle fusion to generate a pre-Golgi intermediate compartment. J Cell Biol *167*, 997-1003.
Yahara, N., Sato, K., and Nakano, A. (2006). The Arf1p GTPase-activating protein Glo3p executes its regulatory function through a conserved repeat motif at its C-terminus. Journal of cell science *119*, 2604-2612.
Yang, J.S., Lee, S.Y., Gao, M., Bourgoin, S., Randazzo, P.A., Premont, R.T., and Hsu, V.W. (2002). ARFGAP1 promotes the formation of COPI vesicles, suggesting function as a component of the coat. J Cell Biol *159*, 69-78.
Ye, K., and Snyder, S.H. (2004). PIKE GTPase: a novel mediator of phosphoinositide signaling. Journal of cell science *117*, 155-161.
Yorimitsu, T., and Sato, K. (2012). Insights into structural and regulatory roles of Sec16 in COPII vesicle formation at ER exit sites. Mol Biol Cell *23*, 2930-2942.
Yoshihisa, T., Barlowe, C., and Schekman, R. (1993). Requirement for a GTPase-activating protein in vesicle budding from the endoplasmic reticulum. Science *259*, 1466-1468.
Yu, X., Breitman, M., and Goldberg, J. (2012). A structure-based mechanism for Arf1-dependent recruitment of coatomer to membranes. Cell *148*, 530-542.
Zendeh-boodi, Z., Yamamoto, T., Sakane, H., and Tanaka, K. (2013). Identification of a second amphipathic lipid-packing sensor-like motif that contributes to Gcs1p function in the early endosome-to-TGN pathway. Journal of biochemistry *153*, 573-587.

Zhao, L., Helms, J.B., Brugger, B., Harter, C., Martoglio, B., Graf, R., Brunner, J., and Wieland, F.T. (1997). Direct and GTP-dependent interaction of ADP ribosylation factor 1 with coatomer subunit beta. Proc Natl Acad Sci U S A *94*, 4418-4423.
Zhao, L., Helms, J.B., Brunner, J., and Wieland, F.T. (1999). GTP-dependent binding of ADP-ribosylation factor to coatomer in close proximity to the binding site for dilysine retrieval motifs and p23. J Biol Chem *274*, 14198-14203.
Zhao, X., Claude, A., Chun, J., Shields, D.J., Presley, J.F., and Melancon, P. (2006). GBF1, a cis-Golgi and VTCs-localized ARF-GEF, is implicated in ER-to-Golgi protein traffic. Journal of cell science *119*, 3743-3753.
Zink, S., Wenzel, D., Wurm, C.A., and Schmitt, H.D. (2009). A link between ER tethering and COP-I vesicle uncoating. Developmental cell *17*, 403-416.

6

Abbreviations

ACAP	ArfGAP with coiled coil, ankyrin repeat and PH domains
ADAP	ArfGAP with dual PH domains
AGAP	ArfGAP with GTPase Domain, ankyrin repeat and PH Domain
AGFG	ArfGAP with FG repeats
AP	adaptor protein complex
APS	ammonium persulfate
Arf	ADP-ribosylation factor
ArfGAP	ADP-ribosylation factor GTPase activating protein
ARAP	ArfGAP with Rho GAP domain, ankyrin repeats and PH domain
ASAP	ArfGAP with SH3 Domain, ankyrin repeat and PH Domain
ATP	adenosine 5′ -triphosphate
BFA	brefeldin A
bp	base pair
BSA	bovine serum albumin
CCV	Clathrin-coated vesicle
cDNA	complementary DNA
COPI	coat protein complex I
COPII	coat protein complex II
DMEM	Dulbecco's modified eagle's medium
DMSO	dimethyl sulfoxide
DNA	desoxyribonucleic acid
DTT	dithiothretiol
EDTA	ethylendiaminetetraacetic acid
ENTH	doamin epsin N-terminal homology domain
ER	endoplasmic reticulum
ERGIC	ER-Golgi intermediate compartment
FCCS	Fluorescence cross-correlation spectroscopy
GAP	GTPase activating protein
GBF1	Golgi-specific brefeldin-A-resistant factor 1
GDP	guanosine 5′ -diphosphate
Gea1/2	guanine nucleotide exchange on Arf protein1/2
GEF	guanosine nucleotide exchange factor
GET	1-5 Golgi to ER traffic protein 1-5
GGA	Golgi-associated γ -adaptin ear homology domain containing, Arf-binding protein
GIT	G-protein-coupled receptor (GPCR)-kinase-interacting ArfGAPs
GM130	cis-Golgi matrix protein of 130 kDa
GMP-PNP	guanosine 5′ -[β,γ -imido]-triphosphate
GTP	guanosine 5′ -triphosphate
GTPγ S	guanosine 5′ -[γ -thio]-triphosphate
HEK293T	cells human embryonic kidney cell line 293, with SV-40 large T-antigen
HeLa cells	human epithelial carcinoma cell line; derived from the patient Henrietta Lacks
HEPES	4-(2-hydroxyethyl)-1-piperazin-ethansulfonic acid
IMAC	immobilized metal affinity chromatography
IPTG	isopropyl-1-thio-β -D-galactopyranoside
KD	dissociation constant
KDELr	KDEL receptor

kb	kilo base pairs
kDa	kilo dalton
LB medium	Luria Bertani medium
MCS	multiple cloning site
NIH/3T3 cells	NIH mouse embryonic fibroblast cell line; 3-day transfer, inoculum 3 x 105 cells
NP-40	Nonidet® P40 (Nonylphenylpolyethylene glycol)
NRK cells	normal rat kidney epithelial cell line
OD	optical density
PBS	phosphate buffer saline
PBS-T	phosphate buffer saline + Tween 20
PCR	polymerase chain reaction
PMSF	phenylmethulsulfonyl fluoride
PDI	protein disulfide isomerase
PVDF	polyvinyldifluoride
Ras G	protein of the Ras (Rat sarcoma) superfamily
RLC	rat liver cytosol
Sar1	secretion-associated and Ras-related protein 1
SDS-PAGE	sodium dodecyl sulfate-polyacrylamide gel electrophoresis
SEC	secretion mutant
SMAP	small ArfGAP proteins
Sf9 cells	cell line derived from Sf21 cell line
TEMED	N, N, N', N'-Tetramethylethylenediamine
TGN	trans Golgi network
TMB	tetramethylbenzidin

Amino Acids Code

A	Ala	Alanine
C	Cys	Cysteine
D	Asp	Aspartic acid
E	Glu	Glutamic acid
F	Phe	Phenylalanine
G	Gly	Glycine
H	His	Histidine
I	Ile	Isoleucine
K	Lys	Lysine
L	Leu	Leucine
M	Met	Methionine
N	Asn	Asparagines
P	Pro	Proline
Q	Gln	Glutamine
R	Arg	Arginine
S	Ser	Serine
T	Thr	Threonine
V	Val	Valine
W	Trp	Tryptophane
Y	Tyr	Tyrosine
Φ	-	bulky, hydrophobic residue
B	-	basic residue
X	-	any residue

Acknowledgements

At the end of my thesis, I would like to thank everyone who contributed to bringing this work to an end.

To begin with, I would like to thank Prof. Dr. Felix Wieland for giving me the opportunity to work on these exciting projects in his lab, for always supporting me to learn new methods, for fruitful discussions and last but not least for allowing me to start my medical studies during the course of my PhD thesis.

I would like to thank Prof. Dr. Britta Brügger for being my second supervisor, for valuable advices and her support throughout the course of my PhD work.

I am grateful to Prof. Dr. Sabine Strahl and Prof. Dr. Thomas Söllner for kindly agreeing to be in my thesis defence committee and to Prof. Thomas Söllner also for being a member of my thesis advisory committee.

I would like to thank the DGF GRK 1188 and Prof. Dr. Felix Wieland for funding.

I would like to thank the GRK 1188 chairmen Prof. Dr. Oliver Fackler and Prof. Dr. Walter Nickel for organizing courses, seminars and monthly meeting, which allowed me to learn interesting methods and to meet pioneers in the field of cell biology and biophysics.

I am deeply grateful to Ingrid Meissner and Alexia Hermann for all the technical support, the invaluable advices on the bench and for always being there at frustrating moments.

I would like to thank Inge Reckmann for her technical support.

I would like to thank Dr. Frank Adolf for all the practical help, the support, the countless discussions and for always being there for me.

I would like to thank Prof. Dr. Ana Garcia-Saez, Dr. Stephanie Bleicken and Dr. Monika Zelman-Femiak for the help with the FCCS experiments and for the fruitful collaboration.

I would like to thank Dr. Rainer Beck for starting the uncoating project and for all the critical comments and discussions.

I would like to thank all the members of the Wieland Lab, past and present, which I had the pleasure to work with. Thank you all for the pleasant working atmosphere in the lab and for all the fun outside the lab.

Last but not least, I am deeply grateful to my parents and especially to my father for all the support though all the years, for the unconditional love, for the endless patients and encouragement.